



**Mittuniversitetet**

MID SWEDEN UNIVERSITY

Thesis for the degree of Doctor of Technology  
Östersund 2016

**NUMERICAL OPTIMIZATION OF PACING STRATEGIES IN  
LOCOMOTIVE ENDURANCE SPORTS**

**David Sundström**

Supervisors:

Professor Mats Tinnsten, Mid Sweden University

Professor Peter Carlsson, Mid Sweden University

Professor Mikael Bäckström, Mid Sweden University

Sports Tech Research Centre

Department of Quality Technology and Management, Mechanical Engineering and  
Mathematics

Faculty of Science, Technology and Media  
Mid Sweden University, SE-831 25 Östersund, Sweden


ISSN 1652-893X

Mid Sweden University Doctoral Thesis 237

ISBN 978-91-88025-51-7



**Sports Tech  
Research Centre**

PART OF  MID SWEDEN UNIVERSITY

Akademisk avhandling som med tillstånd av Mittuniversitetet i Sundsvall framläggs till offentlig granskning för avläggande av teknologie doktorsexamen torsdagen den 25 februari, 2016, klockan 13.00 i sal Q221, Mittuniversitetet, Östersund.

Seminarier kommer att hållas på engelska.

*Investing in your future*



EUROPEAN UNION  
European Regional  
Development Fund

## **NUMERICAL OPTIMIZATION OF PACING STRATEGIES IN LOCOMOTIVE ENDURANCE SPORTS**

**David Sundström**

© David Sundström, 2016

Department of Quality Technology and Management, Mechanical Engineering and  
Mathematics

Mid Sweden University, SE-831 25 Östersund

Sweden

Telephone: +46 (0)771-975 000

Printed by Kopieringen Mid Sweden University, Sundsvall, Sweden, 2016

# **NUMERICAL OPTIMIZATION OF PACING STRATEGIES IN LOCOMOTIVE ENDURANCE SPORTS**

**David Sundström**

Department of Quality Technology and Management, Mechanical Engineering and  
Mathematics

Mid Sweden University, SE-831 25 Östersund, Sweden

ISSN 1652-893X, Mid Sweden University Doctoral Thesis 237; ISBN 978-91-88025-  
51-7



## **ABSTRACT**

This thesis is devoted to the optimization of pacing strategies in two locomotive endurance sports; cross-country skiing and road cycling. It has been established that constant pace and variable power distributions are optimal if purely mechanical aspects of locomotion are considered in these sports. However, there is a lack of research that theoretically investigates optimal pacing for real world athletes who are constrained in their ability to generate power output through the bioenergetics of the human body.

The aims of this thesis are to develop numerical pacing strategy optimization models and bioenergetic models for locomotive endurance sports and use these to assess objectives relevant in optimal pacing. These objectives include: Investigate the impact of hills, sharp course bends, ambient wind, and bioenergetic models on optimal pacing and assess the effect of optimal pacing strategies on performance.

This thesis presents mathematical models for optimization of pacing strategies. These models are divided into mechanical locomotion, bioenergetic, and optimization models that are connected and programmed numerically. The locomotion and bioenergetic models in this thesis consist of differential equations and the optimization model is described by an iterative gradient-based routine. The mechanical model describes the relation between the power output generated by an athlete and his/her locomotion along a course profile, giving the finishing time. The bioenergetic model strives to mimic the human ability to generate power output. Therefore, the bioenergetic model is set to constrain the power output that is used in the mechanical locomotion model. The optimization routine strives to minimize the finishing time in the mechanical locomotion model by varying the distribution of power output along the course, still satisfying the constraints in the bioenergetic model.

The studies contained within this thesis resulted in several important findings regarding the general application of pacing strategies in cross-country skiing and road cycling. It was shown that the constant pace strategy is not optimal if ambient conditions change over the course distance. However, variable power distributions were shown beneficial if they vary in parallel with course inclination and ambient winds to decrease variations in speed. Despite these power variations, speed variations were not eliminated for most variable ambient conditions. This relates to the athlete's physiological restrictions and the effect of these are hard to predict without thorough modeling of bioenergetics and muscle fatigue. Furthermore, it

was shown that substantial differences in optimal power distributions were attained for various bioenergetic models.

It was also shown that optimal braking and power output distributions for cycling on courses that involve sharp bends consisted of three or four phases, depending on the length of the course and the position of the bends. The four phases distinguished for reasonably long courses were a steady-state power phase, a rolling phase, a braking phase, and an all-out acceleration phase. It was also shown that positive pacing strategies are optimal on relatively long courses in road cycling where the supply of carbohydrates are limited. Finally, results indicated that optimal pacing may overlook the effect of some ambient conditions in favor of other more influential, mechanical or physiological, aspects of locomotion.

In summary, the results showed that athletes benefit from adapting their power output with respect not only to changing course gradients and ambient winds, but also to their own physiological and biomechanical abilities, course length, and obstacles such as course bends. The results of this thesis also showed that the computed optimal pacing strategies were more beneficial for performance than a constant power distribution. In conclusion, this thesis demonstrates the feasibility of using numerical simulation and optimization to optimize pacing strategies in cross-country skiing and road cycling.

Keywords: Pacing strategy, optimization, numerical simulation, equations of motion, method of moving asymptotes, cross-country skiing, cycling

## SAMMANDRAG

Avhandlingen handlar om optimering av farthållningsstrategier inom längdskidåkning och landsvägscyckling. Det finns ett utbrett stöd för att konstant fart och varierande effektfördelningar är optimala om endast mekaniska aspekter beaktas i dessa sporter. Ändå saknas teoretiska studier som undersöker optimal farthållning för verkliga idrottsutövare som är begränsade i sin förmåga att generera effekt genom kroppens bioenergetiska system.

Målen med den här avhandlingen är att utveckla metoder för bioenergetik och optimering av farthållningsstrategier i uthållighetsidrott. Dessutom är målet att undersöka påverkan av backar, svängar, omgivande vind och bioenergetisk modellering på den optimala farthållningsstrategin samt att utreda potentialen till prestationsförbättring med optimala farthållningsstrategier.

Avhandling presenterar matematiska modeller för optimering av farthållningsstrategier. Dessa modeller delas in i en mekanisk modell för förflyttning, en bioenergetisk modell och en optimeringsmodell. De mekaniska och bioenergetiska modellerna som presenteras i avhandlingen består av differentialekvation och optimeringsmodellen utgörs av en gradient-baserad algoritm. Den mekaniska modellen beskriver förhållandet mellan utövarens effekt och den resulterande rörelsen längs banan som ger tiden mellan start och mål. Den bioenergetiska modellen beskriver människokroppens olika energisystem och dess begränsningar att generera effekt. Den bioenergetiska modellen interagerar med optimeringsmodellen genom att utgöra dess begränsningar för vad den mänskliga kroppen klarar av. Sammanfattningsvis försöker optimeringsmodellen minimera tiden mellan start och mål i den mekaniska modellen genom att variera effekten längs banan. Samtidigt ser optimeringsmetoden till att denna effektfördelning inte kränker den bioenergetiska modellen.

Studierna som ingår i avhandlingen resulterade i flera viktiga upptäckter om generella tillämpningar av farthållningsstrategier inom längdskidåkning och landsvägscyckling. Det visade sig att konstant fart inte är optimalt om omgivande betingelser varierade längs banans sträckning. Däremot var varierande effektfördelning fördelaktig om den varierar parallellt med banlutning och omgivande vindpåverkan för att minska fartens variationer. Trots denna variation, visade resultaten att fartvariationerna inte eliminerades helt. Detta har att göra med utövarens fysiologiska begränsningar, vars påverkan är svår att förutspå utan genomgående modellering av bioenergetik relaterat till muskeltrötthet. Dessutom

visade resultaten att olika bioenergetiska metoder gav upphov till betydande skillnader i de optimala farthållningsstrategierna.

Resultaten i avhandlingen visade också att optimal effektfördelning vid kurvtagning i landsvägscyklning innehåller tre eller fyra faser. The fyra faser som var utmärkande på relativt långa banor var en tröskelfas, en rullfas, en bromsfas och en maximal accelerationsfas. Resultaten visar också att positiv farthållning är optimal på relativt långa banor i landsvägscyklning där tillgången på kolhydrater är begränsad. Samtidigt visade resultaten på optimala farthållningsstrategier ibland att inverkan av omgivande betingelser förbisågs till fördel för med inflytelserika betingelser som påverkar framdrivningen.

Sammantaget visar resultaten i denna avhandling att utövare gagnas av att anpassa effekten med hänsyn till varierande terräng, omgivande vind, atletens egen fysiologiska och biomekaniska förmåga, banans längd och hinder såsom kurvor. Resultaten visar också att de optimala farthållningsstrategier med varierande effektfördelning som beräknats i denna avhandling förbättrar prestationen jämfört med konstanta effektfördelningar. Sammanfattningsvis visar denna avhandling på möjligheterna att använda numerisk simulering och optimering för att optimera farthållningsstrategier i längdskidåkning och landsvägscyklning.

Nyckelord: Farthållningsstrategi, optimering, numerisk simulering, rörelseekvationer, method of moving asymptotes, längdskidåkning, cykling



## ACKNOWLEDGEMENTS

The work presented in this thesis has been carried out at the Department of Quality Technology and Management, Mechanical Engineering, and Mathematics, Mid Sweden University, Östersund, Sweden. Financial support for this work was provided by the *European Regional Development Fund* and Mid Sweden University.

A number of people have been involved in my work with this thesis, some directly and some indirectly. Firstly, I would like to thank my girlfriend, brother, and my parents for their firm support and understanding. My girlfriend Jannie has been the most understanding life companion ever and my true soulmate when the going got tough during work on this thesis. My brother Martin has also given me great support and encouragement and always has a pun in his back pocket to make my spirits rise. I thank my mother Iren and father Rune for raising me in an impeccable way, for giving me support through thick and thin and for giving me the opportunity to discover my own way of life, both professionally and personally.

Furthermore I would like to thank my supervisor, Professor Mats Tinnsten, and co-supervisors, Professor Peter Carlsson and Professor Mikael Bäckström, for their co-authorship and for the fruitful guidance and discussions that have been more than sufficient for a proper mentorship in my research studies.

Special thanks also go to Dr. Fredrik Ståhl for his co-authorship and the rewarding cooperation and discussion.

I would like to acknowledge the stimulating research environment at the Sports Tech Research Centre at Mid Sweden University in Östersund. Special thanks to Dr. Mats Ainegren, Dr. Marie Crons-kär, Dr. Jonas Danvind, Åsa Danvind, Rebecca Ek, Dr. Andrey Koptioug, Kajsa Nilsson, Dr. Lars-Erik Rännar, and Per Skoglund for their support.

I would also like to express my deepest gratitude to all former and present colleagues in the Q-building at Mid Sweden University's campus in Östersund, for all the interesting and amusing discussions. I am especially grateful to Karin Ahlin, Erik Andersson, Fredrik Andersson, Dr. Glenn Björklund, Giovanni Carraro, Dr. Felix Dobslaw, Dr. Harald Engan, Dr. Kerry McGawley, Lisa Nilsson, Gertrud Nordh, Alexander Patrician, and Professor Erika Schagatay.

Thanks also go to Professor Per Edström for his rigorous review of this thesis.

Finally, I would like to express my gratitude to all the students I have taught on the Bachelor's program in Sports Technology at Mid Sweden University in Östersund. Thanks for enjoyable discussions and for making me learn more than I would otherwise have done.

Östersund, December 2015

A handwritten signature in black ink that reads "David Sundström". The script is fluid and cursive, with the first letter 'D' being particularly large and stylized.

David Sundström

## LIST OF PAPERS

This thesis is mainly based on the following six papers, herein referred to by their Roman numerals:

**Paper I** Numerical optimization of pacing strategy in cross-country skiing.  
David Sundström, Peter Carlsson, Fredrik Ståhl, Mats Tinnsten.  
Structural and Multidisciplinary Optimization 2013, vol. 47 iss. 6, p. 943-950. DOI: 10.1007/s00158-012-0856-7.

### **Author contribution**

The author of this thesis is the lead author of the paper. The author's contribution to the paper includes a literature review, modelling of the efficiency and aerodynamics including the numerical programming, optimization constraint formulation and analysis of the results. The author was responsible for writing the paper, except for section 2.4.

**Paper II** On optimization of pacing strategy in road cycling.  
David Sundström, Peter Carlsson, Mats Tinnsten.  
Proceedings of the 6<sup>th</sup> Asia-Pacific congress on sports technology (APCST) 2013, Hong Kong. Proceedia Engineering vol. 60 p. 118-123.  
DOI: 10.1016/j.proeng.2013.07.062.

### **Author contribution**

The author of this thesis is the lead author of the paper. The author's contribution to the paper includes a literature review, model implementation for mechanics and bioenergetics, optimization problem formulation, the numerical programming, and analysis of the results. The author was responsible for writing the paper.

**Paper III** Comparing bioenergetic models for the optimisation of pacing strategy in road cycling.

David Sundström, Peter Carlsson, Mats Tinnsten.

Sports Engineering 2014 vol. 17 iss. 4 p. 207-215. DOI: 10.1007/s12283-014-0156-0.

**Author contribution**

The author of this thesis is the lead author of the paper. The author's contribution to the paper includes a literature review, model implementation for mechanics and bioenergetics, optimization problem formulation, the numerical programming, and analysis of the results. The author was responsible for writing the paper.

**Paper IV** The influence of course bends on pacing strategy in road cycling.

David Sundström, Peter Carlsson, Mats Tinnsten.

Proceedings of The 2014 conference of the International Sports Engineering Association (ISEA) 2014, Sheffield, UK. Procedia Engineering vol. 72 p. 835-840. DOI: 10.1016/j.proeng.2014.06.141.

**Author contribution**

The author of this thesis is the lead author of the paper. The author's contribution to the paper includes a literature review, model development and implementation for mechanics and bioenergetics, optimization problem formulation, the numerical programming, and analysis of the results. The author was responsible for writing the paper.

**Paper V** On a bioenergetic four compartment model for human exercise.

David Sundström.

Accepted for publication in Sports Engineering 2016.

**Author contribution**

The author of this thesis is the sole author of the paper. The author made a literature review, developed the bioenergetic model by extending a previous model, implemented and programmed it numerically, performed the simulations, and made a comparative analysis of the results. The paper was, of course, written by the author of this thesis.

**Paper VI** Numerical optimization of pacing strategies for variable wind conditions in road cycling.  
David Sundström, Mikael Bäckström.  
Manuscript.

**Author contribution**

The author of this thesis is the lead author of the paper. The author's contribution to the paper includes a literature review, mechanical model development and implementation, optimization problem formulation, the numerical programming, and comparative analysis of the results. The author was responsible for writing the paper.

The published papers are reproduced with kind permission of the publisher.

## Papers not included in this thesis

- Paper a** Optimizing pacing strategies on a hilly track in cross-country skiing.  
David Sundström, Peter Carlsson, Mats Tinnsten  
Proceedings of the 5<sup>th</sup> Asia-Pacific Congress on Sports Technology (APCST), 2011, Melbourne, Australia p. 10-16. DOI: 10.1016/j.proeng.2011.05.044
- Paper b** Optimal distribution of power output and braking for corners in road cycling. Abstract presented at Science and Cycling, 1-2 July, 2015, Utrecht, the Netherlands.
- Paper c** A four compartment model on human exercise bioenergetics  
David Sundström, Mikael Bäckström, Peter Carlsson, Mats Tinnsten.  
Proceedings of the 7<sup>th</sup> Asia-Pacific congress on sports technology (APCST) 2015, Barcelona, Spain. Procedia Engineering vol. 65 p. 118-123. DOI: 10.1016/j.proeng.2015.07.167

## ABBREVIATIONS

2-D	two-dimensional
$A$	projected frontal area
$A_1$	cross-sectional area of the first compartment in a compartment model
$A_2$	cross-sectional area of the second compartment in a compartment model
$A_{AL}$	cross-sectional area of the alactic compartment in Margaria's model and the M-M and M-M-S models
$A_{AWC}$	cross-sectional area of the anaerobic compartment in the CP model
$A_{CHO}$	cross-sectional area of the carbohydrate compartment in the M-M-S model
$A_L$	cross-sectional area of the lactic compartment in Margaria's model and the M-M and M-M-S models
$A_{tot}$	total amount of adenosines
ADP	adenosine diphosphate
AMP	adenosine monophosphate
ATP	adenosine triphosphate
$AWC$	anaerobic work capacity
$a_1, a_2, a_3$	constants in the Hill equation
$a_{tot}$	athlete's total horizontal acceleration
$a_{tot}^{max}$	maximal horizontal acceleration attainable without slipping
$a_s, \ddot{s}$	athlete's acceleration in the course direction
$a_z$	athlete's acceleration in the z-direction
$B$	shape parameter for $\varphi$
BE I-VI	bioenergetic models, see section 2
$B_{AL}$	ventilation tube for the alactic compartment
$B_L$	ventilation tube for the lactic compartment
$b_1$	static component of wheel bearing friction
$b_2$	dynamic coefficient of wheel bearing friction
$C_D$	drag coefficient
$C_D A_{SSP}$	drag area of a skier in the semi-squatting posture
$C_D A_{URP}$	drag area of a skier in the upright posture
$C_D A_\varphi$	continuous function of drag area with respect to $\varphi$
$C_{RR}$	coefficient of rolling resistance
CLNW	constant power simulation on 100 km course without ambient wind
CLW	constant power simulation on 100 km course with ambient wind
CSNW	constant power simulation on 2 km course without ambient wind
CSW	constant power simulation on 2 km course with ambient wind

$CP$	critical power
CP model	critical power model
CPIE	critical power model for intermittent exercise
CPS	constant power strategy
$Cr$	creatine
$Cr_{tot}$	total amount of creatines
$c$	parameter determining the available energy of carbohydrates
$c_{\infty}$	straight course
$c_{7.5}$	course with bend of 7.5 m turning radius
$c_{10}$	course with bend of 10 m turning radius
$D$	number of equally spaced $x$ -coordinates where the constraints were evaluated
DH	double hill course
$Ee_{ADP}$	energy equivalent of one mole ADP
$Ee_{ATP}$	energy equivalent of one mole ATP
$Ee_{PCr}$	energy equivalent of one mole PCr
$F$	net force
$F_{BR}$	bearing friction force
$F_D$	drag force (air resistance)
$F_g$	gravity force
$F_{RR}$	rolling resistance
$F_s$	propulsive force generated by the athlete
$F_s^{max}$	maximal propulsive force generated by the athlete
$F_{\mu k}$	kinetic frictional force
$F_{\mu s}$	static frictional force
$f(x)$	equation for the course section, i.e. $y = f(x)$
GNSS	global navigation satellite systems
$g$	acceleration of gravity ( $9.81 \text{ m}\cdot\text{s}^{-2}$ )
$H$	height measure of compartment model
$H^+$	hydrogen ion
$h$	parameter determining the available anaerobic work or alactic energy
$h_1$	fluid height in the first compartment of a compartment model
$h_2$	fluid height in the second compartment of a compartment model
$I$	mass moment of inertia of the bicycle wheels
$J$	number of optimization variables
$K$	number of distance steps for solving the motion equation
$K_1 - K_{10}$	dissociation constants of the alactic compounds in the M-M-S model
$L$	length of a tube connecting two fluid compartments
$l$	parameter determining the available lactic energy



$M_L$	maximal lactic power
$M_O$	maximal oxidative power
$M_P$	initial maximal power output
$M_R$	maximal lactic replenishment power
$Mg^{2+}$	magnesium ion
M-M	Margaria-Morton
M-M-S	Margaria-Morton-Sundström
$m$	total mass of the athlete and equipment
$N$	normal force between the athlete-equipment system and the ground
$n$	local coordinate normal to course direction
ODE	ordinary differential equation
OLNW	optimal power simulation on 100 km course without ambient wind
OLW	optimal power simulation on 100 km course with ambient wind
OSNW	optimal power simulation on 2.0 km course without ambient wind
OSW	optimal power simulation on 2.0 km course with ambient wind
$P$	power output
$\bar{P}$	maximal power output average
$P_L$	lactic power
$P_m$	maximal power output
$P_{min}$	global minimal power output for optimization problem formulation
$P_{max}$	global maximal power output for optimization problem formulation
$P_O$	aerobic power
$P_R$	lactic replenishment power
PCr	phosphocreatine
$PI$	inorganic phosphate
PSO I-VI	pacing strategy optimization models, see section 2
$pH$	$-\log_{10}[H^+]$
$Q$	number of intersections between $CP$ and the power distribution
QH	quadruple hill course
$R_e$	Reynolds number
$rEC_{AL}$	rate of energy conversion due to alactic degradation
$rEC_{CHO}$	rate of energy conversion due to carbohydrate oxidation
$rEC_{FAT}$	rate of energy conversion due to fat oxidation
$rEC_{FAT}'$	rate of energy conversion due to fat oxidation according to the modified Chenevière model
$rEC_{FAT_1}^{max}$	maximal rate of energy conversion due to fat oxidation at full carbohydrate stores
$rEC_{FAT_2}^{max}$	maximal rate of energy conversion due to fat oxidation at empty carbohydrate stores
$rEC_L$	rate of energy conversion due to sole anaerobic glycolysis

$rEC_L^{max}$	maximal rate of energy conversion due to sole anaerobic glycolysis
$rEC_O^{max}$	maximal rate of energy conversion due to oxidative phosphorylation
$rEC_R^{max}$	maximal rate of energy expenditure due to lactic replenishment
$rEC_R$	rate of energy conversion due to lactic replenishment
$rEE$	rate of energy expenditure
$rEE_0$	y-intercept of the physiological and biomechanical efficiency relationship
$rEE_0^{max}$	initial maximal rate of energy expenditure
$rEE_{mf}^{max}$	maximal rate of energy expenditure due to muscle fatigue
$r_n$	course curvature radius in the vertical plane
$r_t$	tube radius in a compartment model
$r_w$	wheel radius
$r_z$	course curvature radius in the horizontal plane
SP	single plateau course
$s$	local coordinate tangential to course direction
$T$	finishing time (time between start and finish)
TTE	time to exhaustion
$t$	time
$u$	resulting wind speed
$\dot{V}$	volumetric flow rate
$\dot{V}_{max}$	maximal flow through a tube connecting two compartments
$V_m$	active muscle volume
$\dot{V}O_2$	volumetric rate of oxygen consumption
$\dot{V}O_{2max}$	maximal volumetric rate of oxygen consumption
$v, \dot{s}$	athlete's ground speed in the course direction
$v_{lim}$	limit speed where $\eta_{GE}$ is reduced to the half
$v_{max}$	maximal speed attainable without slippage due to normal acceleration
$w$	ambient wind speed
$x$	global horizontal coordinate of the course profile
$y$	global vertical coordinate
$z$	global horizontal coordinate normal to the $x$ - and $y$ -coordinates
$\alpha$	course incline
$\beta$	resulting wind's yaw angle
$\gamma$	ambient wind angle
$\Delta h_{max}$	maximal attainable difference between $h_1$ and $h_2$
$\Delta p$	pressure difference between the ends of a tube
$\delta_1$	dilatation parameter of the fat oxidation relationship ( $rEC_{FAT}'$ ) for full carbohydrate stores

$\delta_2$	dilatation parameter of the fat oxidation relationship ( $rEC_{FAT}'$ ) for empty carbohydrate stores
$\varepsilon$	function dependent on adenosine concentrations in the alactic compound model
$\zeta$	bearing angle of locomotion
$\eta_{GE}$	gross efficiency
$\eta_{PB}$	slope of the physiological and biomechanical efficiency relationship
$\eta_{tr}$	transmission efficiency of the bicycle
$\theta$	geometrical constant in the M-M and M-M-S model
$\kappa_t, \kappa_d, \kappa_m, \kappa_c$	constants in the alactic compound model
$\Lambda$	$\frac{dt}{dx}$
$\lambda$	geometrical constant in the M-M and M-M-S model
$\mu_k$	kinetic friction coefficient
$\mu_s$	static friction coefficient
$\mu_{vis}$	dynamic viscosity of a fluid
$\nu_{vis}$	kinematic viscosity of a fluid
$\xi$	geometrical constant in the M-M-S model
$\rho$	air density
$\rho_{fl}$	fluid density in a compartment model
$\sigma_1$	symmetry parameter of the fat oxidation relationship ( $rEC_{FAT}'$ ) for full carbohydrate stores
$\sigma_2$	symmetry parameter of the fat oxidation relationship ( $rEC_{FAT}'$ ) for empty carbohydrate stores
$\tau_1$	translation parameter of the fat oxidation relationship ( $rEC_{FAT}'$ ) for full carbohydrate stores
$\tau_2$	translation parameter of the fat oxidation relationship ( $rEC_{FAT}'$ ) for empty carbohydrate stores
$\varphi$	reducing function dependent on athlete's speed for gross mechanical efficiency and drag area
$\phi$	geometrical constant in the M-M and M-M-S model

Each single dot over the parameter denotes a differentiation by time, and square brackets applied to any chemical substance denote molar concentration of that substance. Vectors are denoted in bold typeface.



# TABLE OF CONTENTS

ABSTRACT.....	V
SAMMANDRAG.....	VII
ACKNOWLEDGEMENTS.....	IX
LIST OF PAPERS.....	XI
ABBREVIATIONS.....	XV
<b>1. INTRODUCTION .....</b>	<b>1</b>
1.1 DEMANDS OF LOCOMOTIVE ENDURANCE SPORTS .....	1
1.2 LOCOMOTION SIMULATION AND PERFORMANCE PREDICTION .....	3
1.3 MATHEMATICAL MODELING OF BIOENERGETICS .....	4
1.4 PACING STRATEGY.....	4
1.5 AIMS.....	8
<b>2. OUTLINE OF PACING STRATEGY OPTIMIZATION MODELS FOR LOCOMOTIVE ENDURANCE SPORTS.....</b>	<b>11</b>
<b>3. MECHANICS OF LOCOMOTION.....</b>	<b>15</b>
3.1 KINEMATICS.....	15
3.2 KINETICS .....	17
3.2.1 Propulsive force.....	18
3.2.2 Gravity.....	18
3.2.3 Ground reaction force.....	19
3.2.4 Aerodynamics.....	19
3.2.5 Coulumb friction and rolling resistance .....	21
3.2.6 Wheel bearing friction .....	22
3.2.7 Static tire friction .....	22
3.3 EQUATIONS OF MOTION .....	24
3.3.1 Transformation of motion equations.....	25
<b>4. BIOENERGETICS AND BIOMECHANICS.....</b>	<b>27</b>
4.1 BIOENERGETICS .....	27
4.1.1 The critical power model .....	28
4.1.2 Margaria's model.....	29
4.1.3 The Margaria-Morton model.....	31
4.1.4 The Margaria-Morton-Sundström model.....	33
4.1.3 Fluid mechanics of hydraulic compartment models .....	39
4.2 EFFICIENCY.....	41
4.3 FORCE-VELOCITY RELATIONSHIP .....	42

<b>5. NUMERICAL SOLUTION OF ORDINARY DIFFERENTIAL EQUATIONS .</b>	<b>45</b>
5.1 THE EULER METHOD .....	46
5.2 THE 4 <sup>TH</sup> ORDER RUNGE-KUTTA METHOD .....	46
5.3 THE RUNGE-KUTTA-FEHLBERG METHOD .....	47
<b>6. OPTIMIZATION .....</b>	<b>49</b>
6.1 FORMULATION OF A GENERAL OPTIMIZATION PROBLEM .....	49
6.1.1 <i>Optimization variables</i> .....	49
6.1.2 <i>Constraints</i> .....	50
6.1.3 <i>Objective function</i> .....	51
6.2 SOLVING AN OPTIMIZATION PROBLEM .....	52
6.2.1 <i>Analytical optimization</i> .....	52
6.2.2 <i>Numerical optimization</i> .....	53
6.2.3 <i>Approximated sub-problems</i> .....	55
6.2.4 <i>Method of moving asymptotes</i> .....	55
<b>7. THE PACING STRATEGY OPTIMIZATION PROBLEM .....</b>	<b>57</b>
7.1 FORMULATION OF THE OPTIMIZATION PROBLEM .....	57
7.1.1 <i>Objective function</i> .....	57
7.1.2 <i>Constraints</i> .....	57
7.2 NUMERICAL IMPLEMENTATION.....	59
7.3 MODEL UNCERTAINTY AND SENSITIVITY .....	61
<b>8. SUMMARY AND MAIN RESULTS .....</b>	<b>63</b>
8.1 EFFECT OF HILLS ON OPTIMAL PACING IN CROSS-COUNTRY SKIING .....	63
8.2 EFFECT OF HILLS ON OPTIMAL PACING IN ROAD CYCLING .....	63
8.3 IMPACT OF SHARP COURSE BENDS ON OPTIMAL PACING IN ROAD CYCLING.....	65
8.4 IMPACT OF AMBIENT WIND WITH CHANGING DIRECTION ON OPTIMAL PACING IN ROAD CYCLING .....	68
8.5 EFFECT OF VARIOUS BIOENERGETIC MODELS ON THE RESULTS IN PACING STRATEGY OPTIMIZATION .....	73
8.6 EFFECT OF OPTIMAL PACING STRATEGIES ON PERFORMANCE .....	75
8.7 BIOENERGETIC MODEL DEVELOPMENT FOR PACING STRATEGY OPTIMIZATIONS ...	76
8.7.1 <i>Submaximal simulations</i> .....	76
8.7.2 <i>Supramaximal simulations</i> .....	77
8.7.3 <i>All-out simulation</i> .....	79
<b>9. DISCUSSION AND CONCLUSIONS .....</b>	<b>81</b>
9.1 EFFECT OF HILLS ON OPTIMAL PACING IN CROSS-COUNTRY SKIING .....	81

9.2	EFFECT OF HILLS ON OPTIMAL PACING IN ROAD CYCLING .....	81
9.3	IMPACT OF SHARP COURSE BENDS ON OPTIMAL PACING IN ROAD CYCLING .....	82
9.4	IMPACT OF AMBIENT WIND WITH CHANGING DIRECTION ON OPTIMAL PACING IN ROAD CYCLING .....	83
9.5	EFFECT OF VARIOUS BIOENERGETIC MODELS ON THE RESULTS IN PACING STRATEGY OPTIMIZATION .....	85
9.6	EFFECT OF OPTIMAL PACING STRATEGIES ON PERFORMANCE .....	86
9.7	METHODOLOGICAL CONSIDERATIONS .....	87
9.7.1	<i>Mechanics of locomotion</i> .....	87
9.7.2	<i>Bioenergetics</i> .....	87
9.7.3	<i>Optimization</i> .....	88
10.	PERSPECTIVES AND FUTURE DEVELOPMENT .....	89
	REFERENCES .....	93





# **1. INTRODUCTION**

In this thesis, the locomotive endurance sports cross-country skiing and road cycling are studied. Cross-country skiing is studied because of its locomotive nature and as a continuation of previous studies of the author's research group. Furthermore, road cycling is studied because of the author's own interest and active career in the sport. Road cycling is also a suitable field of study considering the rigorous scientific literature available, in which the subject areas of locomotion simulation and pacing strategy optimization are most important to this thesis. Since the present thesis work is preceded by the work in a licentiate thesis (Sundström, 2013), many of the approaches and theories described in the present doctoral thesis were at least in part described in the author's licentiate thesis.

## **1.1 Demands of locomotive endurance sports**

In locomotive sports like cross-country skiing and road cycling, there are both mass start races and individual start races, called time-trials in road cycling. Individual start races minimize the interaction with other competitors while mass start races often involve drafting and the corresponding tactical context. The winner in both types of competition is the one travelling the set distance in less time than the other competitors. Therefore, the most usual performance measure in endurance sports is the duration of travel between start and finish on the race course (finishing time). Thus, the ability to travel at a high average speed for the course distance is a decisive property among endurance athletes. According to the mechanics of locomotion (described in more detail in section 3), average speed depends on a variety of forces that may be formally represented as propulsive and resistive forces. Resistive forces may be friction, rolling resistance, air drag, and gravity. However, for downhill and tailwind locomotion, air drag and gravity correspondingly can act to propel the athlete along with other propulsive forces that the athlete might generate. The ability to generate propulsive forces at speed is referred to as the power output, which is the scalar product of propulsive forces and velocity. Therefore, high locomotive speeds are characterized by high propulsive powers and low restricting forces. The athlete's ability to generate propulsive power output can be trained through various types of physical exercises and will both improve the magnitude of power output that can be maintained and the duration for which that power can be sustained (endurance). These abilities stem from the human body and they are generally studied in the fields of human exercise physiology and biomechanics.

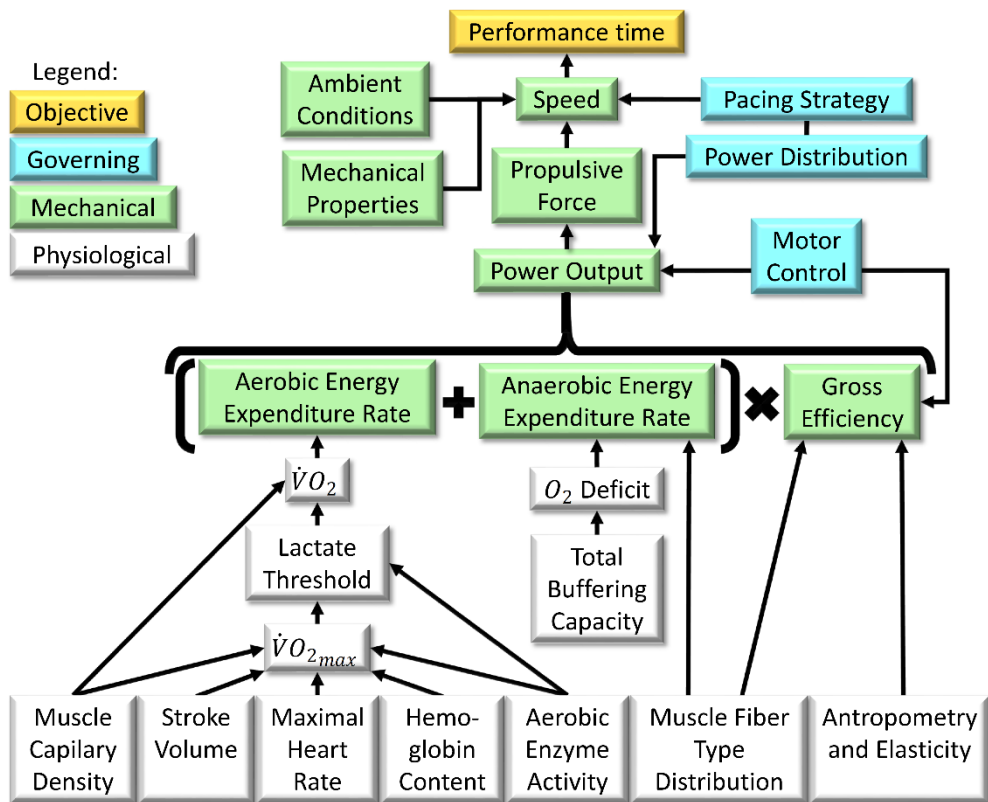


**Figure 1.** Schematic of the pacing strategy or power distribution role in a physiological and mechanical performance model for endurance sports. This illustration is based on the work of Joyner and Coyle (2008).

Athletes generate power output using coordinated muscle contractions. These contractions rely on several processes that operate in parallel to satisfy the energy requirements of each muscle. Some of these processes, anaerobic ones, do not rely on the availability of oxygen and are specialized in short bursts of high intensity work, while other processes, aerobic ones, rely on oxygen delivery and operate to maintain sufficient energy availability for prolonged endurance exercise at lower intensity (section 4.1). In endurance sports, aerobic ability is a key property in keeping a high average speed throughout the course distance. However, anaerobic capacity is also very important for shorter courses and in situations where exercise intensity varies substantially. Gastin (2001) reported that aerobic contribution to total energy requirements averaged 6% for the first 10 s of maximal work rate, while a duration of 180 s resulted in an aerobic contribution of 79%. The remainder of the energy requirements were of course supplied by the anaerobic processes and it is evident that higher relative aerobic contributions are realized in prolonged exercise. Therefore, the measurable aerobic property called the maximal oxygen consumption

rate ( $\dot{V}O_{2max}$ ), is identified as a marker of performance in endurance sports (Robinson et al., 1937). Furthermore, according to Joyner and Coyle (2008), lactate threshold and gross efficiency are also major determinants of endurance sports performance. The lactate threshold is the highest oxygen consumption rate attainable that is still equivalent to steady state lactate production, and efficiency is the ratio between work and energy expenditure. Another performance element is the pacing strategy that is further discussed in section 1.4 and contextualized in Figure 1. This illustration shows a schematic performance model based on the work of Joyner and Coyle (2008). It describes physiological and mechanical properties together with pacing strategy or power distribution.

## 1.2 Locomotion simulation and performance prediction

Understanding the locomotion of athletes is key to the proper analysis of endurance sports performance. Di Prampero et al. (1979) introduced a motion equation for cycling after analyzing the towing of a cyclist at constant speed on a flat track. The force-speed relationship that was reconstructed with the help of data fitting consists of two terms: one independent of speed and one that depends on the square of speed. The first term was identified as rolling resistance and the second as the aerodynamic drag. Olds et al. (1993) introduced the gravity and inertia related terms into the equation for energy requirement in cycling. Olds et al. (1993) considered only constant acceleration and steady speed in their modeling. Further developing the mechanical model of cycling, Martin et al. (1998) introduced transmission efficiency and bearing friction. The model expressions relating power output to speed were also validated by experiments performed in real outdoor circumstances with power output measured at the cranks. Because the model of Martin et al. (1998) is thoroughly validated, it has been applied in many succeeding studies on road cycling performance (Dahmen and Saupe, 2011, Wells et al., 2013, Dahmen and Saupe, 2015) including revised and transformed versions in Papers II-IV and VI.

In cross-country skiing, external forces acting on the athletes and their equipment are not the same as in cycling. There is of course no rolling resistance, no bearing resistance, and no transmission efficiency in the same sense as in cycling. Instead, biomechanical efficiency is likely to be more important and the glide friction between skis and snow provides a considerable resistance to the gliding (Moxnes and Hausken, 2008). Carlsson et al. (2011) introduced a numerical simulation model that solves the motion equations for cross-country skiing. By simulating athletes of different sizes and scaling their power output by allometric relationships, general conclusions of body mass' and course profile's effect on performance were investigated. Furthermore, Moxnes et al. (2013) simulated cross-country skiing on varying terrain and compared the simulation results to on-snow experiments. The

simulation model showed a good fit to experiments and therefore might be used for determining relative performance benefits when various factors change. A similar simulation model in cross-country skiing was introduced, in which the power output was expressed as a function of speed (Moxnes et al., 2014). In the same study, the simulation model was also subject to a sensitivity analysis that investigated the effect of different parameters on performance.

### **1.3 Mathematical modeling of bioenergetics**

Monod and Sherrer (1965) introduced a simplified two-parameter model on fatigue in endurance exercise. This model consists of a constant work rate that is related to the athlete's aerobic properties and a constant work capacity that is related to the anaerobic properties.

Margaria (1976) was the first to introduce a whole body three compartment model to theoretically describe the energetic processes during muscular exercise. Further developments by Morton includes the questioning of Margaria's model (Morton, 1985, Morton, 1986a), the fundamental generalization of the model (Morton, 1986b), specification of its specific geometrical parameters, and the development of maximal power constraints (Morton, 1990). Additionally, Behncke further developed the three compartment model by introducing a shift between carbohydrate and fat oxidation and coupling the carbohydrate level to the glycolysis and lactate production. None of these models use empirical findings on substrate utilization to model separate rates of energy conversion from fats and carbohydrates. Also, none of these models include appropriate efficiency modeling or energy expenditure constraints based on empirical findings of the underlying mechanisms of muscle fatigue.

### **1.4 Pacing strategy**

Pacing strategy in locomotive sports may be defined as the athlete's conscious variation of speed along the course distance. Sometimes the terms pacing strategy and power output distribution are used interchangeably and although these concepts are strongly related, they are interpreted separately in this thesis. The relation between power output and speed makes it possible to adopt a pacing strategy by performing the corresponding distribution of power output. The relation between power and speed can be expressed mathematically as a motion equation. If the event is performed at a maximal power output throughout, it is usually termed an all-out strategy. Using an all-out strategy on a short course with a standstill start and high inertia, the power distribution will obviously be high initially and decrease towards the cessation of the exercise. Simultaneously, speed will increase

throughout this short exercise. With this reasoning, it is clear that a high power start is not necessarily equivalent to a fast start due to inertia or other mechanical constructs such as gravity or various resistive forces. Gradually decreasing speed throughout the duration of the event is termed positive pacing, while gradually increasing speed is referred to as a negative pacing strategy (Abbiss and Laursen, 2008). The adoption of a more or less constant speed may be termed a constant or even pacing strategy. In contrast to a constant pacing strategy, variable pacing strategies involve substantial variations in speed, although many authors define variable pacing as a variable power distribution. For clarity, variable power strategies are termed variable power distributions in this thesis. This may be further conceptualized in cross-country skiing where substantial differences in efficiency between gears have been observed (Ainegren et al., 2013). This results in different rates of energy expenditure for the same mechanical power output in various gears. Therefore, it might be more intuitive to use energy expenditure distributions instead of power distributions in cross-country skiing.

For performance enhancement, optimal pacing strategies aim to vary speed to minimize the time between start and finish. Accordingly, an optimal power distribution varies power output to minimize the finishing time. Furthermore, due to the restrictions on power output that athletes realize, the optimization of pacing strategies is a constrained optimization problem.

To my knowledge the first study investigating pacing in sports was conducted on bipeds' and quadrupeds' locomotion more than 100 years ago and suggests that constant pace is optimal (Kennelly, 1906). This suggestion is based on the inverse polynomial relation between speed and world record times at the time, speculating that intervals with a speed higher than average cannot make up for the time lost in preceding periods of lower than average speed. This theory was later supported by a number of studies in running and cycling (Robinson et al., 1958, Foster et al., 1993, Atkinson et al., 2003). However, it was later shown that the optimal pacing strategy in cycling adapts to ambient conditions when external forces change (Swain, 1997, Atkinson and Brunskill, 2000, Atkinson et al., 2007, Cangle et al., 2011, Boswell, 2012).

By varying power in sync with ambient forces, Swain (1997) showed that variable power strategies are beneficial in variable terrain and ambient wind conditions in a numerical simulation of time-trial cycling. This variable power strategy was also shown to induce lower physiological stress, compared to self-paced strategies on a 16.1 km time-trial experiment (Atkinson and Brunskill, 2000). Atkinson et al. (2007) conducted a similar study but with the mechanical model of Martin et al. (1998) and

confirmed the findings of Swain (1997) regarding variable power strategies in road cycling time-trials. But these predictions showed greater gains than Swain (1997) for varying power in wind and in variable terrain. Atkinson et al. (2007) concluded that this was related to the differences in mechanical models between the two studies. However, more time is spent in uphill and headwind compared to downhill and tailwind, even though power is varied to reduce this effect. So, in accordance with Swain (1997), power has to be compensated in either uphill/headwind or downhill/tailwind to accomplish constant average power or work in every simulation. Therefore, the lack of such compensation in the study of Atkinson et al. (2007) may also result in these greater time gains. Furthermore, these studies did not account for inertia, which explains why high power starts are optimal (de Koning et al., 1999). In addition, de Koning et al. (1999) also concluded that all-out power distribution is optimal in a 1000 m track cycling time-trial, while the 4000 m time-trial benefits from a high power start followed by constant power to the finish line. This requires, of course, a flat track with no ambient wind.

By using a mechanical multibody model of a bicycle and rider, Cangle et al. (2011) optimized the pacing strategy for a 4000 m road cycling time-trial with variable terrain. They used an average power constraint and a constraint on the power variability. Furthermore, they validated the optimal results by comparing experimental results on riders performing constant power and the calculated optimal power distribution. Normalized times were on average 2.9% faster for the optimal power distribution compared to the constant power trials.

Boswell (2012) showed that previous simulation models in road cycling (Swain, 1997, Atkinson et al., 2007) were underestimating the finishing times by excluding the inertial effect. This has a substantial impact when speed fluctuates extensively and therefore affects speed in the initial acceleration phase, when the course gradient is changing, and when decelerations are imposed due to sharp course bends, for instance. Moreover, Wells et al. (2013) confirmed that a high power start is beneficial in time-trial road cycling, through studying variable power distributions on flat courses with no ambient wind.

Investigating the effect of various idealized power distributions (Abbiss and Laursen, 2008), Underwood and Jermy (2014) simulated the track cycling pursuit from experimentally obtained work outputs. Among these constant work simulations, the power strategies involving an all-out start followed by constant or variable power resulted in the fastest finishing time for most of the studied athletes. This partly confirms the findings of de Koning et al. (1999). In the simulation model

of Underwood and Jermy (2014), the mechanics of the course bends were considered and therefore variable power distributions were synchronized with course bends.

Maroński (1994) pioneered the use of calculus of variations and optimal control theory to optimize the pacing strategy in cycling. He proved mathematically that optimal speed was constant for travelling a set course in a set time, regardless of course profile. Furthermore, he showed that the same solution of constant speed was applicable to the problem of minimal time traveling a set distance with fixed work. By applying a circular course with constant wind direction relative to the course, Maroński (1994) also calculated the optimal pacing strategy for variable winds. However, because of the lack of experimental data on the drag areas dependence on the yaw angle, constant drag area was considered. In addition to this limitation, the study of Maroński (1994) did not incorporate any physiological modeling into the optimization, implying that the derived solutions are purely mechanical effects of optimal pacing.

Gordon (2005) introduced the constrained mathematical optimization of pacing strategy by using a simplified simulation model that neglected inertia but used the 3-parameter critical power model (Morton, 1996) to simulate exertion of the rider in road cycling. Gordon (2005) confirmed the findings of Swain (1997) that variable power distribution is optimal for road cycling in varying terrain. However, he also concluded that there is no benefit to varying power in response to changes in ambient wind despite that time gains, albeit small, were achieved in the variable power simulations.

By using an optimal control algorithm and the simulation model of Martin et al. (1998), Dahmen (2012b) performed optimization of the pacing strategy on a fictional 2000 m course profile in road cycling. Three different bioenergetic constraint models were evaluated, including the 3-parameter critical power model (Morton, 1996) and a more realistic 6-parameter model. Furthering the methodological development of pacing strategy optimization, Dahmen (2012a) introduced a new approach by calculating a field of optimal power distributions. As uncertainty always applies to some of the parameters in the simulation models, this field of power distributions might work as a precaution for the rider if any parameter alters from the ideal value.

In the experimental study of Andersson et al. (2010), a cross-country sprint skiing time-trial was investigated in the field with a differential global navigation satellite system on a homologated 1425 m course consisting of two identical laps. Participants opted for an overall positive pacing strategy, which implies that the first lap was run faster than the second lap. In detail, uphill and downhill sections were

faster in the first lap while the flat sections were run faster in the second lap. This may be because the flat sections appeared in the onset and end of each lap meaning that the initial acceleration and the end spurt might have greatly influenced the measured pacing pattern on the flat. Furthermore, Formenti et al. (2015) studied cross-country skiing in a 10 km simulated race where participants opted for a reverse J-shaped pacing strategy.

## 1.5 Aims

The general purpose of this thesis is to further the scientific knowledge of optimal pacing and ultimately support athletes in their strategic mindsets regarding pacing in locomotive endurance sports. To accomplish this purpose three aims are formulated in the field of pacing strategy optimization for locomotive endurance sports. These overall aims are to:

- a) Develop numerical models for optimization of the pacing strategy in cross-country skiing and time-trial road cycling,
- b) Develop more comprehensive bioenergetic models that are suitable for pacing strategy optimizations,
- c) Apply numerical optimization modeling to assess objectives related to pacing strategy optimization. These objectives are to:
  - (i) Assess the effect of hills on optimal pacing.
  - (ii) Investigate the impact of sharp course bends on optimal pacing.
  - (iii) Investigate the impact of ambient wind with changing direction on optimal pacing.
  - (iv) Assess various bioenergetic models' effect on the results in pacing strategy optimization.
  - (v) Assess the effect of optimal pacing strategies on performance.

These objectives are further discretized into more explicit research questions for each paper. These questions include:

- (i) Paper I: How should power output and speed be distributed to optimize performance on a homologated cross-country skiing sprint course of 1425 m?

Paper II: How do different hill set-ups with equal accumulated elevations affect optimal pacing on a 2000 m course in non-drafted road cycling?



- (ii) Paper IV: How should power output and speed be distributed on a 1000 m flat course with one sharp course bend to optimize performance in non-drafted road cycling?  
How does course bend and the corresponding racing line affect performance in non-drafted road cycling on a 1000 m flat course?
  - (iii) Paper VI: How should energy expenditure rate and speed be distributed to optimize performance in non-drafted road cycling of 2 km and 100 km when ambient wind direction is changing relative to the direction of travel and when there is no ambient wind?
  - (iv) Paper III: What are the differences in performance and optimal power distribution between the critical power model for intermittent exercise, the Margaria-Morton model, and a constant power strategy on a 2000 m hilly course in non-drafted road cycling?
- Paper VI: What are the performance differences between an optimized pacing strategy and a constant power strategy when constrained by the Margaria-Morton-Sundström model?
- (v) Papers I, II, III, and VI: How large is the performance enhancement from an optimal pacing strategy compared to a constant power strategy under the assumptions adhering to each paper?

Papers I, II, III, IV, and VI are all responsible to attain aim a), while Paper V is completely designated to aim b).



## **2. OUTLINE OF PACING STRATEGY OPTIMIZATION MODELS FOR LOCOMOTIVE ENDURANCE SPORTS**

Papers I-IV and VI deal with pacing strategy optimization and each of these papers includes certain models for pacing strategy optimization. Paper V, on the other hand, includes models on exercise bioenergetics that may be used in pacing strategy optimization. For simplicity, corresponding pacing strategy optimization models are referred to using the abbreviation PSO, and each bioenergetic model is BE. Each abbreviation is followed by the Roman numeral corresponding to the appended paper (e.g. PSO I corresponds to the pacing strategy optimization model in Paper I). In Papers III and VI there are several bioenergetic models and therefore a complimentary lower case letter is added at the end of the model name to refer to each of these.

Each pacing strategy optimization model (PSO) consists of three integrated sub-models; the mechanical locomotion model, the bioenergetic model (BE), and the optimization model. The locomotion and bioenergetic models in this thesis consist of systems of first-order ordinary differential equations (ODEs) and the optimization model is described by an iterative gradient-based routine. The mechanical model (section 3) describes the relationship between the power output generated by an athlete and his/her locomotion along a cubic spline course profile, giving the finishing time. The bioenergetic model (section 4) strives to mimic the human ability to generate power output and the occurrence of fatigue. Therefore, the bioenergetic model is set to constrain the power output that is used in the mechanical locomotion model to avoid exhaustion. The equations of the locomotion and bioenergetic models are solved using numerical differential equation solvers (section 5). The optimization routine (section 6 and 7) strives to minimize the finishing time in the mechanical locomotion model by varying the distribution of power output along the course, still satisfying the constraints in the bioenergetic model.

All models are mathematical and are programmed using the MATLAB® software. Tables 1 and 2 present the main features of the PSO and BE models respectively, together with the indication on the number of variables and parameters involved, and the solvers used to treat the ODEs for finding corresponding solutions to the modeling equations. All PSO models used the method of moving asymptotes (MMA, section 6.2.4) (Svanberg, 1987, Svanberg, 1993) as optimization routine.

These models are introduced to accomplish the aims of this thesis and to answer the research questions in section 1.5. Aims a) and b) are of course accomplished through the development of the PSO and BE models respectively, which are presented in this

thesis. Furthermore, the research questions of aim c) are answered by implementing the corresponding PSO models adhering to the paper in which the research question is addressed. The treatment of these research questions rely on assumptions regarding the parameters required in the PSO models (i.e. course profile, athlete's mechanical and physiological properties). This means that the results of these studies are specific to certain circumstances and athletes. Therefore, conclusions drawn from these results cannot be universal. However, if representative parameters are applied, it is conceivable to assume that the calculated results are characteristic examples, which may indicate that the nature of the solution might not deviate substantially for similar parameter settings. Therefore, considering that the vast majority of parameters do not vary much in real-world settings, general conclusions might be drawn if changes in the parameters with the greatest variation span is considered.

**Table 1.** Main features of the pacing strategy optimization models presented in this thesis.

Model	Sport	Course length	Number of variables	ODE solver	Obstacle/Object investigated
PSO I	XC skiing	1425 m	75	Runge-Kutta-Fehlberg	Real sprint course
PSO II	Road cycling	2000 m	80	Runge-Kutta-Fehlberg	Hills
PSO III	Road cycling	2000 m	81	4 <sup>th</sup> order Runge-Kutta	Various bioenergetic models on hilly course
PSO IV	Road cycling	1000 m	81	4 <sup>th</sup> order Runge-Kutta	Course bends
PSO VI	Road cycling	2000 m 100 km	1* or 81	Runge-Kutta-Fehlberg	Ambient wind

Note: \*One optimization variable was used to assess constant power distribution.

**Table 2.** Main features of the bioenergetic models presented in this thesis.

Model	Conventional name	Number of dependent variables	Number of parameters	Comment
BE I	Average power	1	1	The total average power output was restricted by a constant value
BE II	Critical power for intermittent exercise	1	2	A single compartment model with constant anaerobic work and critical power
BE III a	Constant power	0	1	Pure mechanical simulation of constant power output No real constraint
BE III b	Critical power for intermittent exercise	1	2	Same as BE II
BE III c	Margaria-Morton	2	10	A three compartment model including a lactic fatigue constraint on the maximal power output
BE IV	Margaria-Morton	2	10	Same as BE III c except for the fatigue constraint which was offset to allow full employment of the compartments
BE V	Margaria-Morton-Sundström	3	43	A four compartment model including a maximal power constraint dependent on the inorganic phosphate concentration
BE VI a	Margaria-Morton-Sundström	3	40	Constant power Same as BE V except for the propulsive force constraint
BE VI b	Margaria-Morton-Sundström	3	43	Same as BE V

Note: Power or energy expenditure rate are independent variables.



### 3. MECHANICS OF LOCOMOTION

Classical mechanics is a subfield of the science of mechanics. It constitutes of a set of physical laws describing the motion of bodies under action of forces and uses systems of mathematical equations to describe static and dynamic events. Some early efforts in classical mechanics were carried out by Galileo Galilei (1564 – 1642), Tycho Brahe (1546 – 1601) and Johannes Kepler (1571 – 1630). However, potentially the greatest contributions to classical mechanics were probably made in parallel by Gottfried Wilhelm Leibniz (1646 – 1716) and Isaac Newton (1643 – 1727). The later published his work in *Philosophiæ Naturalis Principia Mathematica*, where the law of gravity and the three laws of motion are postulated.

In contrast to quantum mechanics, classical mechanics assumes Galilean relativity, meaning time is considered to be absolute. Classical mechanics also assumes Euclidean geometry, which is a good approximation to the properties of physical space when the gravitational field is weak. These principals lay in the foundation of the mechanical simulation models presented in this thesis. The laws of classical mechanics are applicable to macroscopic bodies which are not travelling at speeds near the speed of light.

#### 3.1 Kinematics

In all PSO models, the athlete and his/her equipment is obliged to follow the course that is set up for each model. The course profile is described by a 2-D profile consisting of a connected chain of cubical splines in Cartesian coordinates  $(x, y)$ , see Figures 2 and 3. This relationship is expressed as:

$$y = f(x), \tag{1}$$

where  $f$  represents the cubical relationships of the spline functions connecting the vertical coordinates ( $y$ ) to the horizontal coordinates ( $x$ ). In PSO IV, the course bearing angle is also described by connected cubical splines, but in the horizontal plane only. The advantage of cubical splines is the fact that both the first and second derivatives of the relative coordinates are continuous, which also means that the inclination angle ( $\alpha$ ) and curvature radii in the vertical and horizontal planes ( $r_n$  and  $r_z$ ) are all available for all points from start to finish in the course profile. The course inclination angle is expressed as:

$$\alpha = \tan^{-1} \left( \frac{dy}{dx} \right). \tag{2}$$

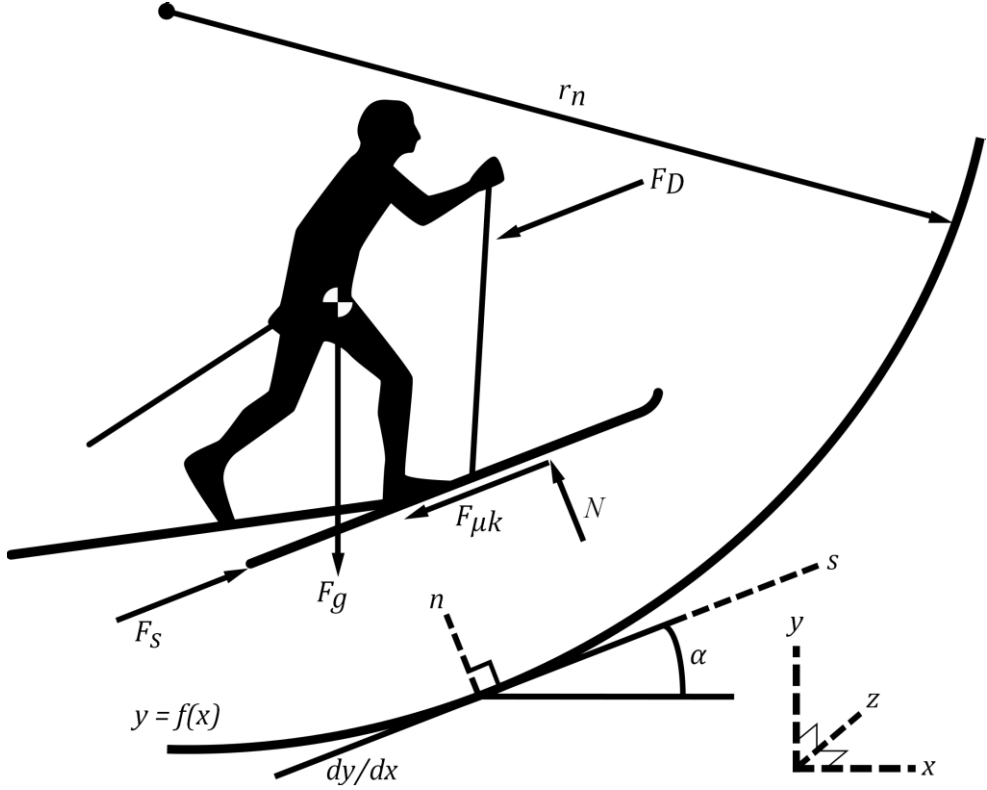


**Figure 2.** Free body diagram of a cross-country skier and an arbitrary course section ( $f(x)$ ) with local ( $s, n$ ) and global ( $x, y, z$ ) coordinates, inclination angle ( $\alpha$ ), and curvature radius ( $r_n$ ). Forces acting on the athlete were the propulsive force ( $F_s$ ), the gravitational force ( $F_g$ ), the normal force ( $N$ ), the drag force ( $F_D$ ), and the glide friction ( $F_{BR}$ ). Note: The athlete and equipment were considered as a point-mass travelling along the course profile.

Furthermore, the curvature radius in the vertical plane is expressed as:

$$r_n = \frac{\left[1 + \left(\frac{dy}{dx}\right)^2\right]^{3/2}}{\frac{d^2y}{dx^2}}. \quad (3)$$

The conversion in speed and acceleration from local coordinates ( $s$ ) to global directions ( $x$ ) were made with the following geometrical conversion equations:

$$\dot{x} = \dot{s} \cos \alpha = v \cos \alpha, \quad (4)$$

$$\ddot{x} = \ddot{s} \cos \alpha = a_s \cos \alpha, \quad (5)$$



where each single dot over the parameter denotes a differentiation by time,  $v$  is the tangential speed, and  $a_s$  is the linear acceleration in the direction of locomotion tangential to the course profile. Scalar calculus is used throughout this thesis and therefore the scalar part of velocity is used in the mathematical description. For the modeling purposes, the athlete's center of mass is set to follow the connected splines associated with both the course profile and, if applicable, the bearing angle splines.

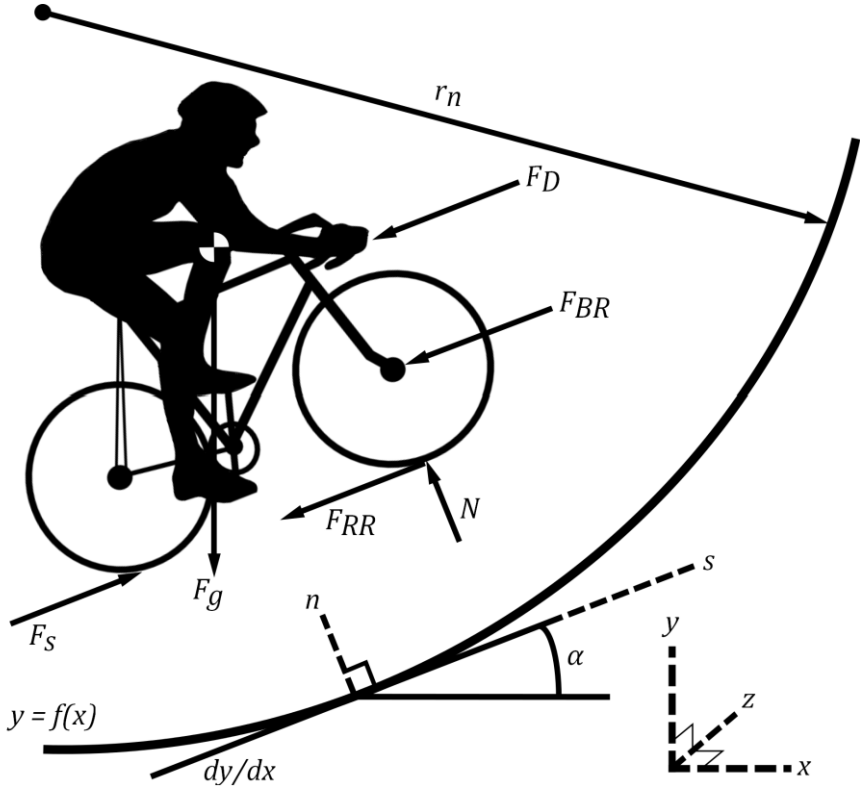


**Figure 3.** Free body diagram of a road bicycle rider and an arbitrary course section ( $f(x)$ ) with local ( $s, n$ ) and global ( $x, y, z$ ) coordinates, inclination angle ( $\alpha$ ), and curvature radius ( $r_n$ ). Forces acting on the athlete were the propulsive force ( $F_s$ ), the gravitational force ( $F_g$ ), the normal force ( $N$ ), the drag force ( $F_D$ ), the rolling resistance ( $F_{RR}$ ), and the bearing resistance ( $F_{BR}$ ). Note: The rider, bicycle and all equipment were considered as a point-mass travelling along the course profile.

### 3.2 Kinetics

According to Newton's second law, the acceleration of a body is parallel and proportional to the force acting on the body and is inversely proportional to the mass of the body. Mathematically, it is expressed as:

$$F = m \cdot a_s \quad (6)$$

where  $F$  is the net force acting on the body and  $m$  is the mass of the body. If only the linear acceleration is accounted for, this is a correct description. However, in PSO II-IV and VI, the angular acceleration of the spinning wheels is accounted for as well and thus an extended version of equation (6) is to be used. Hence, the equation can be rewritten as:

$$F = \left( m + \frac{I}{r_w^2} \right) a_s \quad (7)$$

where  $I$  is the total mass moment of inertia of the wheels and  $r_w$  is the wheel radius. The net force is the sum of the propulsive force and all the resistive forces acting to restrict motion.

### 3.2.1 Propulsive force

The propulsive force ( $F_s$ ) for skiing is expressed as:

$$F_s = \frac{P}{v} \quad (8)$$

where  $P$  is the power output corresponding to the product of force and velocity generated in the direction of locomotion (Figure 2). The gross power output may also comprise the work done in the lateral direction, which may be substantial, not least in the skating technique. However, this lateral motion was not modeled in Paper I. Furthermore, the propulsive force ( $F_s$ ) for cycling (Figure 3) is expressed as:

$$F_s = \frac{P \cdot \eta_{tr}}{v} \quad (9)$$

where  $P$  is the propulsive power output generated by the rider at the pedals and  $\eta_{tr}$  is the mechanical efficiency of the bicycle's transmission.

### 3.2.2 Gravity

The gravitational force is parallel and proportional to the acceleration of gravity which is directed to the center of the earth. The acceleration of gravity is considered to be constant for the area of interest in all simulation models and it is always acting downward in a vertical direction (negative  $y$ -direction). The gravitational force can therefore be expressed as:

$$F_g = m \cdot g \quad (10)$$

where  $g$  is the acceleration of gravity.

### 3.2.3 Ground reaction force

Changes in the course inclination angle ( $\alpha$ ) alter the ground reaction force, here referred to as the normal force ( $N$ ). This force between the ground surface and the means of locomotion (Figures 2 and 3) can be expressed as:

$$N = m \left( g \cos \alpha + \frac{v^2}{r_n} \right) \quad (11)$$

where  $r_n$  is the course curvature radius in the vertical ( $x$ - $y$ ) plane.

### 3.2.4 Aerodynamics

A reasonable approximation of the aerodynamic drag exerted on a blunt body travelling in a static fluid can be calculated by the equation:

$$F_D = \frac{1}{2} C_D A \cdot \rho \cdot v^2 \quad (12)$$

where  $C_D$  is the drag coefficient,  $A$  is the projected frontal area and  $\rho$  is the air density. This was the equation used for the aerodynamic drag force in PSO I-IV. The applicability of this equation fails when speeds are low, i.e. at low Reynolds numbers ( $R_e < \sim 1000$ ), because of the relatively larger impact of skin friction. At the starting speed (minimal speed) of the slowest starting model (PSO VI), the Reynold's number was about  $R_e \approx 60\,000$ .

Drafting is not considered in any of the models presented in this thesis. However, ambient wind velocity is the subject of evaluation in PSO VI. Ambient wind velocity affects the aerodynamic drag and thereby the locomotion of an endurance athlete. Variable strong winds are common in road cycling races located in open areas and therefore both the magnitude and the direction of ambient wind velocities are important. To account for variable wind conditions in PSO VI, the aerodynamic drag force in the direction of travel was expressed as:

$$F_D = \frac{1}{2} C_D A \cdot \rho \cdot u^2 \cos \beta = \frac{1}{2} C_D A \cdot \rho \cdot u (v + w \cos \gamma) = \frac{1}{2} C_D A \cdot \rho [(v + w \cos \gamma)^2 + (w \sin \gamma)^2]^{\frac{1}{2}} (v + w \cos \gamma) \quad (13)$$

where  $w$  is the ambient wind speed,  $\gamma$  is the ambient wind angle and  $u$  is the resulting wind speed, see Figure 4.

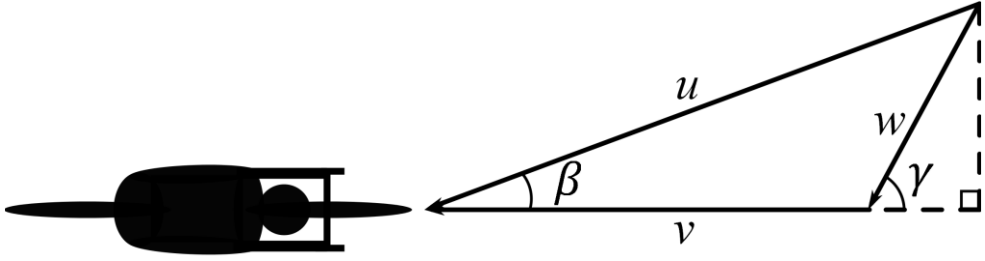


**Figure 4.** Geometrical description of wind speed due to locomotion ( $v$ ), ambient wind speed ( $w$ ), ambient wind angle ( $\gamma$ ), resulting wind speed ( $u$ ), and resulting wind's yaw angle ( $\beta$ ). It is assumed in this figure that air has a relative motion and the rider is the zero velocity reference.

In PSO VI, the projected drag area  $C_D A$  is set to vary with the resulting wind's yaw angle according to the findings of Fintelman et al. (2014). That study investigates the variation of  $C_D A$  at a wide range of yaw angles ( $\beta$ ) between 0 and 90°. The full range of yaw angles are then acquired by extrapolating the mirror image of  $C_D A$  values in the 0 to 90° range to the angles of 90 to 180°. In PSO VI, only the ambient wind direction is set to change, but equation (11) may also be used when variable wind speed is considered.

In cross-country skiing, significant crosswinds are not very common because the courses are commonly set in the forested areas. However, it is common for cross-country skiers to crouch, or assume a semi-squatting posture, at high speeds (Figure 5) thus changing the effective drag area.

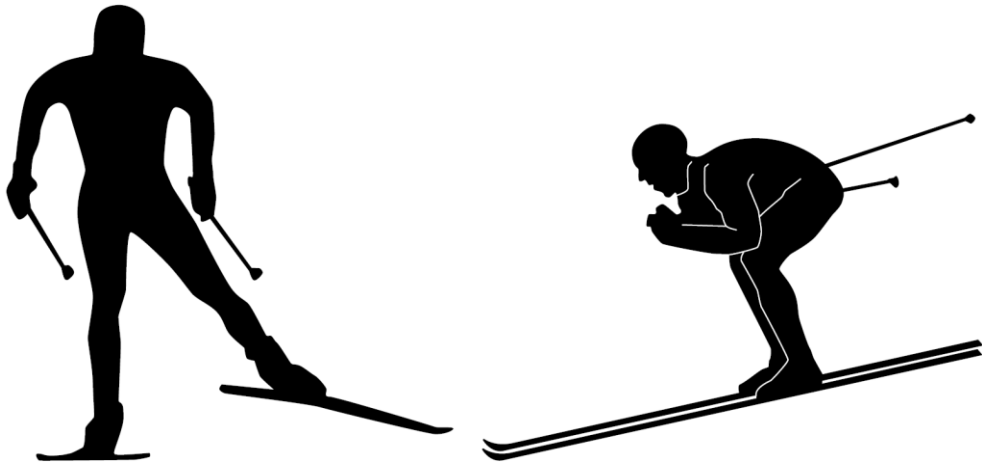


**Figure 5.** Upright (left) and semi-squatting (right) postures in cross-country skiing.

This reduces the drag area but restricts the athlete's ability to generate power output. In PSO I, The effective drag area is calculated as:

$$C_D A_\varphi = C_D A_{URP} \cdot \varphi + C_D A_{SSP} (1 - \varphi) \quad (14)$$

where  $C_D A_{URP}$  is the athlete's drag area in the upright posture and  $C_D A_{SSP}$  is the drag area in the semi-squatting posture. The reducing function  $\varphi$  in equation (14) that is introduced in PSO I, is expressed as:

$$\varphi = \frac{1}{2} - \frac{1}{\pi} \tan^{-1}(B(v - v_{lim})) \quad (15)$$

where  $B$  was a parameter that controls the shape of the function and  $v_{lim}$  was the limit speed where the skier's drag area assumes the mean value of drag areas in the upright and semi-squatting postures. A graphical representation of  $\varphi$  may be seen in Figure 6.

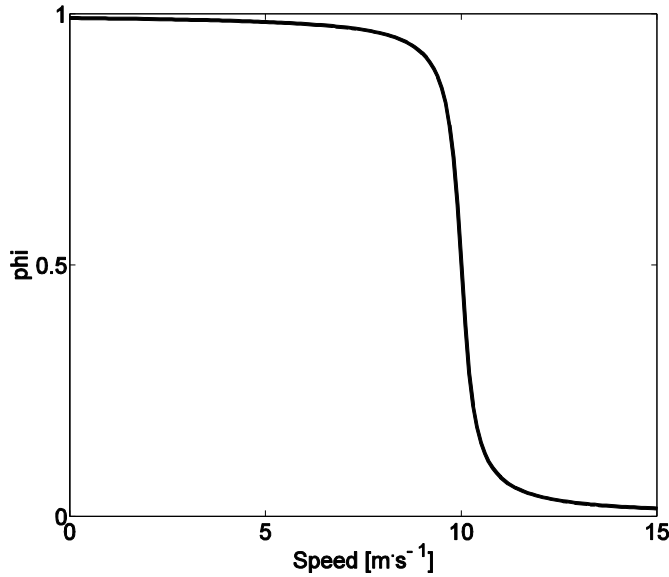


**Figure 6.** The reducing function plotted against speed of locomotion.

In PSO II-IV, the drag area was estimated by the allometric scaling equations derived by Heil (2001, 2002).

### 3.2.5 Coulumb friction and rolling resistance

In PSO I, the glide friction between snow and skis is modeled as so-called Coulumb friction. This type of friction depends both on the normal force and the kinetic

friction coefficient. Usually, the friction coefficient varies between 0.02-0.10 (Colbeck, 1994) for various snow conditions and ski properties. The expression for the kinetic friction force  $F_{\mu k}$  (Figure 2) is formulated as:

$$F_{\mu k} = \mu_k \cdot N = \mu_k \cdot m \left( g \cos \alpha + \frac{v^2}{r_n} \right) \quad (16)$$

where  $\mu_k$  is the kinetic friction coefficient. For PSO II-IV and VI, the rolling resistance between the road and the tires was also set to be proportional to the normal force. The coefficient of rolling resistance is usually between 0.002 (Kyle, 1996) and 0.008 (Pugh, 1974) on smooth asphalt roads, depending on the tire construction and material as well as the inflation pressure (Grappe et al., 1999). The rolling resistance (Figure 3) can be expressed as:

$$F_{RR} = C_{RR} \cdot N = C_{RR} \cdot m \left( g \cos \alpha + \frac{v^2}{r_n} \right) \quad (17)$$

where  $C_{RR}$  is the coefficient of rolling resistance.

### 3.2.6 Wheel bearing friction

The friction emerging from the wheel bearings creates a restricting torque on the bicycle wheels. Although, this resistance is inherent for the bicycle itself, bearing friction may be considered as an external force restricting locomotion. It has been shown that this force is nearly independent of the normal force acting on the bearing, but depends on the rotational speed and the type of bearing and lubricant (Dahn et al., 1991). According to the measurements by Dahn et al. (1991), the friction in greased cartridge bearings with a normal load of 27 kg on each wheel can be expressed as

$$F_{BR} = b_1 + b_2 \cdot v \quad (18)$$

where  $b_1$  and  $b_2$  are constants derived from the study of Dahn et al. (1991).

### 3.2.7 Static tire friction

While cornering the bicycle, friction between the tires and the road will keep the wheels on track through the corner. Without this frictional grip force the center of mass would continue in a straight line motion tangential to the horizontal plane curve. The frictional grip force will push the rider-bicycle system in the horizontal plane, executing the normal acceleration required to turn. This normal acceleration may be expressed as:

$$a_z = \frac{v^2}{r_z} \quad (19)$$

where  $r_z$  is the turning radius in the horizontal plane describe as:

$$r_z = \frac{ds}{d\zeta} \quad (20)$$

where  $\zeta$  is the bearing angle in radians. In PSO IV, the grip friction between the tires and the road (Figure 3) is described as Coulumb friction with constant friction coefficient:

$$F_{\mu_s} \leq \mu_s \cdot N = \mu_s \cdot m \left( g \cos \alpha + \frac{v^2}{r_n} \right) \quad (21)$$

where  $\mu_s$  is the static friction coefficient. PSO IV only considers courses with no elevation variation and therefore  $r_n \approx \infty$  and  $\alpha = 0$ . Furthermore, the static friction force (equation 21) is only responsible for the lateral acceleration (z-direction) (equation 19) in PSO IV. Therefore a constraint on the maximal speed limit through the corner can be expressed as:

$$v \leq \sqrt{r_z \mu_s g} = v_{max} \quad (22)$$

where  $v_{max}$  is the maximal attainable speed possible without slipping. However, equation (22) does not account for the tangential acceleration due to pedaling or braking. To incorporate both acceleration components the constraint has to be expressed as:

$$a_{tot} = \sqrt{a_s^2 + a_z^2} = \sqrt{a_s^2 + \frac{v^4}{r_z^2}} \leq \mu_s g = a_{tot}^{max} \quad (23)$$

where  $a_{tot}$  is the total horizontal acceleration, and  $a_{tot}^{max}$  is the maximal attainable horizontal acceleration possible without slipping (Paper b). A geometrical illustration of the acceleration components in equation (23) can be seen in Figure 7. The model in Paper b does not account for variable terrain and, therefore, the s- and x-coordinates coincide in this grip constraint.

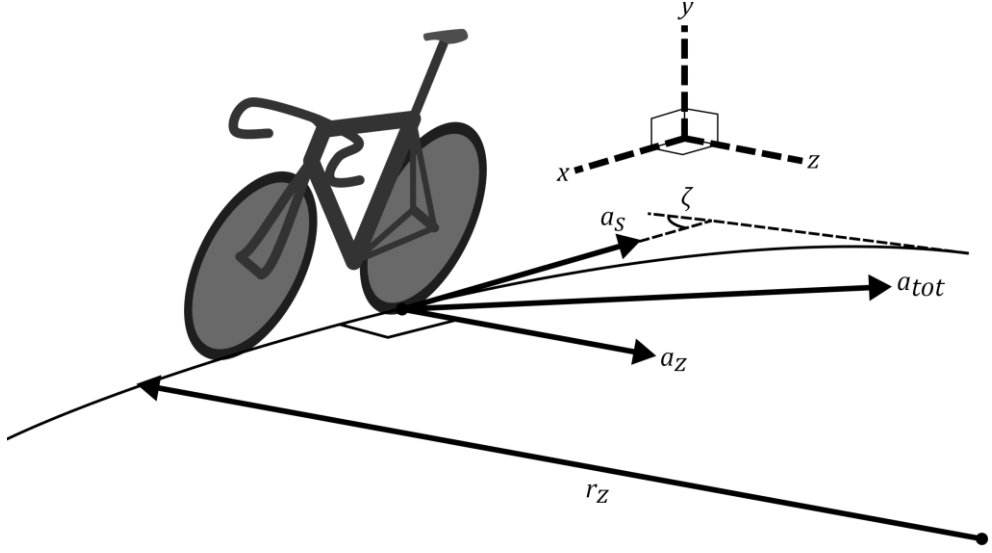


**Figure 7.** The total acceleration ( $a_{tot}$ ) in the horizontal plane involved in the grip constraint in Paper b (equation 23) is expressed as the vector sum of the tangential ( $a_s$ ) and lateral ( $a_z$ ) acceleration components. The lateral acceleration depends on the turning radius ( $r_z$ ) which depends on the change in bearing angle ( $\zeta$ ). Note that the directions of the global coordinates  $x$  and  $z$  are only momentarily valid as the bicycle turns.

### 3.3 Equations of motion

All mechanical simulation models (PSO I-IV and VI) presented in this thesis describe the locomotion of a point particle. These mechanical simulation models work in a forward dynamics mode, meaning that the power output is predetermined and thereby the force and motion are simultaneously calculated by the model. The athlete and equipment masses (PSO I) along with the mass moment of inertia of the bicycle wheels (PSO II-IV and VI) are the only inertia considered for the particle traveling the course profile in these mechanical simulation models.

Newton's second law of motion (equation 7) can be used to formulate a motion equation in the direction of locomotion ( $s$ ) for road cycling:

$$F_s - F_g \sin \alpha - F_D - F_{RR} - F_{BR} = \left( m + \frac{I}{r_w^2} \right) a_s. \quad (24)$$

By introducing the expression for each external force (equations 9-10, 13, and 17-18) the motion equation may be rewritten as:



$$\begin{aligned} & \frac{P \cdot \eta_{tr}}{v} - m \cdot g \sin \alpha - \frac{1}{2} C_D A \cdot \rho [(v + w \cos \gamma)^2 + (w \sin \gamma)^2]^{\frac{1}{2}} (v + w \cos \gamma) - C_{RR} \cdot \\ & m \left( g \cos \alpha + \frac{v^2}{r_n} \right) - b_1 + b_2 \cdot v = \left( m + \frac{I}{r_w^2} \right) a_s. \end{aligned} \quad (25)$$

This equation can be further rewritten for the global coordinate  $x$ -direction as:

$$\begin{aligned} & \left[ \frac{P \cdot \eta_{tr}}{v} - m \cdot g \sin \alpha - \frac{1}{2} C_D A \cdot \rho [(v + w \cos \gamma)^2 + (w \sin \gamma)^2]^{\frac{1}{2}} (v + w \cos \gamma) - C_{RR} \cdot \right. \\ & \left. m \left( g \cos \alpha + \frac{v^2}{r_n} \right) - b_1 + b_2 \cdot v \right] \cos \alpha = \left( m + \frac{I}{r_w^2} \right) a_s \cos \alpha = \left( m + \frac{I}{r_w^2} \right) \ddot{x}. \end{aligned} \quad (26)$$

### 3.3.1 Transformation of motion equations

In all PSO models, the equations of motion were transformed so that the horizontal position ( $x$ ) was the independent variable while time was the dependent variable. This was done by using the following relationships between time, horizontal position, and course profile:

$$\ddot{x} = a_s \cos \alpha = \ddot{s} \cos \alpha = -\frac{d^2 t}{dx^2} \left( \frac{dt}{dx} \right)^{-3}, \quad (27)$$

$$\frac{\dot{x}}{\cos \alpha} = \dot{s} = v = \left( \frac{dt}{dx} \cos \alpha \right)^{-1}. \quad (28)$$

The transformed motion equation was acquired through the substitution of equations (27) and (28) into equation (26), forming the following motion equation:

$$\begin{aligned} & \frac{d^2 t}{dx^2} = -\left( \frac{dt}{dx} \right)^4 \frac{P \cdot \eta_{tr}}{m + I_w / r_w^2} \cos^2 \alpha + \\ & \frac{C_D A \cdot \rho}{2(m + I_w / r_w^2)} \sqrt{\left( \frac{dt}{dx} \cos \alpha + \left( \frac{dt}{dx} \right)^2 w \cos \gamma \right)^2 + \left( \left( \frac{dt}{dx} \right)^2 w \sin \gamma \right)^2} \left( 1 + \frac{dt}{dx} w \cos \gamma \cos \alpha \right) + \\ & \frac{dt}{dx} \frac{m}{m + I_w / r_w^2} \left[ \left( \frac{dt}{dx} \right)^2 g \cos \alpha (C_{RR} \cos \alpha + \sin \alpha) + \frac{dt}{dx} \frac{b_1 \cos \alpha + b_2}{m} + \frac{C_{RR}}{R_v \cos \alpha} \right] + \frac{dt}{dx} \frac{\tan \alpha}{R \cos \alpha}. \end{aligned} \quad (29)$$

Finally, to make the motion equation solvable, it was transformed into a system of first order ordinary differential equations, through introducing a new variable denoted  $\Lambda$ :

$$\begin{aligned} & \frac{d\Lambda}{dx} = -\Lambda^4 \frac{P \cdot \eta_{tr}}{m + I_w / r_w^2} \cos^2 \alpha + \frac{C_D A \cdot \rho}{2(m + I_w / r_w^2)} \sqrt{\left( \frac{\Lambda}{\cos \alpha} + \Lambda^2 w \cos \gamma \right)^2 + (\Lambda^2 w \sin \gamma)^2} (1 + \Lambda \cdot \\ & w \cos \gamma \cos \alpha) + \Lambda \frac{m}{m + I_w / r_w^2} \left[ \Lambda^2 \cdot g \cos \alpha (C_{RR} \cos \alpha + \sin \alpha) + \Lambda \frac{b_1 \cos \alpha + b_2}{m} + \frac{C_{RR}}{R_v \cos \alpha} \right] + \\ & \Lambda \frac{\tan \alpha}{R \cos \alpha}, \\ & \Lambda = \frac{dt}{dx}. \end{aligned} \quad (30)$$

The benefit of this transformation is that the differential equation solver stops at predetermined distances so that finishing time and split times can be more accurately calculated. In most cases, such as competitions in locomotive sports, athletes travel a preset distance rather than a preset duration. Therefore, transformed motion equations give the best congruence to real world conditions. This way of solving motion equations also facilitates the use of adaptive step-size determination for reduced calculation times and improved accuracy. The process of transforming motion equations is more thoroughly described in Paper I.

## **4. BIOENERGETICS AND BIOMECHANICS**

All endurance athletes rely on skeletal muscle contraction to generate the forces necessary for locomotion. The action of a resulting force in the direction of movement will perform work with a magnitude equal to the product of force and displacement. Furthermore, power output, which is an important determinant of performance, may be expressed as the derivative of work with respect to time. Therefore, the modeling of work and power output are critical parts in the formulation of mathematical pacing strategy optimization problems. In most cases, the natural restrictions adhering to the athlete's biomechanical or bioenergetic properties are used as constraints in the formulation of the optimization problem. Hence, various biomechanical and bioenergetic models are presented along with their corresponding maximal power output or other expressions of mechanical or physiological derivatives.

### **4.1 Bioenergetics**

Muscle contractions rely on an energetic substrate called adenosine triphosphate (ATP) to fuel the relative movement of muscle filaments in the myofibrils. This contraction is activated by the nervous system's often conscious signals originating from the brain. As ATP is nearly exclusively the only immediate substrate for muscle contraction, ATP availability is critical to power output and thereby performance.

In humans, ATP is provided to the cells by aerobic and anaerobic pathways. Anaerobic pathways include the alactic conversion of adenosine diphosphate (ADP) and phosphocreatine (PCr) into ATP and creatine. This is the fastest pathway for forming ATP, but its capacity is very limited. The anaerobic breakdown of carbohydrates into lactic acid through glycolysis (lactic pathway) is about 2 times slower (at maximal rate) but 2-15 times greater in capacity compared to the alactic pathway (Sahlin, 1986). The aerobic pathways depend on oxygen for the phosphorylation of mainly carbohydrates and fats. The maximal oxidative phosphorylation of carbohydrates is about 3 times slower than the maximal rate of the alactic pathway, while phosphorylating fats is about 6 times slower (Sahlin, 1986). With "well filled stores", total carbohydrate capacity is about 3 500 times greater than that of the alactic stores while the available fat reserves may be more than 20 000 times greater (Sahlin, 1986). These energetic processes work in parallel to satisfy the energy requirements of the muscles. The concentration of ATP is closely regulated in these energy supplying processes to satisfy the requirements of energy to the muscle. The wide range of maximal rates of energy conversion and total capacity for these energetic pathways is enough to fulfil the ATP requirements

of work ranging from short high intensity bursts of activity to prolonged medium and low intensity work.

The studies contained within this thesis are all compartment models, in which each compartment comprises a specific category of energetic substrate for a specific energetic pathway. Compartment discretization into muscle fiber motor units and the order of fiber type activations (Liu et al., 2002, Xia and Fray Law, 2008, James and Green, 2012, Gede and Hubbard, 2014) are not considered in this thesis.

#### 4.1.1 The critical power model

The critical power concept (CP model) was first introduced by Monod and Sherrer (1965) to model muscular work and local muscular fatigue. The critical power model may be regarded as a hydraulic compartment model with a constant aerobic work rate (critical power,  $CP$ ) and a constant anaerobic work capacity ( $AWC$ ) available for exercise at intensities above  $CP$ . A hydraulic two-compartment description of the critical power model is shown in Figure 8 (left). Mathematically, the original critical power model may be expressed with the following differential equation:

$$P = CP + A_{AWC} \frac{dh}{dt} \quad (31)$$

where  $CP$  is the critical power,  $h$  is the parameter determining the available anaerobic work, and  $A_{AWC}$  is the cross-sectional area of the anaerobic compartment. The original critical power concept does not account for the replenishment of anaerobic energy at rest or low power outputs and therefore  $\frac{dh}{dt}$  cannot attain negative values.

Morton and Billat (2004) introduced the critical power model for intermittent exercise (CPIE) (BE II and BE III b) (Figure 8, right). This model allows for the anaerobic work capacity to be restored when power is less than the critical power ( $CP$ ). This model has the same expression for power output as the original critical power model (equation 31) and the associated bioenergetic constraint may be expressed as:

$$0 \leq h \leq 1. \quad (32)$$

Morton (1996) also introduced a maximal power constraint for the CP model, but this expression was not applied in any of the author's papers quoted in this thesis.

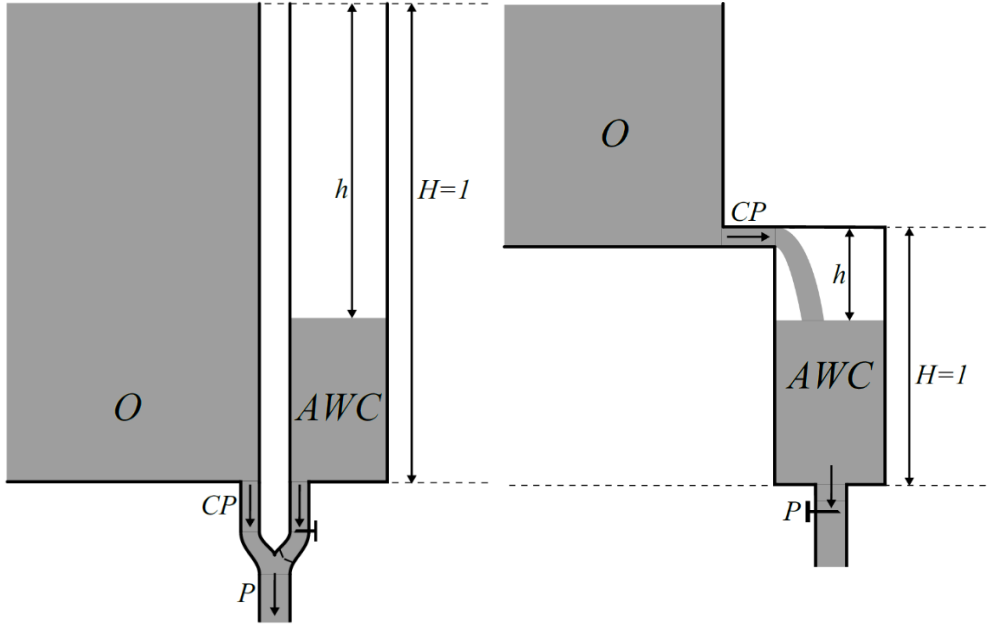


**Figure 8.** Hydraulic representation of the original critical power model (left) and the critical power model for intermittent exercise (right). *O* represents the store of fat and carbohydrate available for oxidative phosphorylation and *AWC* represents the anaerobic energy store.

#### 4.1.2 Margaria's model

Margaria (1976) was the first to introduce a compartment model that distinguishes between alactic (*AL*) and lactic (*L*) energy pathways. Furthermore, Margaria's model incorporates the slow component of oxygen uptake kinetics and accounts for the slower nature of lactic replenishment (as compared to lactic production). The model of Margaria can be expressed by the following differential equations:

$$P = A_{AL} \frac{dh}{dt} + P_O + P_L - P_R = A_{AL} \frac{dh}{dt} + P_O + A_L \frac{dl}{dt} \quad (33)$$

where  $h$  and  $l$  are the variables describing the energy content in the *AL* and *L* compartments respectively,  $A_{AL}$  and  $A_L$  are the cross-sectional areas of these compartments,  $P_L$  and  $P_R$  are the powers associated with lactic formation and replenishment respectively, and  $P_O$  is the power related to oxidative phosphorylation which is expressed as:

$$P_O = \begin{cases} 2M_O h, & 0 \leq h < \frac{1}{2} \\ M_O, & \frac{1}{2} \leq h \leq 1 \end{cases} \quad (34)$$

where  $M_O$  is the maximal oxidative power. Furthermore, the lactic energy flow,  $A_L \frac{dl}{dt}$  is expressed as:

$$A_L \frac{dl}{dt} = \begin{cases} 0, & 0 \leq h < \frac{1}{2} \text{ and } l = 0 \\ M_L(2h - 1 - l), & l + \frac{1}{2} \leq h \leq 1 \\ M_R(2h - 1 - l), & h \leq l + \frac{1}{2} \leq 1 \text{ and } l > 0 \end{cases} \quad (35)$$

where  $M_L$  is the maximal lactic power and  $M_R$  is the maximal rate of lactic replenishment. Further restrictions on the state variables ( $h$  and  $l$ ) must also apply. This includes equation (32) and the following equation:

$$0 \leq l \leq \frac{1}{2}. \quad (36)$$

A hydraulic representation of the Margaria model is shown in Figure 9. Furthermore, Margaria (1976) suggests a maximal power constraint that relates to variable  $h$  according to:

$$P_m = M_P(1 - h) \quad (37)$$

where  $P_m$  is the maximal power output and  $M_P$  is the initial maximal power output in a well-rested athlete.

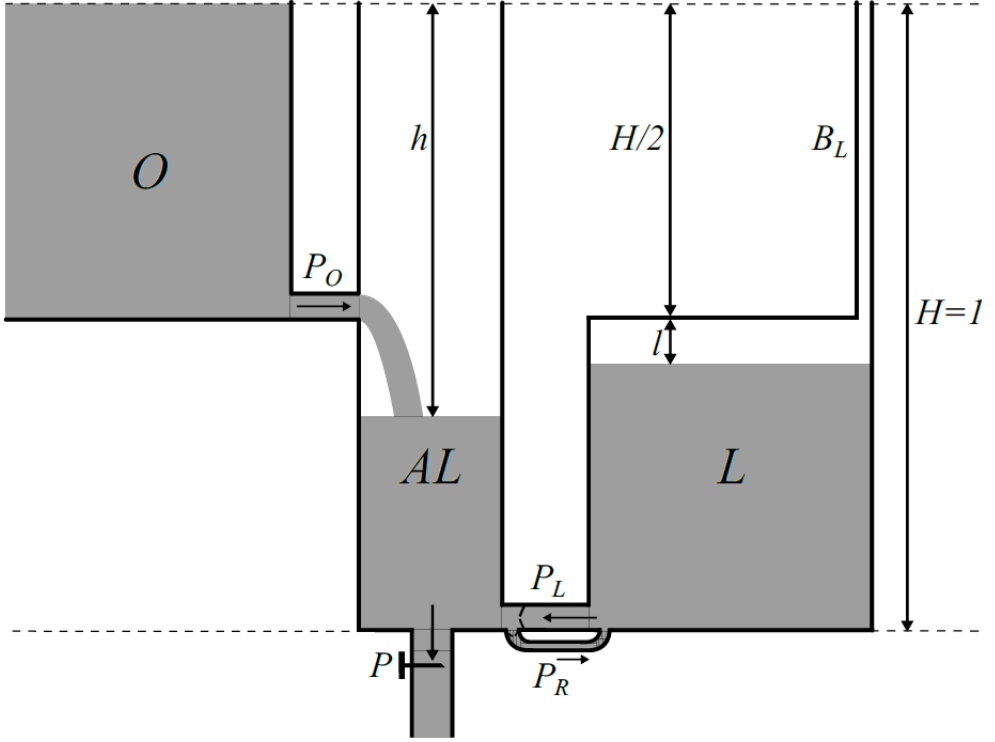


**Figure 9.** Hydraulic representation of Margaria's original model.

#### 4.1.3 The Margaria-Morton model

Morton solved Margaria's model mathematically and showed its discordance with empirical findings (Morton, 1985, Morton, 1986a). Subsequently, Morton performed further developments of Margaria's model to form the generalized Margaria-Morton (M-M) model (Morton, 1986b, Morton, 1990). The M-M model presented in Figure 10 was used in BE III c and BE IV; mathematically it may be expressed by equation (33) together with the following differential equations:

$$P_O = \begin{cases} M_O \frac{h}{1-\phi}, & 0 \leq h < 1 - \phi \\ M_O, & 1 - \phi \leq h \leq 1 \end{cases} \quad (38)$$

$$A_L \frac{dl}{dt} = \begin{cases} 0, & 0 \leq h < 1 - \theta \text{ and } l = 0 \\ M_L \frac{h-\theta-l}{1-\theta-\lambda}, & l + \theta \leq h \leq 1 - \lambda \\ M_R \frac{h-\theta-l}{1-\lambda}, & h \leq l + \theta \leq 1 - \lambda \text{ and } l > 0 \\ M_L \frac{1-\theta-\lambda-l}{1-\theta-\lambda}, & 1 - \lambda \leq h \end{cases} \quad (39)$$

In these equations, the geometrical parameters  $\phi$ ,  $\theta$ , and  $\lambda$  are represented in Figure 10. In addition to these equations, further restrictions are applicable to the state variables ( $h$  and  $l$ ):

$$0 \leq h \leq 1 - \phi, \quad (40)$$

$$0 \leq l \leq 1 - \theta - \lambda. \quad (41)$$

Morton (1990) also suggests expressions of the maximal power output for the M-M model. One expression relates the maximal power output to the level in the  $AL$  vessel, similar to Margaria's model (Margaria, 1976). Another suggestion is that maximal power output depends on the level in the  $L$  compartment. Morton formulated this relation as:

$$P_m = M_P \frac{1-\theta-\lambda-l}{1-\theta-\lambda}. \quad (42)$$

This model was used in BE III c. However, a modified expression of the maximal power output for the M-M model was implemented into BE IV. This modified formulation takes care that the maximal power output will not fall below the lactate threshold in contrast to equation (42) which allows the maximal power output to reach zero at empty  $L$  compartment. This modified formulation is expressed as:

$$P_m = M_P - \frac{l(M_P - M_O(1-\lambda))}{1-\theta-\lambda}. \quad (43)$$

Further extensions regarding that shift from carbohydrate oxidation to fat oxidation in prolonged exercise were introduced by Behncke (1993). However, empirical findings (Watt et al., 2002) indicate that the shift from carbohydrate to fat oxidation is more gradual than in the model by Behncke (1993).



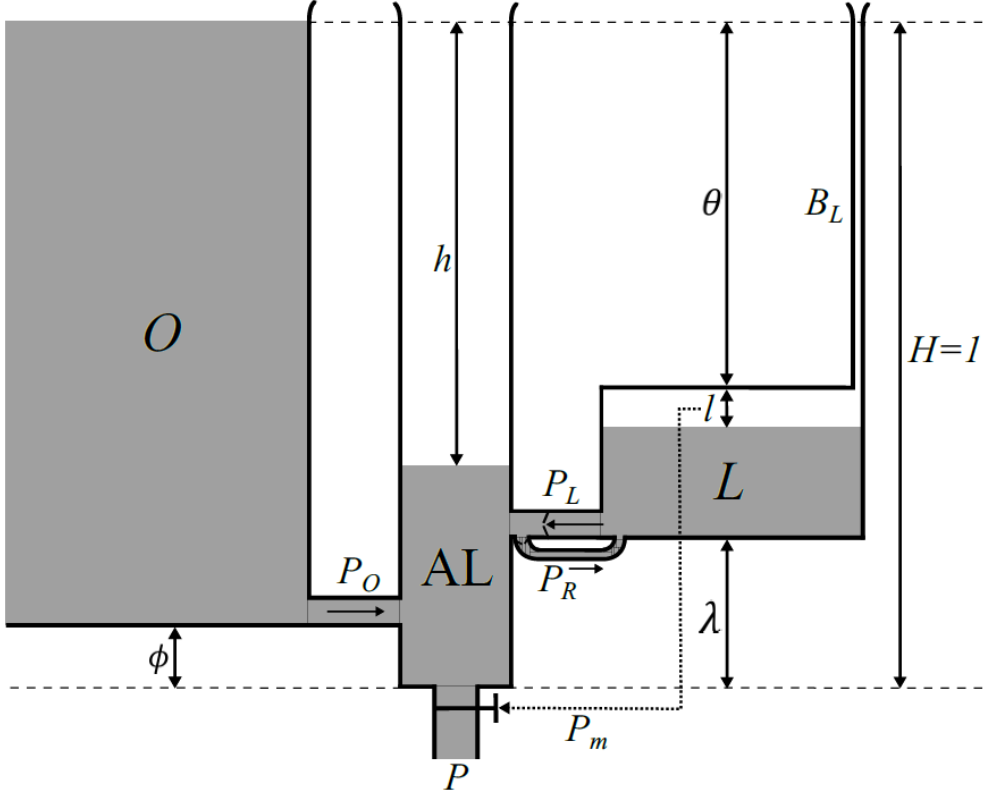


**Figure 10.** Hydraulic representation of the generalized Margaria-Morton model.  $B_L$  is a narrow tube with negligible volume.

#### 4.1.4 The Margaria-Morton-Sundström model

The Margaria-Morton-Sundström (M-M-S) model is an extension to the M-M model that also incorporates the regulation of oxidative substrate utilization (BE V and BE VI). Therefore, the M-M-S model has separate fat and carbohydrate compartments where carbohydrate stores are finite, thus imposing further restrictions during prolonged exercise. Furthermore, regulation of the lactic energy flow is further adjusted by the variable carbohydrate store. In contrast to the previous models presented in this thesis, the M-M-S model describes the flow of chemical energy rather than work rate or power. This enables modeling of efficiency. A hydraulic representation of the M-M-S model is shown in Figure 11 and the mathematical description is based on the following differential equation:

$$rEE = rEC_{FAT} + rEC_{CHO} + rEC_{AL} + rEC_L - rEC_R = rEC_{FAT} + rEC_{CHO} + A_{AL} \frac{dh}{dt} + A_L \frac{dl}{dt} \quad (44)$$

where  $rEE$  is the rate of energy expenditure,  $rEC_{FAT}$  and  $rEC_{CHO}$  are the rates of energy conversion due to fat and carbohydrate oxidation respectively, and  $rEC_L$  and  $rEC_R$  are the rates of energy conversion due to sole anaerobic glycolysis and gluconeogenesis respectively. Furthermore,  $rEC_{AL}$  is the rate of energy conversion due to alactic substrate degradation. In this equation, the rate of energy conversion due to fat oxidation is expressed as:

$$rEC_{FAT} = \begin{cases} 0, & rEC_{FAT}' \leq 0 \text{ and} & 0 \leq h + \xi < 1 - \phi \\ rEC_{FAT}', & 0 \leq rEC_{FAT}' < rEC_0^{max} \frac{h}{1-\phi} \text{ and} & 0 \leq h + \xi < 1 - \phi \\ rEC_0^{max} \frac{h}{1-\phi}, & rEC_0^{max} \frac{h}{1-\phi} \leq rEC_{FAT}' \text{ and} & 0 \leq h + \xi < 1 - \phi \\ rEC_0^{max}, & rEC_0^{max} \leq rEC_{FAT}' \text{ and} & 1 - \phi \leq h + \xi \end{cases} \quad (45)$$

where  $rEC_0^{max}$  is the maximal rate of energy conversion using oxidative phosphorylation and  $rEC_{FAT}'$  is modelled as a modified version of the one suggested by Chenevière et al. (2009):

$$rEC_{FAT}' = rEC_{FAT1}^{max} \frac{1-\phi-c}{1-\phi} \sin \left[ \left( \frac{h+\xi}{1-\phi} \pi \frac{\frac{1}{\pi\sigma_1}}{\pi+2\delta_1} + \delta_1 + \tau_1 \right)^{\sigma_1} \right] + rEC_{FAT2}^{max} \frac{c}{1-\phi} \sin \left[ \left( \frac{h+\xi}{1-\phi} \pi \frac{\frac{1}{\pi\sigma_2}}{\pi+2\delta_2} + \delta_2 + \tau_2 \right)^{\sigma_2} \right] \quad (46)$$

where  $rEC_{FAT1}^{max}$  and  $rEC_{FAT2}^{max}$  are the maximal rates of energy conversion due to fat oxidation for full ( $c = 0$ ) and empty ( $c = 1 - \phi$ ) carbohydrate energy stores respectively. Furthermore,  $\delta_1$ ,  $\delta_2$ ,  $\tau_1$ ,  $\tau_2$ ,  $\sigma_1$ , and  $\sigma_2$  are the dilatation, translation, and symmetry parameters of the fat oxidation model for full and empty carbohydrate stores respectively. The rate of energy conversion from carbohydrate oxidation is expressed as:

$$rEC_{CHO} = \begin{cases} rEC_0^{max} \frac{h}{1-\phi} - rEC_{FAT}', & 0 \leq h + \xi < 1 - \phi \\ rEC_0^{max}, & 1 - \phi \leq h + \xi \end{cases} \quad (47)$$

The resulting rate of lactic energy store depletion is expressed as:

$$A_L \frac{dl}{dt} = \begin{cases} 0, & 0 \leq h + \xi < 1 - \theta \text{ and } l = 0 \\ rEC_L^{max} \frac{1-\phi-c}{1-\phi} \frac{h+\xi-\theta-l}{1-\theta-\lambda}, & l + \theta \leq h + \xi \leq 1 - \lambda \\ rEC_R^{max} \frac{h+\xi-\theta-l}{1-\theta-\lambda}, & h + \xi \leq l + \theta \leq 1 - \lambda \text{ and } l > 0 \\ rEC_L^{max} \frac{1-\phi-c}{1-\phi} \frac{1-\theta-\lambda-l}{1-\theta-\lambda}, & 1 - \lambda \leq h + \xi \end{cases} \quad (48)$$

where  $rEC_L^{max}$  is the maximal rate of energy conversion due to sole glycolysis and  $rEC_R^{max}$  is the maximal rate of energy conversion due to gluconeogenesis. Finally, the resulting rate of carbohydrate store depletion is expressed as:

$$A_{CHO} \frac{dc}{dt} = rEC_{CHO} + 16A_L \frac{dl}{dt}. \quad (49)$$

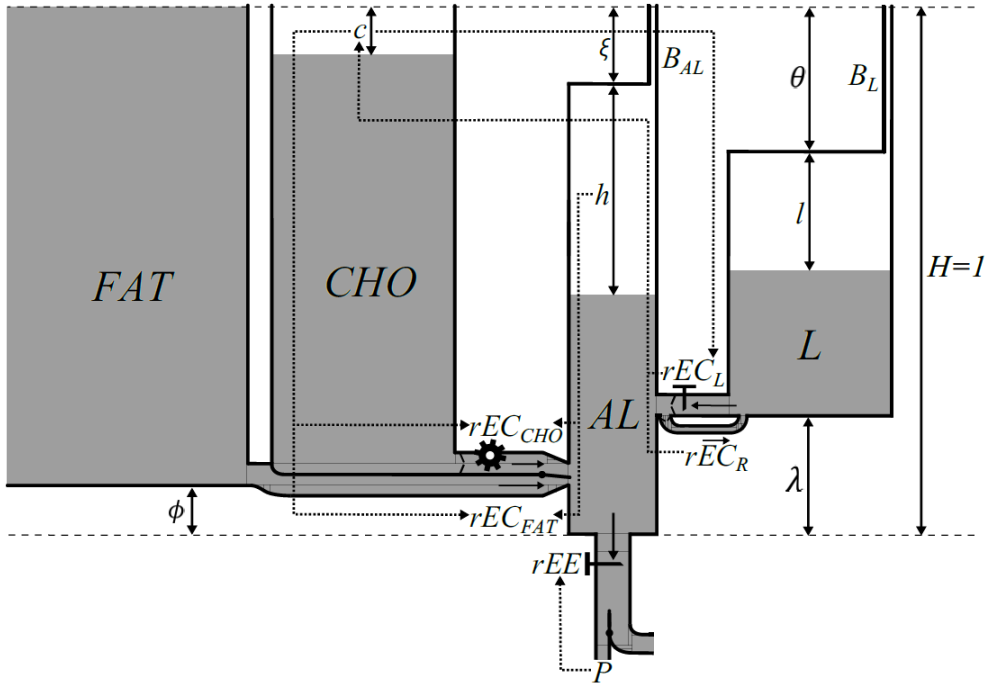


**Figure 11.** Hydraulic representation of the Margaria-Morton-Sundström model. The  $B_{AL}$  and  $B_L$  tubes are both narrow and have negligible volume.

The state variables of the M-M-S model ( $c$ ,  $h$  and  $l$ ) must also obey the following restrictions to retain the physical properties of a hydraulic compartment model:

$$0 < c < 1 - \phi, \quad (50)$$

$$0 < h < 1 - \xi, \quad (51)$$

$$0 < l < 1 - \theta - \lambda. \quad (52)$$

Previous models' expressions for maximal power output have been based on different assumptions of muscle fatigue. Among these, muscle fatigue is considered to depend on the remaining anaerobic work (equation 37), the remaining alactic work (equation 42), or the remaining lactic work (equation 43). However, empirical findings establish that inorganic phosphate concentration  $[PI]$  is a major cause of metabolic muscle fatigue (Westerblad et al., 2002). Therefore, the maximal energy expenditure in the M-M-S model is expressed as a function of  $[PI]$ :

$$rEE_{mf}^{max} = rEE_0^{max} \left( 1 - \frac{[PI]}{2[A_{tot}]} \right) \quad (53)$$

where  $rEE_0^{max}$  is the initial maximal rate of energy expenditure,  $[A_{tot}]$  is the total concentration of adenosines and the concentration of inorganic phosphate is expressed as:

$$[PI] = [ADP] + 2[AMP] \quad (54)$$

where  $[AMP]$  and  $[ADP]$  are the concentrations of adenosine monophosphate and adenosine diphosphate respectively. The mentioned concentrations of alactic substances are available in the M-M-S model by adopting chemical equilibrium equations to the  $AL$  compartment. This assumption not only presupposes chemical equilibrium but also constant sarcoplasmic volume and minimal inter-muscle differences in alactic substances' concentration.

The total energy content in the  $AL$  compartment is built up by the concentrations of each substance, their energy equivalents, and the total muscle volume of the active muscles. Therefore, the total alactic energy may be expressed as:

$$A_{AL}h = (Ee_{PCr} \cdot [PCr] + Ee_{ATP} \cdot [ATP] + Ee_{ADP} \cdot [ADP]) \cdot V_m \quad (55)$$

where  $Ee_{PCr}$ ,  $Ee_{ATP}$ , and  $Ee_{ADP}$  are the energy equivalents (Gibb's free energy to amount ratios) of PCr, ATP, and ADP respectively,  $[PCr]$  is the concentration of PCr, and  $V_m$  is the active muscle volume. The equilibrium equations utilized in the M-M-S model were suggested by McGilvery and Murray (1974) and include not only the alactic substances but also the  $pH$  and magnesium ion concentration ( $[Mg^{2+}]$ ) in the sarcoplasm. These equations are based on the following conservation laws:

$$[A_{tot}] = [ATP] + [ADP] + [AMP] \quad (56)$$

$$[Cr_{tot}] = [PCr] + [Cr] \quad (57)$$

where  $[Cr_{tot}]$  is the total concentration of creatines and  $[Cr]$  is the concentration of creatine. Furthermore, dissociation constants for each individual reaction in the *AL* compartment may be expressed as:

$$K_1 = [HATP^{3-}]/[H^+][ATP^{4-}], \quad (58)$$

$$K_2 = [HADP^{2-}]/[H^+][ADP^{3-}], \quad (59)$$

$$K_3 = [HAMP^-]/[H^+][AMP^{2-}], \quad (60)$$

$$K_4 = [HPCr^-]/[H^+][PCr^{2-}], \quad (61)$$

$$K_5 = [MgATP^{2-}]/[Mg^{2+}][ATP^{4-}], \quad (62)$$

$$K_6 = [MgADP^-]/[Mg^{2+}][ADP^{3-}], \quad (63)$$

$$K_7 = [MgAMP]/[Mg^{2+}][AMP^{2-}], \quad (64)$$

$$K_8 = [MgPCr]/[Mg^{2+}][PCr^{2-}], \quad (65)$$

$$K_9 = \frac{[AMP^{2-}][ATP^{4-}]}{[ADP^{3-}]^2}, \quad (66)$$

$$K_{10} = [ATP^{4-}][Cr]/[H^+][ADP^{3-}][PCr^{2-}]. \quad (67)$$

In these expressions,  $[H^+]$  is the hydrogen ion concentration and the superscript indicates the ionic charge. These constants in combination with constant values of the concentrations  $[H^+]$  and  $[Mg^{2+}]$  may form the following constants:

$$\kappa_t = 1 + K_1[H^+] + K_5[Mg^{2+}], \quad (68)$$

$$\kappa_d = 1 + K_2[H^+] + K_6[Mg^{2+}], \quad (69)$$

$$\kappa_m = 1 + K_3[H^+] + K_7[Mg^{2+}], \quad (70)$$

$$\kappa_c = 1 + K_4[H^+] + K_8[Mg^{2+}], \quad (71)$$

which are used to formulate the total concentrations of ATP, ADP, AMP, and PCr:

$$[ATP] = \kappa_t [ATP^{4-}], \quad (72)$$

$$[ADP] = \kappa_d [ADP^{3-}], \quad (73)$$

$$[AMP] = \kappa_m [AMP^{2-}], \quad (74)$$

$$[PCr] = \kappa_c [PCr^{2-}]. \quad (75)$$

By combining these expressions (equations 72 to 75) with equations (56) to (71), expressions were derived for each substrate as a function of  $[ATP^{4-}]$ :

$$[ATP] = \kappa_t [ATP^{4-}], \quad (76)$$

$$[ADP] = \frac{[ATP^{4-}]\varepsilon}{2K_9\kappa_m}, \quad (77)$$

$$[AMP] = \frac{[ATP^{4-}]\varepsilon^2}{4K_9\kappa_m}, \quad (78)$$

$$[PCr] = \frac{[Cr_{tot}]}{1 + \frac{K_{10}[H^+]\varepsilon'}{2K_9\kappa_c\kappa_m}} \quad (79)$$

where:

$$\varepsilon = \left( \kappa_d^2 - 4K_9\kappa_m\kappa_t + 4K_9\kappa_m \frac{[A_{tot}]}{[ATP^{4-}]} \right)^{\frac{1}{2}} - \kappa_d. \quad (80)$$

A plot of equations (77) to (79) is shown in Figure 12, in which constants and total concentrations of adenosine and creatine from Paper V are used. Although similar parameters were used, the appearance of Figure 12 is not entirely equal to the one presented in McGilvery and Murray (1974) where  $[ADP]$  at one point reaches higher than both  $[AMP]$  and  $[ATP]$ . The original M-M-S model also incorporates restrictions on the maximal propulsive force and efficiency modelling. However, these functionalities are presented in sections 4.2 and 4.3.

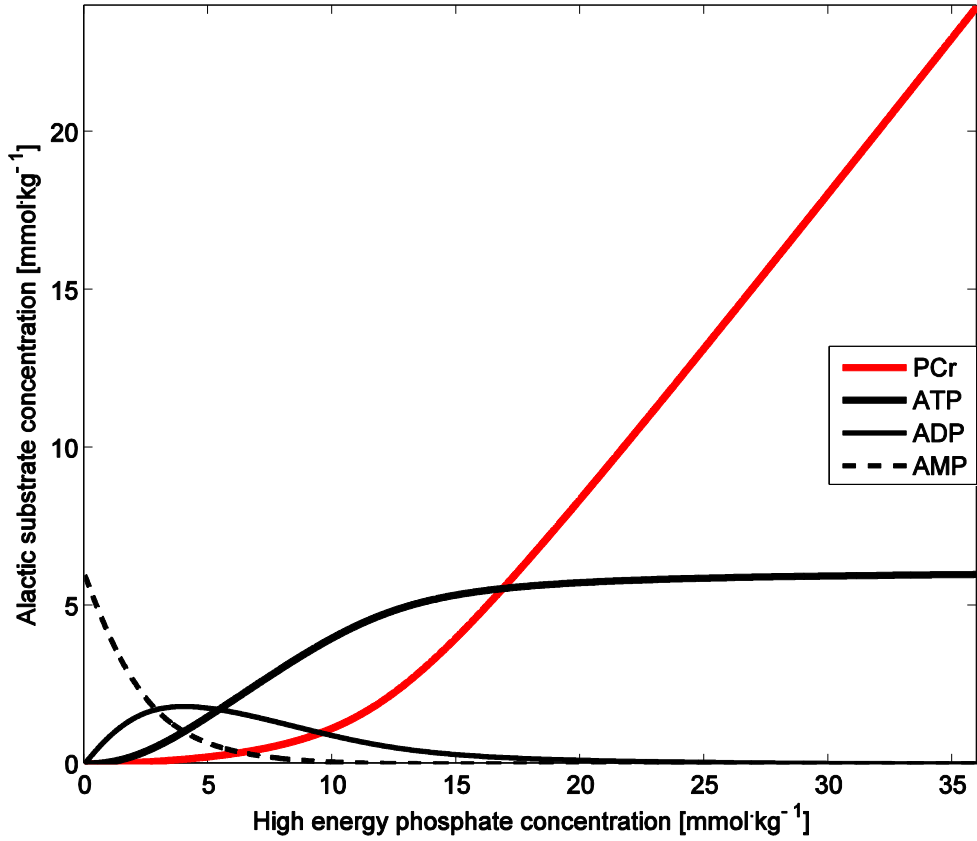


**Figure 12.** Equilibrium concentrations [PCr], [ATP], [ADP], and [AMP] as the function of total charged phosphate of all phosphagenes in muscle. The tissue has a total concentration of  $24 \text{ mmol} \cdot \text{kg}^{-1}$  of Cr and PCr, and a total concentration of  $6 \text{ mmol} \cdot \text{kg}^{-1}$  of ATP, ADP and AMP, with a pH of 7.05 and  $[\text{Mg}^{2+}]$  of  $0.5 \text{ mmol} \cdot \text{l}^{-1}$

#### 4.1.3 Fluid mechanics of hydraulic compartment models

The dynamics of a full-body hydraulic compartment model are governed by the fluid mechanical law called the Hagen-Poiseuille equation. This equation is valid for incompressible Newtonian fluids in laminar flow through long tubes with constant cross-sectional areas.

Suppose we have a hydraulic system that consists of two fluid filled compartments of constant cross-sectional area connected with a tube at the bottom. The fluid flow between compartments is then described by the following equation:

$$\Delta p = \dot{V} \frac{8\mu_{vis}L}{\pi r_t^4} \quad (81)$$

where  $\Delta p$  is the pressure difference between the ends of the tube,  $L$  is the length of the tube,  $\mu_{vis}$  is the dynamic viscosity of the fluid,  $\dot{V}$  is the volumetric flow rate and  $r_t$  is the tube radius. The assumptions of the Hagen-Poiseuille equation are that the fluid is incompressible and Newtonian, the flow is laminar through a pipe of constant circular cross-section that is substantially longer than its diameter, and there is no acceleration of fluid in the tube. The pressure difference between the ends of the pipe can be expressed as:

$$\Delta p = \left( \frac{h_1}{A_1} - \frac{h_2}{A_2} \right) \pi r_t^2 \rho_{fl} g \quad (82)$$

where  $h_1$  and  $h_2$  are the fluid heights in the first and second compartments respectively,  $A_1$  and  $A_2$  are the cross-sectional areas of the first and second compartments respectively,  $\rho_{fl}$  is the fluid density, and  $g$  is the acceleration of gravity. Substituting equation (81) into (82) gives the relationship for the volumetric flow  $\dot{V}$  as a function of the fluid level heights in the different compartments,  $h_1(t)$  and  $h_2(t)$ :

$$\dot{V} = \left( \frac{h_1(t)}{A_1} - \frac{h_2(t)}{A_2} \right) \frac{\rho_{fl} g \pi^2 r_t^6}{8 \mu_{vis} L} = \left( \frac{h_1(t)}{A_1} - \frac{h_2(t)}{A_2} \right) \frac{g \pi^2 r_t^6}{8 v_{vis} L} \quad (83)$$

where  $v_{vis}$  is the kinematic viscosity and the quotient outside of the brackets in equation (83) is constant. The direction of flow will always be from the higher level fluid compartment to the compartment with the lower fluid level (from high pressure to low pressure). If  $\dot{V}$  is positive, the flow will be from compartment 1 to compartment 2. The highest flow rate for constant compartment cross-sectional areas is achieved when the difference in level between the compartments is maximal. Hence, equation (83) may be expressed to depend on the maximal flow ( $\dot{V}$ ) through the tube:

$$\dot{V} = \dot{V}_{max} \left( \frac{h_1(t) - h_2(t)}{\Delta h_{max}} \right) \quad (84)$$

where  $\dot{V}_{max}$  is the maximal flow through the tube occurring at  $\Delta h_{max}$  which is the maximal attainable difference between  $h_1$  and  $h_2$ .



## 4.2 Efficiency

The strict mechanical definition of efficiency is the ratio between work performed and energy expended. Therefore, the relationship between power output ( $P$ ) and rate of energy expenditure ( $rEE$ ) may be expressed as:

$$P = rEE \cdot \eta_{GE} \quad (85)$$

where  $\eta_{GE}$ , by definition, is the gross efficiency. In cross-country skiing, the skier's ability to generate power output will decrease at high speeds because of the equivalent increase in muscle contraction speed, which dramatically decreases the muscle force exerted by the athlete. In BE I this is modeled by reducing the mechanical efficiency at high speeds through multiplication by the same reducing function  $\varphi$  as in equation (15), section 3.2.4 (Figure 6). Concerning efficiency,  $v_{lim}$  in equation (15) is the limit speed where the efficiency is reduced to half of  $\eta_{GE}$ . Varying mechanical efficiencies associated with different skiing techniques (classic or freestyle) and different gears (e.g. double poling and diagonal stride) (Sidossis et al., 1992, Sandbakk et al., 2010) are not considered in BE I.

In cycling, the speed at which efficiency falls is significantly higher than in cross-country skiing. This is due to the use of chain wheel gearing in cycling that effectively enables a wide range of gears even at relatively high speeds. Therefore, no decrease in efficiency was programmed in BE II to BE VI. However, in BE V and VI efficiency was modeled using a linear relationship:

$$P = (rEE - rEE_0)\eta_{PB} \quad (86)$$

where  $\eta_{PB}$  is the slope and  $rEE_0$  is the y-intercept of the physiological/biomechanical efficiency relationship.  $\eta_{PB}$  may be estimated by the delta efficiency which refers to the difference in work divided by the difference in energy expenditure between two different exercise intensities. This linear efficiency relationship is shown to adhere to the actual muscle efficiency better than a simple gross efficiency measure (Gaesser and Brooks, 1975). A graphical representation of the linear efficiency relationship is shown in Figure 13.

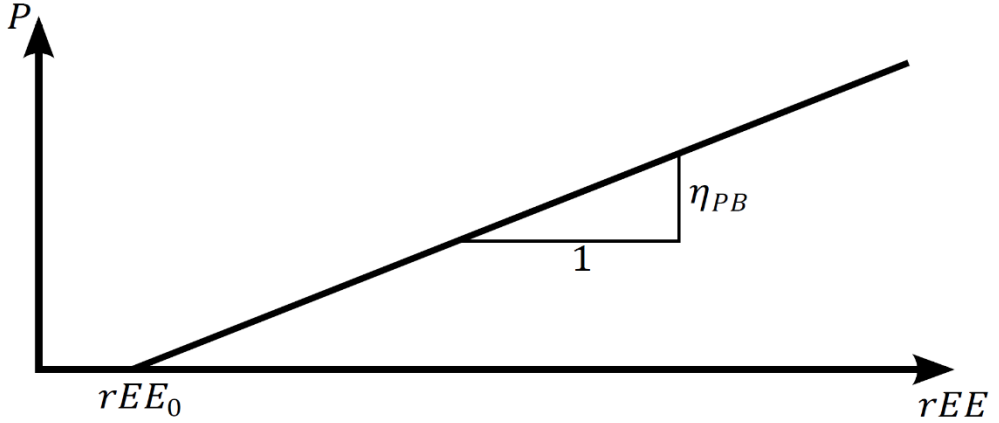


**Figure 13.** Graphic illustration of the efficiency relationship in equation (86) with the power output ( $P$ ), the rate of energy expenditure ( $rEE$ ), the  $y$ -intercept ( $rEE_0$ ), and the slope ( $\eta_{PB}$ ) of the relationship.

### 4.3 Force-velocity relationship

A muscle's ability to produce force in concentric contraction is dependent on the contraction velocity. The variation of maximal voluntary muscle contraction force with the contraction velocity may be described using the Hill equation (Hill, 1938). Assuming that the contraction velocity of the muscle is proportional to the translational speed ( $v$ ) in the initial part of a race, the Hill equation may be expressed as:

$$F_s^{max} = \left( \frac{a_1}{v+a_2} - a_3 \right) \quad (87)$$

where  $F_s^{max}$  is the maximal propulsive force, while  $a_1$ ,  $a_2$ , and  $a_3$  are constants. According to the Hill equation, the maximal propulsive power output ( $P_s^{max}$ ) also varies with speed and assumes a maximum value at a certain speed, whereas lower and higher speeds result in lower maximal power outputs (Figure 14).

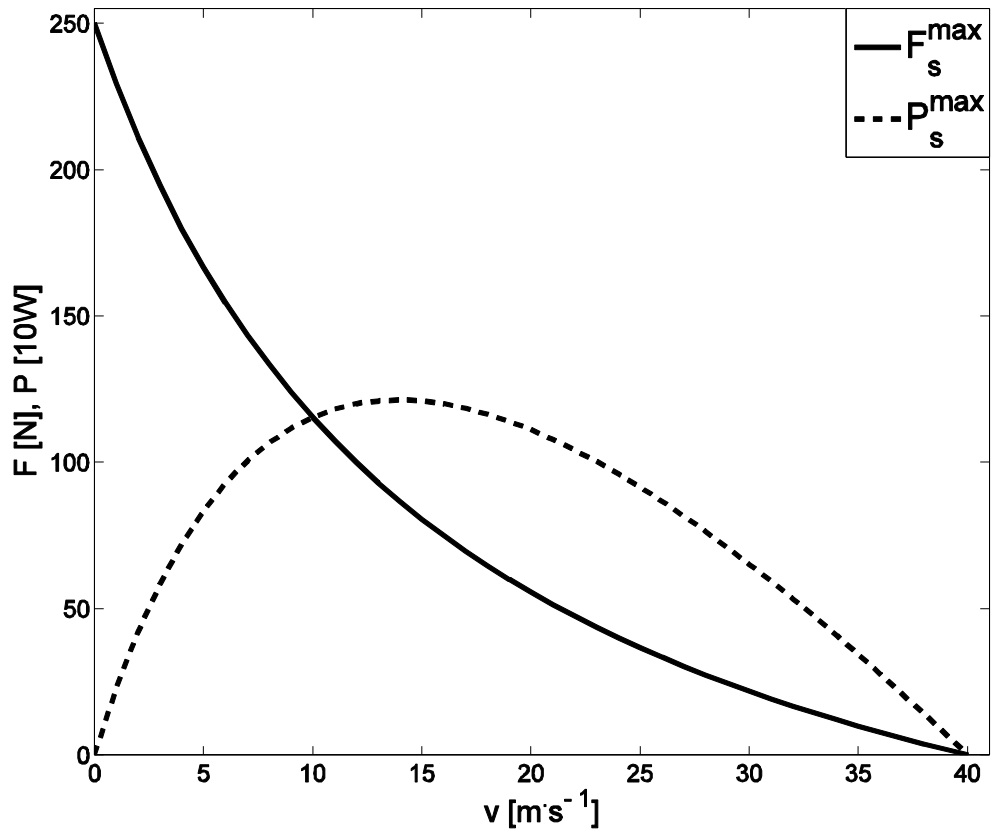


**Figure 14.** A plot of the force-velocity ( $F_s^{\text{max}}$ ) and power-velocity ( $P_s^{\text{max}}$ ) relationships expressed as the Hill equation (equation 87) with  $a_1 = 5600 \text{ kg}\cdot\text{s}^{-1}$ ,  $a_2 = 16 \text{ m}\cdot\text{s}^{-1}$ , and  $a_3 = 100 \text{ N}$ .



## 5. NUMERICAL SOLUTION OF ORDINARY DIFFERENTIAL EQUATIONS

A differential equation is an equation for an unknown function of one or several variables that relates to the values of the function itself and its derivatives. Ordinary differential equations (ODE) are differential equations containing a function of one variable and its derivatives. In many practical applications, differential equations describe a course of events (dynamics). The motion equation derived in section 3.3 describes the dynamics of an athlete's locomotion on a two-dimensional course and the systems of differential equations for an athlete's bioenergetics in section 4.1 describe the dynamics of energy flow. However, to determine the locomotion and the flow of energy explicitly, these differential equations must be solved. This may or may not be done analytically, but in most cases a numerical solution may be used which is more practical and sometimes the only way to acquire a solution. The numerical differential equation solvers often use some iterative routines for solving discrete steps in the independent variable.

For the motion equation solutions in PSO I-IV and VI, for every iteration the inverse of horizontal speed for the current position is calculated by using the step length ( $\Delta x$ ), the inverse of horizontal speed ( $\frac{dt}{dx}$ ), and the inverse of horizontal acceleration ( $\frac{d^2t}{dx^2}$ ) from the previous solution (at previous step). Furthermore, the duration of each step is calculated by the step length and the current inverse of horizontal speed. The process may be repeated for the new position, thus continuing the numerical solution. A system of two first order ODEs for the mechanics of the models presented in this thesis may be expressed as:

$$\begin{cases} \frac{d\Lambda}{dx} = \frac{d^2t}{dx^2} = f_1(x, \Lambda(x)) \\ \Lambda = \frac{dt}{dx} = f_2(x, t(x)) \\ \Lambda(x_0) = \Lambda_0 \\ t(x_0) = t_0 \end{cases} \quad (88)$$

where  $\Lambda$  is the extra variable introduced in section 3.3 to transform the second order differential equation into a system of two first order differential equations. Furthermore,  $x$  is the horizontal coordinate,  $t$  is time,  $f_1$  and  $f_2$  are the equations of motion that express the inverse of horizontal acceleration and the inverse of horizontal speed respectively (equation 30).  $x_0$ ,  $t_0$ , and  $\Lambda_0$  are the initial values of horizontal position, time, and inverse of horizontal speed.

## 5.1 The Euler method

A basic numerical method for solving an initial value ODE is the Euler method. It effectively uses an iterative process based on the finite difference approximations of the derivatives to solve the ODE. Thus we formulate these finite differences for the two coupled dependent variables:

$$\frac{d\Lambda}{dx} = f_1(x, \Lambda(x)) \approx \frac{\Lambda(x+\Delta x) - \Lambda(x)}{\Delta x}, \quad (89)$$

$$\Lambda(x) = f_2(x, t(x)) \approx \frac{t(x+\Delta x) - t(x)}{\Delta x}, \quad (90)$$

where  $\Delta x$  is the horizontal distance step. One step is easily solved with the Euler method by solving equation (90) for  $t(x + \Delta x)$ :

$$t(x + \Delta x) \approx t(x) + \Delta x \cdot f_2(x, t(x)). \quad (91)$$

However, to be able to solve the next step we also need to solve equation (89) for  $\Lambda(x + \Delta x)$ :

$$\Lambda(x + \Delta x) = f_1(x + \Delta x, t(x + \Delta x)) \approx \Lambda(x) + \Delta x \cdot f_1(x, \Lambda(x)). \quad (92)$$

## 5.2 The 4<sup>th</sup> order Runge-Kutta method

A method for solving ODEs that is more accurate than the Euler method is the 4<sup>th</sup> order Runge-Kutta method (R-K 4) (Kutta, 1901), which was used in PSO III and IV to solve the motion equation. Due to the formulation of the constraints (section 6.1.2) in PSO III and IV using linear regression, constant distance steps were required, which makes the R-K 4 a suitable solver with small errors. For the R-K 4, equation (91) may be rewritten as:

$$t(x + \Delta x) \approx t(x) + \frac{\Delta x}{6} (k_1 + 2k_2 + 2k_3 + k_4), \quad (93)$$

where the coefficients are expressed as:

$$k_1 = f_2(x, t(x)), \quad (94)$$

$$k_2 = f_2\left(x + \frac{\Delta x}{2}, t(x) + \frac{\Delta x}{2} k_1\right), \quad (95)$$

$$k_3 = f_2\left(x + \frac{\Delta x}{2}, t(x) + \frac{\Delta x}{2} k_2\right), \quad (96)$$

$$k_4 = f_2(x + \Delta x, t(x) + \Delta x \cdot k_3). \quad (97)$$

The corresponding term for the inverse horizontal speed (equation 92) is also reformulated according to equation (93).

### 5.3 The Runge-Kutta-Fehlberg method

An even more sophisticated method than the 4<sup>th</sup> order Runge-Kutta method is the Runge-Kutta-Fehlberg method (R-K-F) (Fehlberg, 1969). This method was used for solving the motion equations in PSO I, II, and VI and is a combination of 4<sup>th</sup> and 5<sup>th</sup> order Runge-Kutta formulas. At the cost of only one additional computation, the R-K-F can estimate the computation error, therefore allowing corrections in the step size ( $\Delta x$ ) that adapts to keep the error small. Therefore, R-K-F may have higher accuracy than the R-K 4 solver if step size is properly constrained. Equation (91) in the Euler method may be exchanged for the following two estimates:

$$t_4(x + \Delta x) \approx t(x) + \Delta x \left( \frac{25}{216} k_1 + \frac{1408}{2565} k_3 + \frac{2197}{4104} k_4 - \frac{1}{5} k_5 \right), \quad (98)$$

$$t_5(x + \Delta x) \approx t(x) + \Delta x \left( \frac{16}{135} k_1 + \frac{6656}{12825} k_3 + \frac{28561}{56430} k_4 - \frac{9}{50} k_5 + \frac{2}{55} k_6 \right), \quad (99)$$

where  $t_4$  and  $t_5$  are the 4<sup>th</sup> and 5<sup>th</sup> order estimates of the time in each step, and the coefficients in these formulas are expressed as:

$$k_1 = f_2(x, t(x)), \quad (100)$$

$$k_2 = f_2\left(x + \frac{\Delta x}{4}, t(x) + \frac{\Delta x}{4} k_1\right), \quad (101)$$

$$k_3 = f_2\left(x + \frac{3\Delta x}{8}, t(x) + \frac{\Delta x}{32}(3 \cdot k_1 + 9 \cdot k_2)\right), \quad (102)$$

$$k_4 = f_2\left(x + \frac{12}{13}\Delta x, t(x) + \frac{\Delta x}{2197}(1932 \cdot k_1 - 7200 \cdot k_2 + 7296 \cdot k_3)\right), \quad (103)$$

$$k_5 = f_2\left(x + \Delta x, t(x) + \Delta x \left( \frac{439}{216} \cdot k_1 - 8 \cdot k_2 + \frac{3680}{513} \cdot k_3 - \frac{845}{4104} \cdot k_4 \right)\right), \quad (104)$$

$$k_6 = f_2\left(x + \Delta x, t(x) + \Delta x \left( -\frac{2^3}{3^3} \cdot k_1 + 2 \cdot k_2 - \frac{3544}{2565} \cdot k_3 + \frac{1859}{4104} \cdot k_4 - \frac{11}{40} \cdot k_5 \right)\right). \quad (105)$$

The error of the 4<sup>th</sup> order formula in the R-K-F method which is in the order of  $O(\Delta x^5)$ , can be estimated by comparing the solution to the more accurate 5<sup>th</sup> order solution. The estimated error is expressed as:

$$Er_t = |t_5(x + \Delta x) - t_4(x + \Delta x)| = \Delta x \left| \frac{1}{360} \cdot k_1 - \frac{128}{4275} \cdot k_3 - \frac{2197}{75240} \cdot k_4 + \frac{1}{50} \cdot k_5 + \frac{2}{55} \cdot k_6 \right|. \quad (106)$$

Of course, equation (92) in the Euler method may as well be reformulated according to R-K-F (equations 98 and 99).



## 6. OPTIMIZATION

Optimization is all about finding the best solution possible in a predetermined set of circumstances. The field of optimization research grew in the 1960s, along with advances in the area of transistor-based computers, which enabled high speed numerical computing. Optimization methods can be applied to almost every kind of engineering problem; even the field of economics assimilates the benefits of optimization. Mathematical optimization can be divided into analytical and numerical optimization. Analytical optimization (section 6.2.1) is constrained to simpler problems, while numerical optimization (section 6.2.2) can be applied to a much broader range of problems.

In this thesis the term optimal is not interpreted as an absolute, but rather a relative term. The optimal solution is the best solution given by an optimization method under certain conditions and optimization assumptions including convergence criteria. Therefore, there may be better solutions to the pacing strategy optimization problems than the optimal solutions presented in this thesis. For reasons of simplicity, the variables and function denotations in this chapter will differ from the terms listed in the abbreviations section of this thesis.

### 6.1 Formulation of a general optimization problem

An optimization problem is generally formulated to minimize a certain quantity given a defined domain. The domain may be defined by variables ( $\mathbf{x}$ ) and their domain as well as various constraints. Mathematically, a general constrained optimization problem may be formulated as:

$$\begin{array}{ll} \text{Minimize} & f(\mathbf{x}) \\ \text{Subject to} & \mathbf{h}(\mathbf{x}) = 0 \\ & \mathbf{g}(\mathbf{x}) \leq 0 \end{array} \quad (107)$$

where  $\mathbf{x}$  is a vector of optimization variables,  $f(\mathbf{x})$  is the objective function, while  $\mathbf{h}(\mathbf{x})$  and  $\mathbf{g}(\mathbf{x})$  are vectors with equality and inequality constraints respectively. Problems that do not contain any constraints are called unconstrained problems. Many optimization problems have the same fundamental structure and can therefore be solved with various optimization methods.

#### 6.1.1 Optimization variables

In order to optimize an objective function, some parameters inherent in such function must be allowed to change. These parameters are usually called

optimization variables to the problem and the number of variables must be finite. In many applications, optimization variables are allowed to attain continuous values within a specified range of variation.

### 6.1.2 Constraints

A set of optimization variables results in a measure of the objective function. However, not all sets of variables are practically possible. Hence, constraints are introduced to restrict the optimization variables. Constraints that only restrict the domain of the optimization variable are most commonly named geometrical or side constraints and constraints that limit the performance or behavior of the system are named functional or behavioral constraints. All constraints must be functions of the optimization variables to have an effect on the problem. A set of variables is termed a feasible solution if it lies within the defined domain of the system, with all constraints satisfied. Moreover, a set of variables that does not satisfy the constraints is termed an infeasible solution. If a variable set directly touches a constraint, this constraint is termed active. Most optimal solutions are located where two or more constraints are simultaneously active.

Considering a hypothetical optimization problem with two variables ( $\mathbf{x} = [x_1, x_2]$ ) and four inequality constraints ( $\mathbf{g}(\mathbf{x}) \leq 0$ ), the domain of the system can be divided into feasible and infeasible regions (Figure 15).

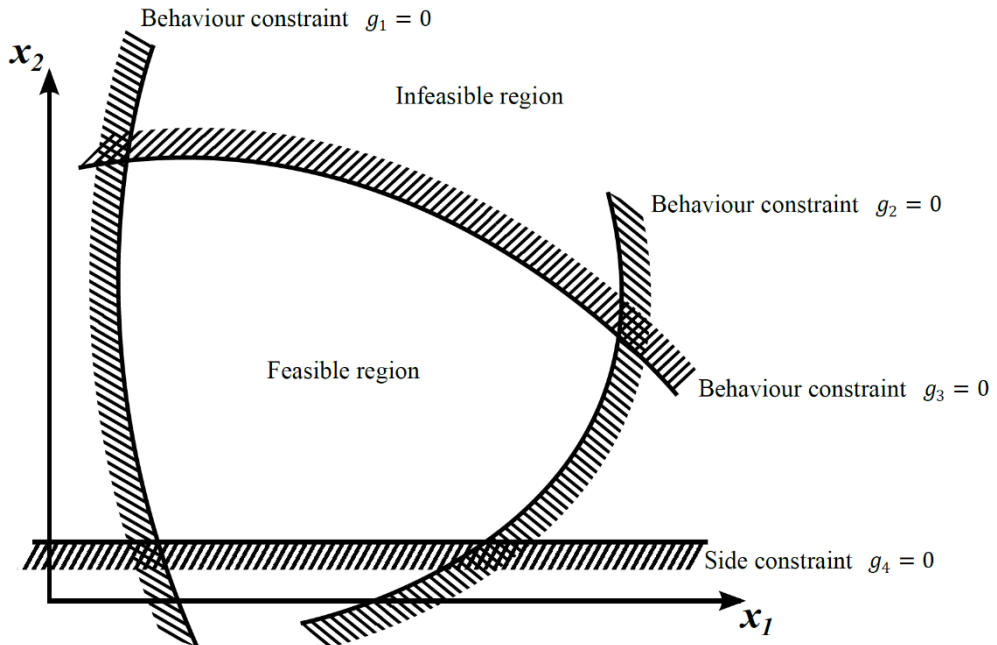


**Figure 15.** Inequality constraints plotted onto the surface of two variables.

### 6.1.3 Objective function

Among the sets of variables that satisfy all constraints there may be sets that are better than others. To evaluate which variable set is the best one, an objective function is formulated as a function of the optimization variables. The objective function (which sometimes is termed cost function) describes the quantity to be optimized. In the majority of optimization problems, the objective function is set to be minimized. However, in some cases the purpose of the optimization is to maximize a function. Instead of reformulating the mathematics of optimization for maximization, the problem may be reformulated as a minimization of the negative equivalent of the original objective function.

By adding an objective function into the constraints set illustrated by Figure 15, the optimization problem may be presented as depicted in Figure 16. Now the objective function contours increase in the same order as the subscript numerals, such that  $f_6 > f_5 > f_4 > f_3 > f_2 > f_1$ . The optimal solution to this optimization problem is available at  $\mathbf{x} = \mathbf{x}^*$

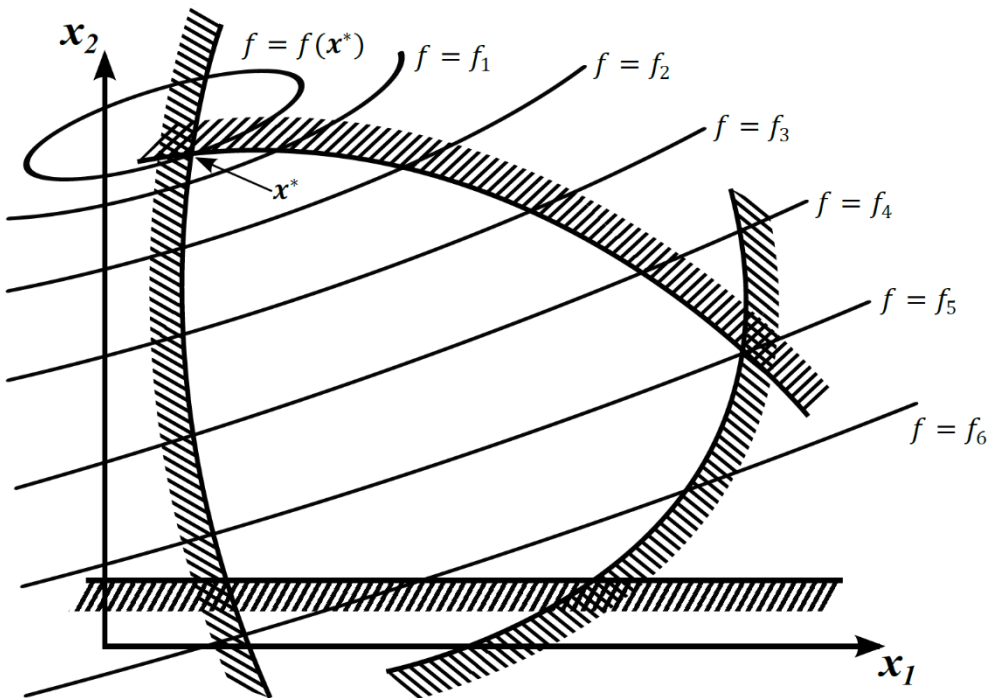


**Figure 16.** Objective function contours plotted together with the constraints.

## 6.2 Solving an optimization problem

### 6.2.1 Analytical optimization

The most fundamental optimization example is to find the minimum of an ordinary analytical function without constraints. If it is possible to analytically differentiate the function, the solution is easy to find. For problems where there is more than one variable and non-linear constraints are considered, the solution is not that obvious. For such a problem, it is a good idea to use the method of Lagrange multipliers. Consider an optimization problem with only inequality constraints:

$$\begin{array}{ll} \text{Minimize} & f(\mathbf{x}) \\ \text{Subject to} & \mathbf{g}(\mathbf{x}) \leq \mathbf{0} \end{array} \quad (108)$$

With the use of the Lagrange multiplier vector  $\boldsymbol{\lambda} = (\lambda_1, \lambda_2, \dots, \lambda_p)$ , the Lagrangian function can be expressed as:

$$L(\mathbf{x}, \boldsymbol{\lambda}) = f(\mathbf{x}) + \boldsymbol{\lambda} \cdot \mathbf{g}(\mathbf{x}) \quad (109)$$

It can be shown that a stationary point of equation (109) can be the solution of equation (108). The gradient of the Lagrangian function, along with some other conditions, creates the first order necessary conditions also called Karush-Kuhn-Tucker conditions for an inequality constrained problem:

$$\nabla f(\mathbf{x}) + \boldsymbol{\lambda} \cdot \nabla \mathbf{g}(\mathbf{x}) = \mathbf{0} \quad (110)$$

$$\boldsymbol{\lambda} \cdot \mathbf{g}(\mathbf{x}) = 0 \quad (111)$$

$$\mathbf{g}(\mathbf{x}) \leq \mathbf{0}, \boldsymbol{\lambda} \geq \mathbf{0} \quad (112)$$

By rewriting equation (110) as  $\nabla f(\mathbf{x}) = -\boldsymbol{\lambda} \cdot \nabla \mathbf{g}(\mathbf{x})$ , one can see that the gradient of the objective function must be a linear combination of the active constraints' gradients (Figure 17).

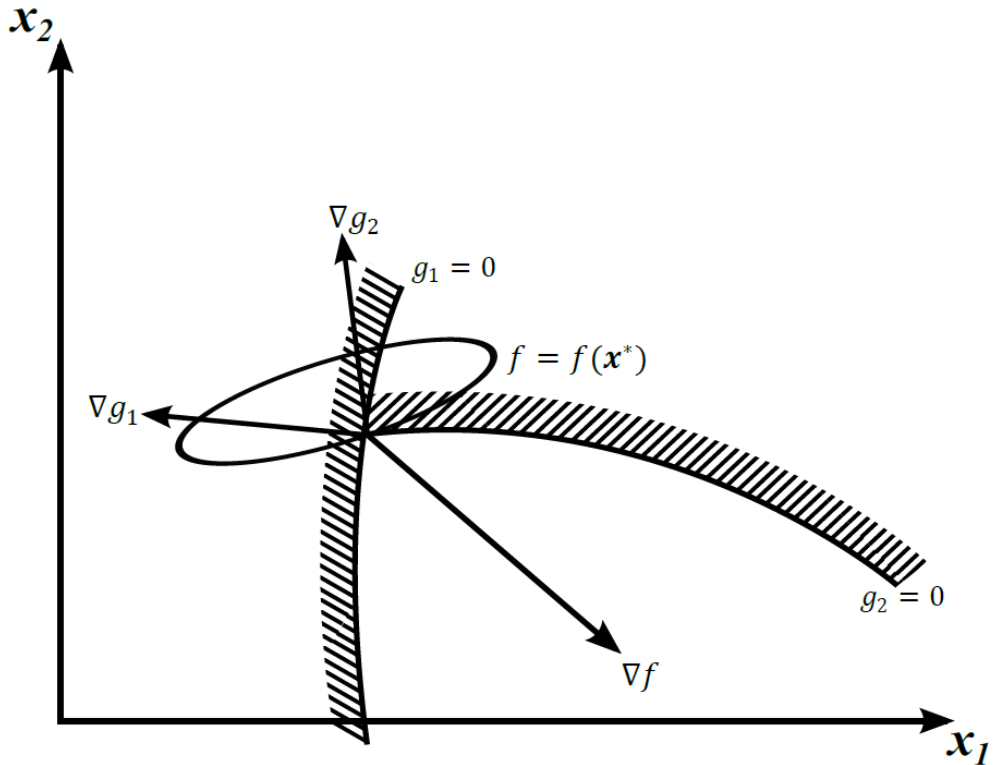


**Figure 17.** Geometrical representation of the Karush-Kuhn-Tucker conditions including the gradients of the objective function and two active inequality constraints at the optimal solution.

An alternative formulation of the Karush-Kuhn-Tucker conditions may be used for problems that also have to obey equality constraints. However, these analytical optimization methods are generally ineffective when functions are strongly nonlinear, or the number of variables or constraints is too high. Furthermore, many engineering applications are unable to create the objective function and/or the constraints in explicit form. These objective functions and constraints are perhaps only available by numerical simulation and therefore require numerical optimization routines to be applied.

### 6.2.2 Numerical optimization

There are various numerical optimization routines that can estimate the optimal solution with good accuracy. These methods are generally depending on iterative numerical computations ultimately leading to a minimum. Optimization methods may be categorized into gradient based methods and non-gradient based methods. Gradient based methods compute the gradients of the objective function and the

constraints to find the direction of improvement and therefore better estimate an improved solution in each iteration. Gradient based methods are favorable for problems that are continuously differentiable. On the other hand, non-gradient based methods are favorable when gradients are unattainable, as these methods only make use of function evaluations. A general description of a gradient based numerical optimization routine can be expressed as:

- Step I. Guess initial set of variables  $\mathbf{x}^{(0)}$  and calculate the solution.
- Step II. For  $k = 0, 1, \dots, N$   
If  $\mathbf{x}^{(k)}$  is optimal, stop.
- Step III. Calculate an improved estimate of the solution  
 $\mathbf{x}^{(k+1)} = \mathbf{x}^{(k)} + \alpha_k \cdot \mathbf{d}^{(k)}$ .
- Step IV. Repeat from Step II.

Here,  $\mathbf{d}^{(k)}$  is the search direction and  $\alpha_k$  is the step length in that direction. Usually, the optimality is determined by some kind of convergence criterion. A convergence criterion may be formulated as an inequality, where the norm of the step size vector or the relative step size decrement in each iteration must be lower than preset minimum values. Another convergence criterion defines how the relative objective function improvement must be lower than a threshold value. When the convergence criterion is satisfied, the optimization will stop and the best feasible solution (lowest objective function) is termed optimal.

However, for some problems it is hard to create an adequate convergence criterion if, for instance, the solution is not gradually decreasing between every iteration. Furthermore, the decrease of the solution or the step-size decrease may fluctuate even between iterations of gradual decreasing objective function. One alternative formulation is therefore to program the model to compute a predetermined number of iterations  $N$  and let the best solution out of these iterations be the optimal one.

Even if a convergence criterion is used and the solution converges to a stationary solution, it cannot be put beyond doubt that the provided optimal solution represents nothing but a local minimum. A local minimum is a minimum lower than the nearby variable sets in the feasible region, yet higher than the true global minimum. Numerical gradient based optimization methods are incapable of distinguishing a local minimum from a global minimum and therefore the only way to be certain of the nature of the attained optimal solution is to use multiple starting values of the optimization variables. Even this method leaves room for uncertainty, but at least it reduces the risk of mistaking a local minimum for a global minimum. Some non-gradient based optimization methods, also called global optimization

methods are more reliable in distinguishing between local and global minima. However, they are usually not suitable for complex implicit simulation programs such as the ones presented in section 3 and 4. Global optimization methods usually require more function evaluations to be performed in order to attain the optimal solution however better suited for non-continuous functions.

### 6.2.3 Approximated sub-problems

There are numerical methods for constrained gradient-based optimization that use approximated sub-problems  $\tilde{P}$  to estimate the real problem  $P$ . The sub-problems are created between Step II and Step III in the algorithm in the previous section. The approximations are obtained through linear Taylor series expansions for the objective function and constraints (termed  $\tilde{f}(\mathbf{x})$  and  $\tilde{\mathbf{g}}(\mathbf{x})$ ). The problem in equation (108) can be approximated with the following linearized sub-problem ( $\tilde{P}^{(k)}$ ) using Taylor expansion around  $\mathbf{x}^{(k)}$ :

$$\begin{aligned} \tilde{P}^{(k)}: & \\ \text{Minimize} \quad & \tilde{f}(\mathbf{x}) = f(\mathbf{x}^{(k)}) + \nabla f(\mathbf{x}^{(k)}) \cdot (\mathbf{x} - \mathbf{x}^{(k)}) \\ \text{Subject to} \quad & \tilde{\mathbf{g}}(\mathbf{x}) = \mathbf{g}(\mathbf{x}^{(k)}) + \nabla \mathbf{g}(\mathbf{x}^{(k)}) \cdot (\mathbf{x} - \mathbf{x}^{(k)}) \leq \mathbf{0} \end{aligned} \tag{113}$$

The above problem (equation 113) can easily be solved with linear programming methods such as the Simplex method. The original problem in equation (108) is solved as a sequence of linearized sub-problems, where the linearization is carried out for every iteration. However, the change of the optimization variables may not be too large, as the Taylor expansion is only valid in the vicinity of the original point of linearization. Hence, a concept called move limits is utilized. These limits are set to constrain the change of the design within each iteration and the limits are usually adjusted between iterations. The move limits may be expressed as:

$$\underline{\mathbf{x}} \leq \mathbf{x} \leq \bar{\mathbf{x}} \tag{114}$$

where  $\underline{\mathbf{x}}$  is the lower limit of the optimization variables  $\mathbf{x}$  and  $\bar{\mathbf{x}}$  is the upper limit.

### 6.2.4 Method of moving asymptotes

The method of moving asymptotes (MMA) (Svanberg, 1987, Svanberg, 1993) is based on approximated sub-problems. However, the approximated objective function  $\tilde{f}(\mathbf{x})$  and the constraints  $\tilde{\mathbf{g}}(\mathbf{x})$  of MMA are obtained through linearization in variables of the type  $1/(x_j - l_j)$  and  $1/(u_j - x_j)$ , where  $l_j$  and  $u_j$  are the lower and upper asymptotes of  $x_j$ , thus  $l_j \leq x_j \leq u_j$ . Consequently, the approximated MMA sub-problem  $\tilde{P}^{(k)}$  can be expressed as:

$$\tilde{p}^{(k)}; \quad (115)$$

Minimize

$$\tilde{f}^{(k)}(\mathbf{x}) = f(\mathbf{x}^{(k)}) + \sum_{j=1}^J \left[ \left( \frac{p_{0j}^{(k)}}{u_j^{(k)} - x_j} + \frac{q_{0j}^{(k)}}{x_j - l_j^{(k)}} \right) - \left( \frac{p_{0j}^{(k)}}{u_j^{(k)} - x_j^{(k)}} + \frac{q_{0j}^{(k)}}{x_j^{(k)} - l_j^{(k)}} \right) \right]$$

Subject to

$$\tilde{g}_i^{(k)}(\mathbf{x}) = g_i(\mathbf{x}^{(k)}) + \sum_{j=1}^J \left[ \left( \frac{p_{ij}^{(k)}}{u_j^{(k)} - x_j} + \frac{q_{ij}^{(k)}}{x_j - l_j^{(k)}} \right) - \left( \frac{p_{ij}^{(k)}}{u_j^{(k)} - x_j^{(k)}} + \frac{q_{ij}^{(k)}}{x_j^{(k)} - l_j^{(k)}} \right) \right] \leq 0$$

$$\text{If } \frac{\partial f}{\partial x_j} > 0 \text{ then } p_{0j}^{(k)} = (u_j^{(k)} - x_j^{(k)})^2 \cdot \frac{\partial f}{\partial x_j} \text{ and } q_{0j}^{(k)} = 0$$

$$\text{If } \frac{\partial g_i}{\partial x_j} > 0 \text{ then } p_{ij}^{(k)} = (u_j^{(k)} - x_j^{(k)})^2 \cdot \frac{\partial g_i}{\partial x_j} \text{ and } q_{ij}^{(k)} = 0$$

$$\text{If } \frac{\partial f}{\partial x_j} < 0 \text{ then } p_{0j}^{(k)} = 0 \text{ and } q_{0j}^{(k)} = -(x_j^{(k)} - l_j^{(k)})^2 \cdot \frac{\partial f}{\partial x_j}$$

$$\text{If } \frac{\partial g_i}{\partial x_j} < 0 \text{ then } p_{ij}^{(k)} = 0 \text{ and } q_{ij}^{(k)} = -(x_j^{(k)} - l_j^{(k)})^2 \cdot \frac{\partial g_i}{\partial x_j}$$

$$\text{If } \frac{\partial f}{\partial x_j} = 0 \text{ then } p_{0j}^{(k)} = 0 \text{ and } q_{0j}^{(k)} = 0$$

$$\text{If } \frac{\partial g_i}{\partial x_j} = 0 \text{ then } p_{ij}^{(k)} = 0 \text{ and } q_{ij}^{(k)} = 0$$

where  $j = 1, \dots, J$  (number of variables),  $i = 1, \dots, I$  (number of constraints) and all derivatives  $\frac{\partial f}{\partial x_j}$  and  $\frac{\partial g_i}{\partial x_j}$  are evaluated at  $\mathbf{x}^{(k)}$ .



## 7. THE PACING STRATEGY OPTIMIZATION PROBLEM

### 7.1 Formulation of the optimization problem

Pacing strategy optimization is the matter of finding the optimal way of varying speed in locomotion. Moreover, pacing strategy optimization in endurance sports is generally applied to optimize performance, which may be expressed in terms of finishing time. This formulation requires a specified course profile and many other parameters to be solvable. In mathematical terms, the objective function is the time duration between start and finish. This is calculated by the solution of the motion equation. Moreover, certain restrictions must apply so that the solution does not exceed reasonable limits. These restrictions are formulated as mathematical constraints dependent on quantities in the bioenergetic model and motion equation solutions.

#### 7.1.1 Objective function

The objective function in all PSO models is formulated as:

$$T = \sum_{i=1}^K \Delta t_i \quad (116)$$

where  $T$  is the total time between start and finish,  $K$  is the total number of discrete distance steps, and  $\Delta t_i$  is the time corresponding to each distance step in the motion equation solution.

#### 7.1.2 Constraints

The constraints for each pacing strategy optimization model are formulated as:

**PSO I:**

$$\frac{1}{2T} \sum_{i=1}^{K-1} (P_i + P_{i+1}) \Delta t_k \leq \bar{P}, \quad (117)$$

$$P_{min} \leq P_j \leq P_{max}, \quad j = 1, \dots, J \quad (118)$$

where  $P_i$  and  $P_{i+1}$  are the magnitudes of power output at steps  $i$  and  $i + 1$  respectively. These values are available through linear interpolation of the optimization variables.  $\bar{P}$  is the preset maximal average power output limit,  $P_{min}$  and  $P_{max}$  are the preset minimal and maximal power output limits respectively, and  $J$  is the total number of optimization variables. PSO I also included a constant power simulation to evaluate the effect of the optimal pacing strategy.

**PSO II:**

$$0 \leq h_q \leq 1, \quad q = 1, \dots, J + Q \quad (119)$$

$$P_{min} \leq P_j \leq P_{max}, \quad j = 1, \dots, J \quad (120)$$

where  $h_q$  is the variable determining the available anaerobic work in the C PIE model and  $Q$  is the number of intersections between the critical power and the linear interpolation of the optimization variables. PSO II also included a constant power simulation to evaluate the effect of the optimal pacing strategy.

### PSO III, BE III a:

There was no optimization involved in the PSO III, BE III a. Therefore, only a constant power output simulation (with the same average power as PSO III, BE III b) was performed, and compared to the following bioenergetic models.

### PSO III, BE III b:

Same as in PSO II.

### PSO III, BE III c:

$$0 \leq h_i < 1, \quad i = 1, \dots, K \quad (121)$$

$$0 \leq l_i < 1 - \theta - \lambda, \quad i = 1, \dots, K \quad (122)$$

$$P_{min} \leq P_i \leq P_{m_i}, \quad i = 1, \dots, K \quad (123)$$

where  $h_i$  and  $l_i$  are the variables determining the available alactic and lactic energies respectively and  $P_{m_i}$  is the maximal instant power output limit in the M-M model.

### PSO IV:

$$0 \leq h_i < 1, \quad i = 1, \dots, K \quad (124)$$

$$0 \leq l_i < 1 - \theta - \lambda, \quad i = 1, \dots, K \quad (125)$$

$$P_{min} \leq P_i \leq P_{m_i}, \quad i = 1, \dots, K \quad (126)$$

$$0 \leq v_i \leq v_{max_i}, \quad i = 1, \dots, K \quad (127)$$

where  $v_i$  is the translational speed in the direction of travel and speed and  $v_{max_i}$  is the maximal instant speed limit due to static grip friction.

**PSO VI, BE VI a:**

$$0 \leq c_d < 1 - \phi, \quad d = 1, \dots, D \quad (128)$$

$$0 \leq h_d < 1 - \xi, \quad d = 1, \dots, D \quad (129)$$

$$0 \leq l_d < 1 - \theta - \lambda, \quad d = 1, \dots, D \quad (130)$$

$$rEE_0 \leq rEE_d \leq rEE_{mf}^{max}, \quad d = 1, \dots, D \quad (131)$$

where  $c_d$ ,  $h_d$ , and  $l_d$  are the variables determining the available carbohydrate, alactic, and lactic energies respectively,  $rEE_0$  is the minimal or resting rate of energy expenditure,  $rEE_{mf}^{max}$  is the maximal instant power output of the M-M-S model and  $D$  is the number of equally spaced  $x$ -coordinates where the constraints were evaluated.

**PSO VI, BE VI b:**

BE VI b was also constrained by equations (128-131) in combination with the following maximal propulsive force constraint:

$$0 \leq F_{s_d} \leq F_s^{max}, \quad d = 1, \dots, D \quad (132)$$

where  $F_s^{max}$  is the maximal instant propulsive force.

## 7.2 Numerical implementation

All numerical expressions of every model presented in this thesis were implemented using the MATLAB® software and executed on a personal computer. Where possible, generic MATLAB® functions were utilized to simplify the source code. Due to copyright restrictions, no source code of the models presented in this thesis is publicly available, although research cooperation may be an exception. Depending on the parameter settings, large differences in computation times were obtained. Without going into detail and describing a thorough investigation on the sensitivity of various parameters' impact on the calculation time, general correlations can be identified by the comprehensive simulation work that has been performed. Some of the factors that have a major effect on the computation time are: the number of

optimization variables, course length, accuracy of the differential equation solvers for motion equation and bioenergetic model, distance between lower and upper asymptotes (section 6.2.4), and number of perturbations used in the numerical gradient calculation method.

Previous experience has shown that similar optimization problems are successfully solved using MMA. Therefore, all models for the optimization of pacing strategies (PSO I-IV and VII) in this thesis use MMA (section 6.2.4) to optimize the pacing strategy. Other optimization routines embedded in the MATLAB® Optimization Toolbox™ and Global Optimization Toolbox, such as the interior point method, the sequential quadratic programming method, and the generalized pattern search method were also tested but without success.

The partial derivatives building up the gradients of the objective function ( $\nabla T$ ), as well as the constraints ( $\nabla g$ ), are calculated numerically using either the forward difference approximation (PSO I and II) or the five-point stencil (PSO III, IV, and VI). The forward difference approximation for the objective function in pacing strategy optimization is expressed as:

$$\frac{dT}{dP_j} \approx \frac{T(P_j + \Delta P_j) - T(P_j)}{\Delta P_j}, \quad j = 1, \dots, J \quad (133)$$

where  $\Delta P_j$  is the variable perturbation. The five-point stencil for the first derivative is formulated as:

$$\frac{dT}{dP_j} \approx \frac{-T(P_j + 2\Delta P_j) + 8T(P_j + \Delta P_j) - 8T(P_j - \Delta P_j) + T(P_j - 2\Delta P_j)}{12\Delta P_j}, \quad j = 1, \dots, J. \quad (134)$$

The five-point stencil approximates the derivative more accurately but needs about four times the computation time of the forward difference approximation due to three additional computations for every optimization variable ( $T(P_j + 2\Delta P_j)$ ,  $T(P_j + \Delta P_j)$ ,  $T(P_j - \Delta P_j)$ ,  $T(P_j - 2\Delta P_j)$ ). A schematic description of the optimization process for pacing strategies is illustrated in Figure 18. The change in variables proposed by MMA is  $\mathbf{P}_{imp}$  and  $\mathbf{P}_{opt}$  for the improved and optimum solutions, respectively. The initial estimate of the variable values is set to  $\mathbf{P}_{ini}$  (Figure 18). For most of the calculations presented in this thesis  $\mathbf{P}_{ini}$  is set to a constant valued distribution within the feasible domain of the optimization problem. However, in PSO IV,  $\mathbf{P}_{ini}$  is not feasible in the course bend calculations due to the constraint in equation (127). The magnitude of the constant valued  $\mathbf{P}_{ini}$  is chosen with respect to the athlete's physiological ability and the nature of the course and ambient circumstances. The final solution termed the optimal pacing strategy or optimal power distribution

( $P_{opt}$ ) is the best feasible solution among all suggested solutions in the optimization iterations.

Initial power distribution

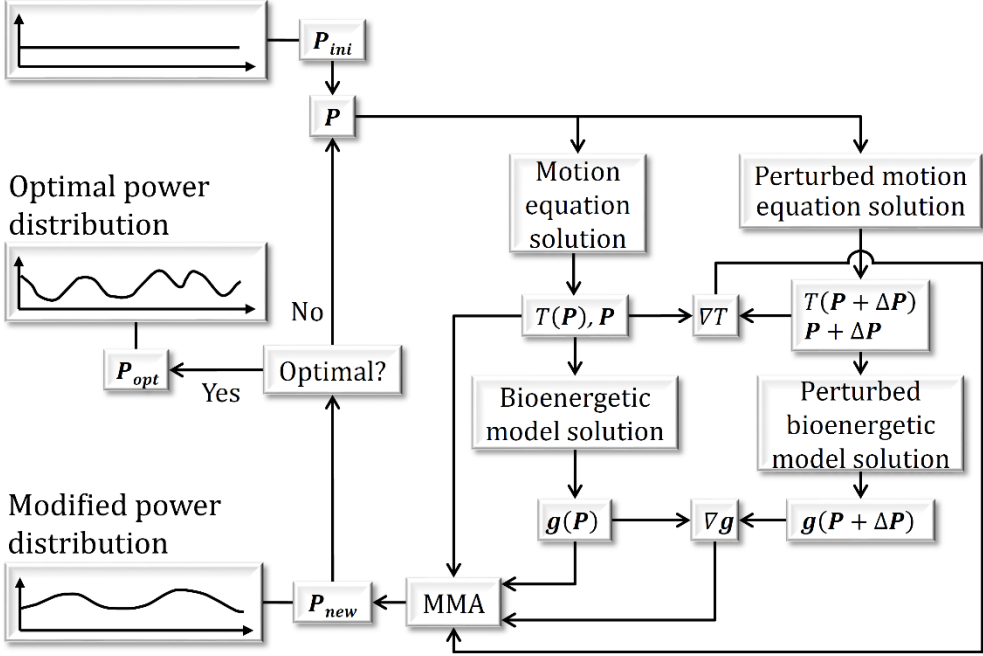


**Figure 18.** Flow chart of the pacing strategy optimization problem where finishing time  $T$  is the objective function, the power output  $P$  is the vector of optimization variables and  $g$  is the vector of constraints from the bioenergetic model.  $P_{ini}$ ,  $P_{new}$ , and  $P_{opt}$  are the initial, improved and optimal vectors of optimization variables (power distributions).

### 7.3 Model uncertainty and sensitivity

No uncertainty analyses were conducted for any of the models presented in this thesis. Furthermore, no extensive sensitivity analyses were performed regarding the parameters associated with the pacing strategy optimization models discussed in this thesis. However, due to the formulation of these models, some general conclusions can be drawn regarding their sensitivity. In this analysis it is essential that both the absolute magnitude of each parameter is considered, as well as the potential of that parameter's variation. Firstly, considering the expressions for the motion equation (e.g. equation 30) and the bioenergetic model (e.g. equations 45-80) and its restrictions (e.g. equations 128-132) in PSO VI, it can easily be concluded that some parameters have a great effect on the finishing time. The drag area of the

athlete may vary within a reasonably broad range and affects the aerodynamic drag force that assumes significant magnitudes at regular speeds, restricting speed and thereby performance. For the same reason, ambient winds may have a great effect on performance. Furthermore, the gravitational force is always of a constant magnitude, but will only affect the athlete's locomotion during uphill and downhill sections (i.e. during nonzero course gradients). These gradients may vary only slightly, but nonetheless significantly affect performance due to the high magnitude of the gravitational force.

The full model's sensitivity to the bioenergetic model's parameters is largely dependent on exercise duration. In the M-M-S model (section 4.1.4) for instance, the carbohydrate store, the maximal rate of oxidative phosphorylation, and the maximal rate of fat oxidation greatly influence performance in prolonged exercise. However, in short duration exercise, performance relies more on the anaerobic energy supplying systems. Therefore, performance in short duration exercise is more sensitive to changes in the energy of the lactic and alactic stores, and the maximal rate of energy expenditure and the rate of lactic energy conversion. Intermittent exercise may result from varying terrain or other ambient conditions and is characterized by recurring periods of high and low power outputs. The parameter that limits the replenishment of lactic energy is more sensitive to changes in intermittent exercise than to all-out exercise or exercise on flat and straight courses with a constant wind velocity. Furthermore, the anaerobic capacities in the alactic and lactic compartment also influence performance more in intermittent exercise than in steady power output exercise.

## 8. SUMMARY AND MAIN RESULTS

### 8.1 Effect of hills on optimal pacing in cross-country skiing

In Paper I, the pacing strategy was optimized for a cross-country skier travelling a sprint course of 1425 m. The optimal pacing strategy with the corresponding power distribution was compared to a simulation using constant power that was equal to the average power in the optimal pacing strategy. The optimization was run for 20 iterations which resulted in a finishing time of 187.4 s that was 6.5% faster than the constant power simulation. The optimal power distribution showed great variability in parallel with course gradient. The optimal power distribution and the corresponding pacing strategy are illustrated in Figure 19.

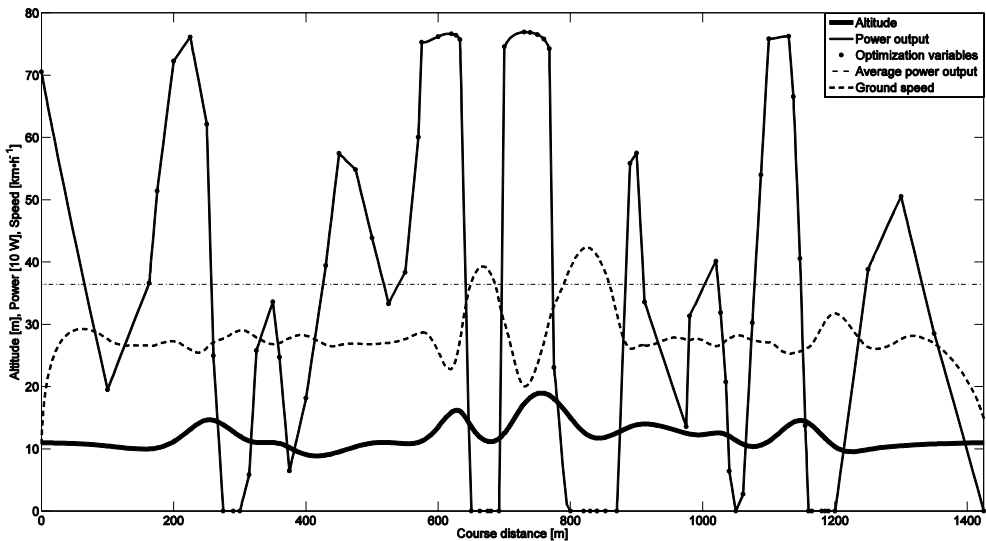


**Figure 19.** Course profile, speed, optimal power output distribution and average power output for a world class male skier of 78 kg. Calculations are made using PSO I.

### 8.2 Effect of hills on optimal pacing in road cycling

In Paper II, the aim was to optimize pacing for road cycling, using the critical power model for intermittent exercise on three 2000 m hilly courses and compare the results for various hill set-ups. Furthermore, comparisons were also made between optimal pacing strategies and constant power strategies using the average power of the optimal strategies. The optimization routine completed 30 iterations for each course, and the finishing times were  $T_{SP} = 171.1$  s,  $T_{DH} = 156.9$  s, and  $T_{QH} = 151.9$  s, for the single plateau (SP), double hill (DH), and quadruple hill (QH) courses respectively. The variances of speed for the optimal pacing strategies were 6.54%,

1.18%, and 0.84%, while the time gains of these pacing strategies compared to constant power simulations were 3.0%, 5.0%, and 2.3% for the SP, DH, and QH courses respectively. In comparison to the initial energy levels, the remaining energies in the anaerobic compartments (AWC) at the finish line were 0.041%, 0.41%, and 0.22% for the SP, DH, and QH courses respectively. Course profiles, optimal pacing strategies and power output distributions are shown in Figure 20.

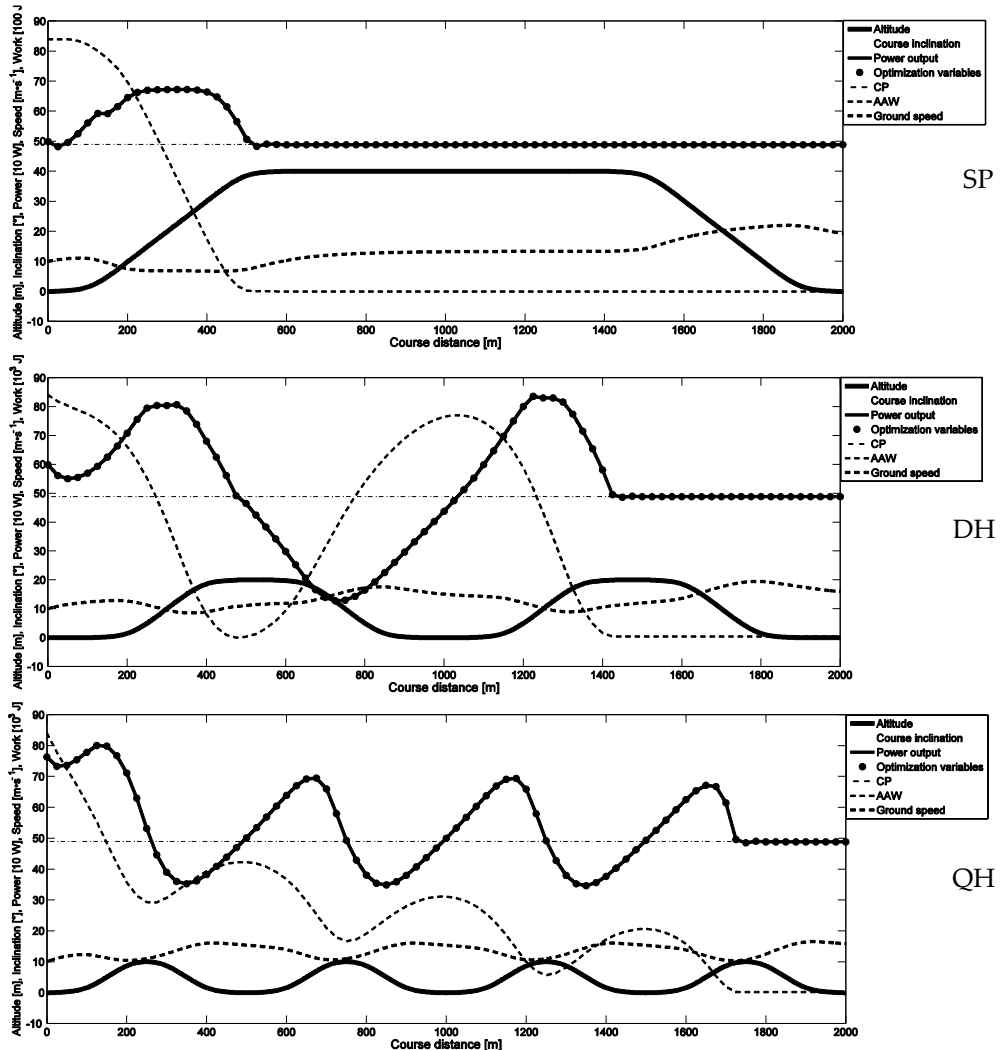


**Figure 20.** Optimal pacing strategies and power output distributions for the rider on the single plateau (SP), double hill (DH) and quadruple hill (QH) courses. Results are calculated by PSO II.



The optimal power distributions in Paper II varied in sync with course gradients in each optimal strategy, so different course profiles resulted in differing optimal pacing strategies.

### 8.3 Impact of sharp course bends on optimal pacing in road cycling

In Paper IV, the aim was to investigate how power output and speed should be distributed to optimize performance in non-drafted road cycling on a flat 1000 m course with one sharp bend. Furthermore, the aim was also to investigate the effect of racing line on performance. Therefore, optimal power distributions and the corresponding pacing strategies were calculated for three courses with the same length; two of the courses had a minimal turning radius of 7.5 ( $c_{7.5}$ ) and 10 m ( $c_{10}$ ) respectively and one course was straight ( $c_{\infty}$ ). The two different turning radii could be considered as two different racing lines through the same course bend. Bearing angle profiles, pacing strategies, power output distributions, and anaerobic compartments' energy levels are illustrated in Figure 21.

The finishing times were  $T_{\infty} = 70.7$  ,  $T_{10} = 76.0$ , and  $T_{7.5} = 77.0$  s, while the speed variances were 2.1, 3.3, and 3.9  $\text{m}\cdot\text{s}^{-1}$ , for  $c_{\infty}$ ,  $c_{10}$ , and  $c_{7.5}$  respectively. In comparison to the initial energy levels, the remaining alactic energies at the finish line were 10.1, 9.93, and 10.2%, while the remaining lactic energies were 8.35, 15.7, and 15.5%, for  $c_{\infty}$ ,  $c_{10}$ , and  $c_{7.5}$  respectively. The average power outputs were 691, 631, and 626 W while the kinetic energies spent due to braking were 0, 2522, and 3235 J for  $c_{\infty}$ ,  $c_{10}$ , and  $c_{7.5}$  respectively. Moreover, the minimal speeds due to braking were 8.28 and 7.16  $\text{m}\cdot\text{s}^{-1}$  for  $c_{10}$ , and  $c_{7.5}$  respectively.

Paper b is not one of the appended papers in this thesis because it is only a peer-reviewed conference abstract that was presented orally. However, since this paper contributes to achieving the main aims of Paper IV, some of its results, including previously unpublished data, are presented here. Instead of just restricting the normal acceleration due to static friction, Paper b's restriction accounted for the total horizontal acceleration including the tangential component that is directly influenced by the braking or propulsive force on the wheels. The course had a length of 500 m with a 90° course bend halfway through at a minimal turning radius of 6.5 m. Moreover, the optimization completed 40 iterations, which resulted in the power output distribution shown in Figure 22. Furthermore, Table 3 summarizes a selection of results from this optimal solution.

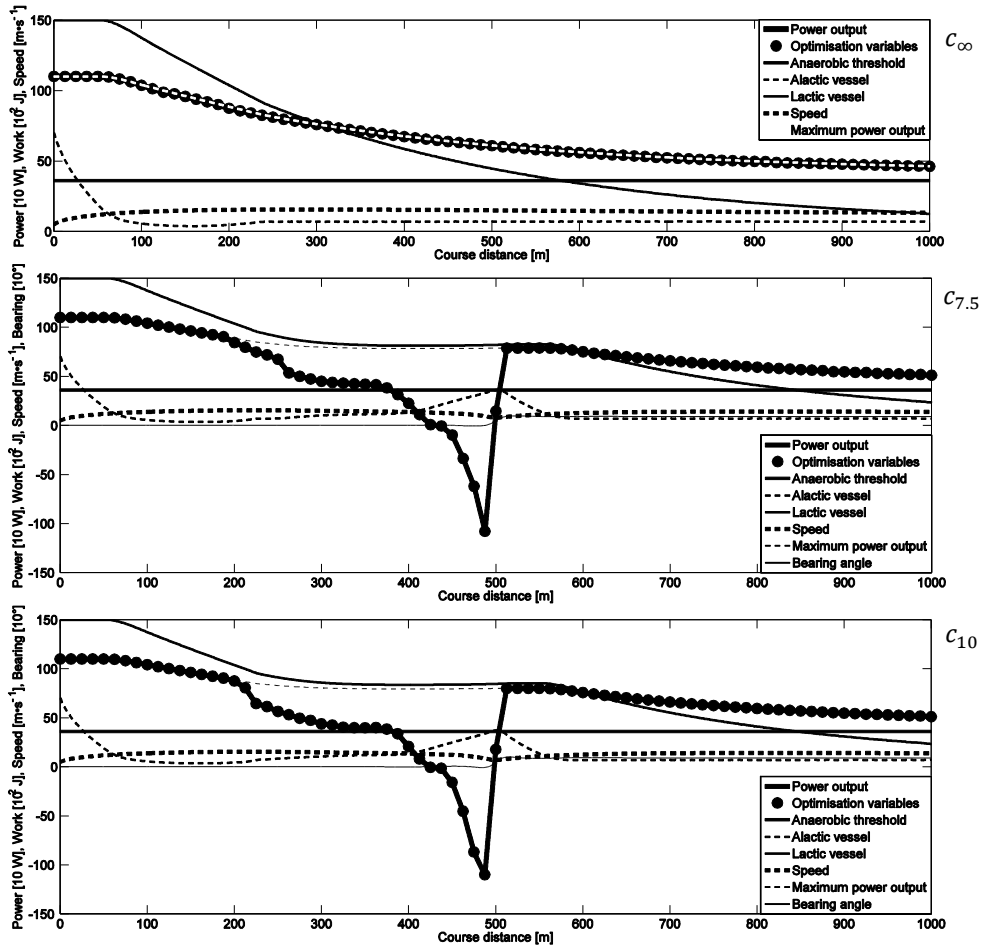


**Figure 21.** Optimal pacing strategies, power distributions, anaerobic thresholds, alactic and lactic compartment levels, maximal power constraints, and bearing angles, for the straight course ( $c_{\infty}$ ) and the curved courses with 7.5 m ( $c_{7.5}$ ) and 10 m ( $c_{10}$ ) radii in PSO IV. The Maximum power constraint was colored white in  $c_{\infty}$ , for visibility.

**Table 3.** Results from Paper b and previously unpublished data from the same study.

Finishing time [s]	40.5
Propulsive time [s]	37.6
Braking time [s]	1.9
Freewheeling time [s]	1.0
Speed variance [ $\text{m}\cdot\text{s}^{-1}$ ]	0.0038
Average propulsive power [W]	829
Average braking power [W]	1970
Remaining alactic energy [%]	12.2
Remaining lactic energy [%]	35.2
Maximal frictional force [N]	576
Maximal propulsive force [N]	220
Average propulsive force [N]	73
Maximal braking force [N]	539
Average braking force [N]	197
Tip over braking force [N]	$\sim 490 - 540$

The results presented in Figure 22, including the dynamics of braking, may also be more thoroughly observed in close proximity to the course bend. Figure 23 shows the acceleration components of the motion in this segment and the maximal attainable acceleration due to the maximal grip friction of the tires. The shark fin shaped graph in Figure 23 is the tangential acceleration component. Regarding the well-known relation between acceleration and force, this may be seen as representative of the optimal distribution of braking force.

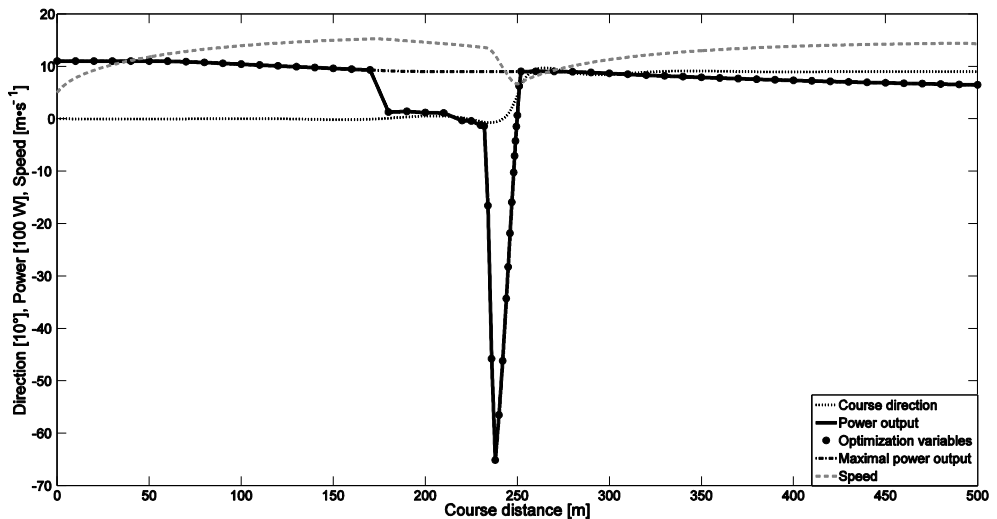


**Figure 22.** Optimal pacing strategy and power output distribution including braking pattern for a corner with a minimal turning radius of 6.5 m. Negative power output is considered braking power.

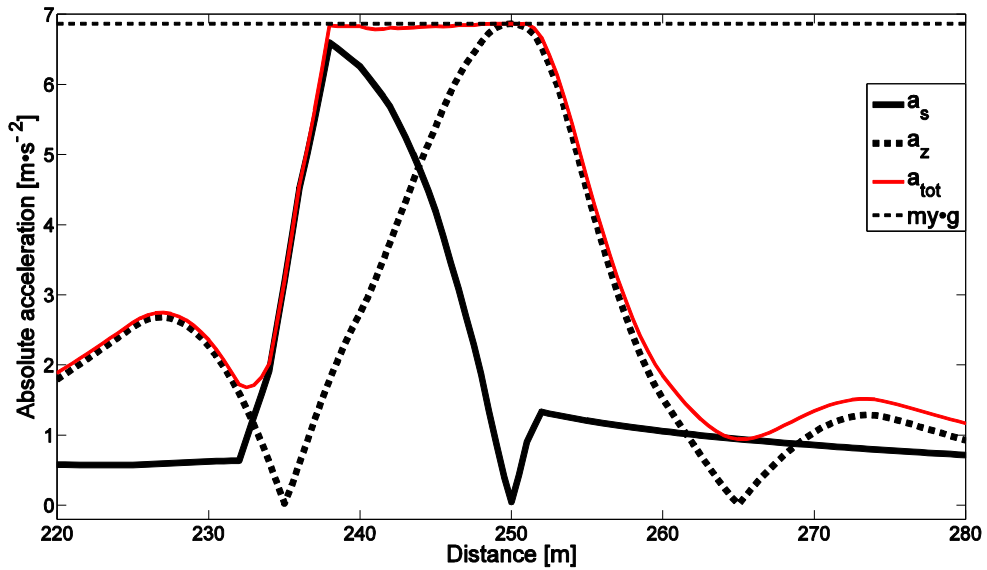


**Figure 23.** Tangential and normal acceleration components for optimal braking and maximal allowable acceleration due to static friction in a square corner with a minimal turning radius of 6.5 m.

## 8.4 Impact of ambient wind with changing direction on optimal pacing in road cycling

The aim of Paper VI was to investigate how energy expenditure rate and speed should be distributed to optimize performance in non-drafted road cycling on flat 2 and 100 km courses when ambient wind direction is changing or when there are no ambient winds? Therefore, four different courses were simulated, two were 2 km long and two were 100 km long. Moreover, one of each course length contained ambient wind with constant speed but varying directions relative to the course. The other two courses were simulated without the impact of ambient wind. All four courses were simulated and optimized for both one and 81 optimization variables resulting in eight simulations. The 81-variable optimizations resulted in the optimal power distributions and the one-variable optimizations resulted in constant power distributions which did not violate the optimization constraints. The eight simulations were named CSNW, CSW, CLNW, CLW, OSNW, OSW, OLNW, and OLW, where C stands for constant power strategy (one variable), O denotes optimal power distribution (81 variables), S stands for short course (2 km), L is for long course (100 km), NW stands for no ambient wind, and W denotes a course where ambient wind is present. A full list of numerical outputs from the eight pacing strategy simulations in Paper VI are presented in Tables 4 and 5. Optimal pacing strategies and energy expenditure rate distributions for Paper VI are shown in

Figures 24-27. The energy expenditure rate distribution in Figures 24-27 are equivalent to the power distributions depicted in Figures 19-22 and 28-29.

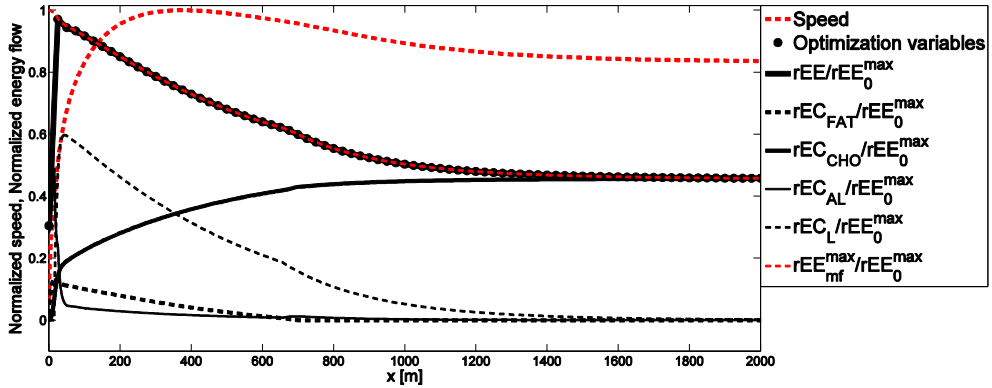


**Figure 24.** Optimal pacing strategy, energy expenditure rate distribution, and relative metabolic subsystem contribution, in no ambient wind on a 2000 m course.

The constant power strategies resulted in finishing times of 170.8, 177.4, 10351, and 11188 s for the CSNW, CSW, CLNW, and CLW simulations respectively. Furthermore, the optimal power distributions resulted in finishing times of 161.0, 168.6, 10146, and 11028 s for the OSNW, OSW, OLNW, and OLNW simulations respectively. Consequently, the optimal power distributions gave time gains of 5.7, 4.9, 2.0, and 1.4% compared to the constant power distributions for SNW, SW, LNW, and LW courses respectively.

**Table 4.** Numerical results from simulation of the constant and optimal power distributions on the short courses with and without ambient wind (2000 m) in PSO VI.

Simulation	CSNW	OSNW	$\Delta$ [%]	CSW	OSW	$\Delta$ [%]
Ambient wind	No			Yes		
Power distribution	Constant	Optimal		Constant	Optimal	
Finishing time [s]	170.8	161.0	-5.7	177.4	168.6	-4.9
Average speed [ $\text{m}\cdot\text{s}^{-1}$ ]	11.71	12.42	6.1	11.28	11.86	5.2
Maximal speed [ $\text{m}\cdot\text{s}^{-1}$ ]	12.36	14.33	16.0	14.44	16.93	17.2
Total work [kJ]	65.85	72.42	10.0	67.83	75.11	10.7
Average $P$ [W]	385.6	449.8	16.7	382.4	445.5	16.5
Total energy expenditure [kJ]	284.9	311.5	9.3	293.5	323.2	10.1
Total energy conversion from fat oxidation [kJ]	42.75	11.15	-73.9	44.01	11.14	-74.7
Total energy conversion from carbohydrate oxidation [kJ]	158.6	213.9	34.9	165.7	225.5	36.1
Total alactic energy conversion [kJ]	11.48	11.67	1.6	11.50	11.67	1.5
Total lactic energy conversion [kJ]	72.11	74.85	3.8	72.38	74.88	3.4
Average $rEE$ [W]	1668	1935	16.0	1655	1917	15.8
Average $rEC_{FAT}$ [W]	250.3	69.23	-72.3	248.1	66.04	-73.4
Average $rEC_{CHO}$ [W]	928.4	1328	43.0	934.0	1338	43.3
Average $rEC_{AL}$ [W]	67.23	72.49	7.8	64.85	69.23	6.7
Average $rEC_L$ [W]	422.3	464.9	10.1	408.1	444.1	8.8
Maximal relative constraint violation	7.074e-07	1.378e-04	193.8	9.183e-04	1.060e-05	-98.8
Relative objective function improvement in the last optimization iteration	8.694e-07	8.759e-07	0.7	1.908e-04	2.294e-08	-100.0

Note:  $\Delta$  is the relative difference between constant and optimal power distributions expressed as a percentage.

The total energy expenditures were higher in each of the OSW, OLW, CSW, and CLW simulations compared to the OSNW, OLNW, CSNW, and CLNW simulations respectively. However, the average power outputs and energy expenditure rates were greater in all simulations, excluding ambient wind, compared to the equivalent power distributions on the ambient wind courses.

**Table 5.** Numerical results from simulation of the constant and optimal power distributions on the long courses with and without ambient wind (100 km) in PSO VI.

Simulation	CLNW	OLNW	$\Delta$ [%]	CLW	OLW	$\Delta$ [%]
Ambient wind	No			Yes		
Power distribution	Constant	Optimal		Constant	Optimal	
Finishing time [s]	10351	10146	-2.0	11188	11028	-1.4
Average speed [ $\text{m}\cdot\text{s}^{-1}$ ]	9.661	9.856	2.0	8.938	9.068	1.5
Maximal speed [ $\text{m}\cdot\text{s}^{-1}$ ]	9.671	11.52	19.1	12.95	14.35	10.8
Total work [kJ]	2056	2137	3.9	2192	2274	3.7
Average $P$ [W]	198.6	210.6	6.0	196.0	206.2	5.2
Total energy expenditure [kJ]	9230	9551	3.5	9853	1018	3.3
Total energy conversion from fat oxidation [kJ]	6833	7016	2.7	7438	7648	2.8
Total energy conversion from carbohydrate oxidation [kJ]	2366	2514	6.3	2386	2512	5.3
Total alactic energy conversion [kJ]	6.588	5.840	-11.4	6.500	5.859	-9.9
Total lactic energy conversion [kJ]	21.52	12.20	-43.4	20.41	12.45	-39.0
Average $r_{EE}$ [W]	891.7	941.3	5.6	880.6	923.2	4.8
Average $r_{EC_{FAT}}$ [W]	660.1	691.4	4.7	664.7	693.5	4.3
Average $r_{EC_{CHO}}$ [W]	228.6	247.8	8.4	213.2	227.8	6.8
Average $r_{EC_{AL}}$ [W]	0.6365	0.5756	-9.6	0.5809	0.5313	-8.5
Average $r_{EC_L}$ [W]	2.079	1.203	-42.1	1.824	1.129	-38.1
Maximal relative constraint violation	4.033e-04	0	-100	9.978e-04	0	-100
Relative objective function improvement in the last optimization iteration	6.943e-08	1.468e-06	2014	1.568e-08	1.308e-06	8242

Note:  $\Delta$  is the relative difference between constant and optimal power distributions expressed as a percentage.

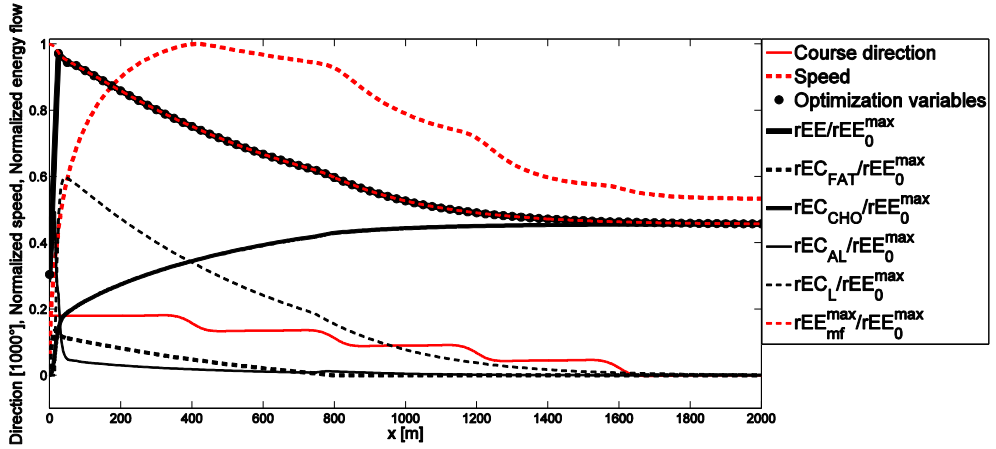


**Figure 25.** Optimal pacing strategy, energy expenditure rate distribution, relative metabolic subsystem contribution, and course direction, on a 2000 m course with an ambient wind of  $5 \text{ m} \cdot \text{s}^{-1}$  which changes from tailwind to headwind in five equal angle increments.

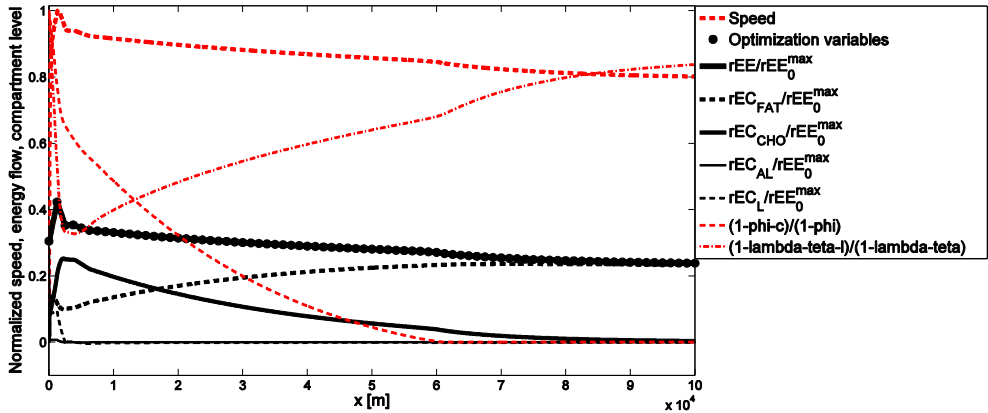


**Figure 26.** Optimal pacing strategy, energy expenditure rate distribution, and relative metabolic subsystem contribution, in no ambient wind on a 100 km course.



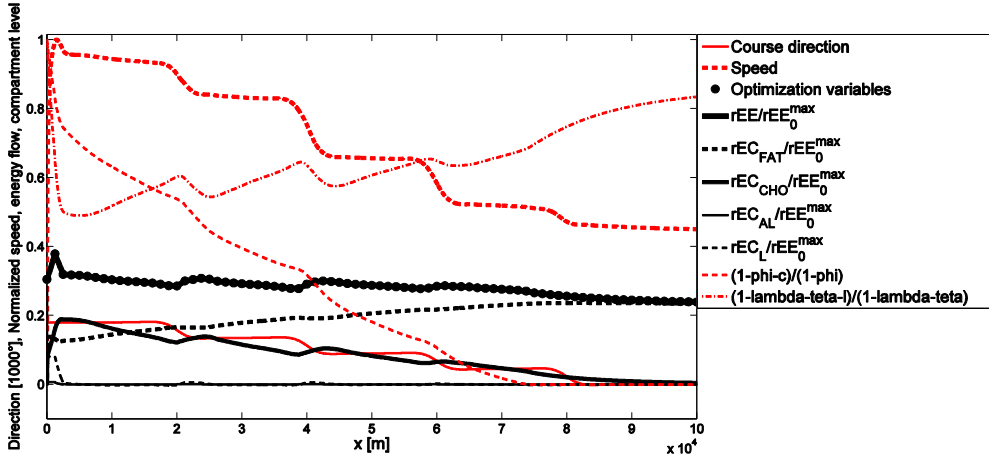


**Figure 27.** Optimal pacing strategy, energy expenditure rate distribution, relative metabolic subsystem contribution, and course direction, on a 100 km course with an ambient wind of  $5 \text{ m}\cdot\text{s}^{-1}$  which changes from tailwind to headwind in five equal angle increments.

## 8.5 Effect of various bioenergetic models on the results in pacing strategy optimization

In Paper III, the aim was to evaluate the effect of different bioenergetic models on the optimal pacing strategy and the estimated performance. The M-M model (BE III c) was compared to the CPIE model (BE III b) and a constant power simulation (BE III a). The QH course profile from Paper II was used and the optimization carried out 60 iterations for the M-M and CPIE models respectively. The finishing times (performance) were  $T_{CPS} = 165.2$ ,  $T_{CPIE} = 158.2$ , and  $T_{MM} = 159.3 \text{ s}$  and the variances of speed were 7.8, 2.1, and  $5.3 \text{ m}\cdot\text{s}^{-1}$ , for the constant power, CPIE, and M-M models respectively. Furthermore, in comparison to the initial levels of energy, the remaining anaerobic energies at the finish line were 0.045% in the CPIE simulation, while they were 15 and 37% for the AL and L compartments respectively in the M-M model. Course profile, pacing strategies, power output distributions, and anaerobic compartments' energy levels can be seen in Figures 28 and 29 for the optimal simulations of the CPIE and M-M model respectively. Furthermore, a comparison in pacing strategies between the constant power, CPIE, and M-M models is illustrated in Figure 30.

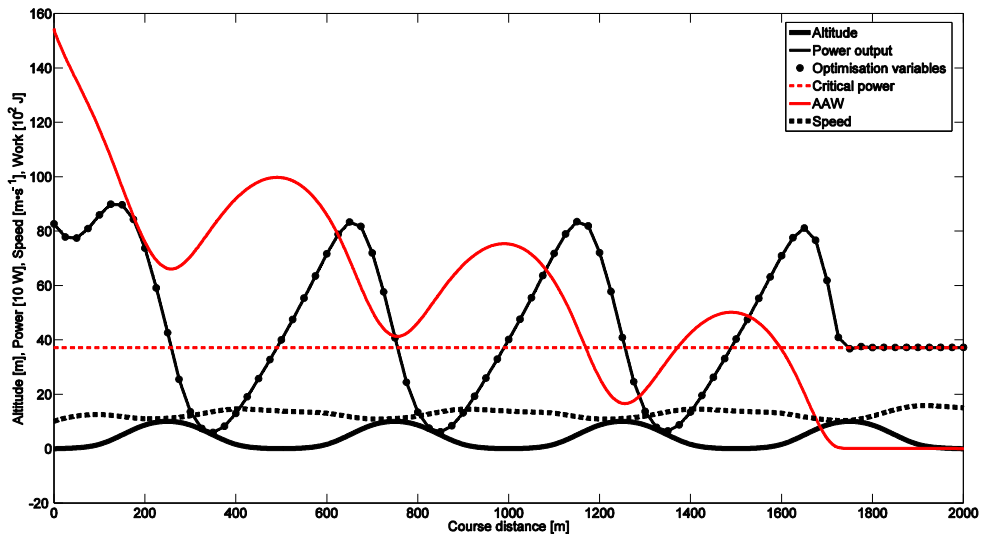


**Figure 28.** Optimal pacing strategy, power distribution, critical power, anaerobic work compartment level (AAW), and course profile, calculated by PSO III and constrained by BE III b (CPIE model).

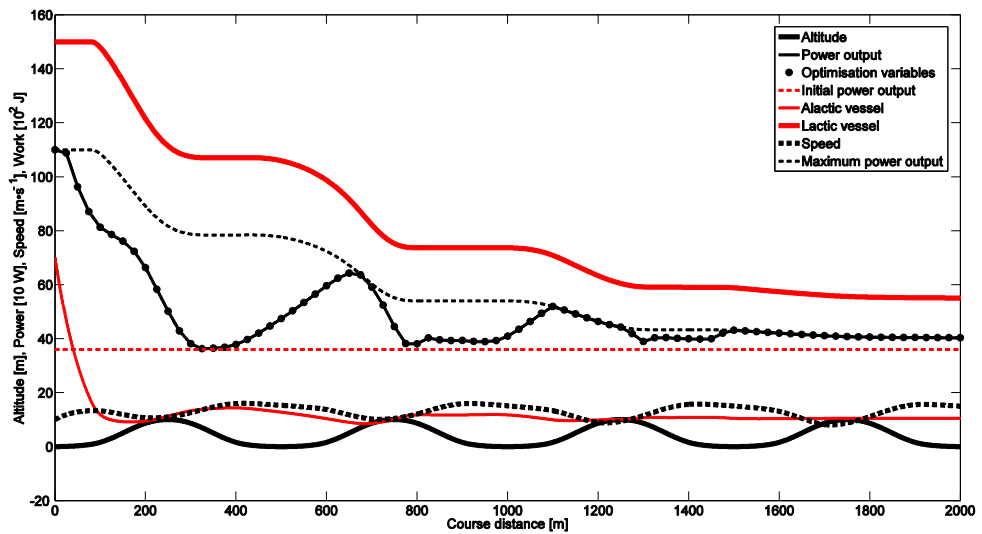


**Figure 29.** Optimal pacing strategy, power distribution, initial power, alactic and lactic compartment levels, maximal power constraint, and course profile, calculated by PSO III and constrained by BE III c (M-M model).

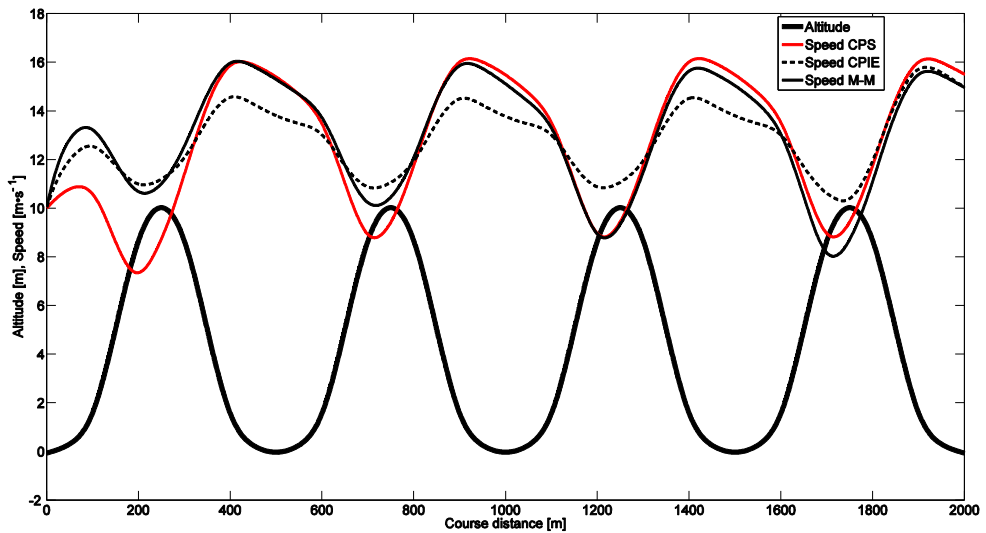


**Figure 30.** Course profile and optimal pacing strategies for the three modeling approaches in PSO III.

## 8.6 Effect of optimal pacing strategies on performance

The estimated improvements from adopting optimal power distributions compared to constant power strategies for the studies contained within this thesis are summarized in Table 6.

**Table 6.** Numerical result comparisons for simulation of constant and optimal power distributions in Paper I, II, II, and VI.

Paper	Sport	BE model	Course	Obstacle	Finishing time [s]		$\Delta$ [%]
					Constant	Optimal	
I	XC-Skiing	Average power	-	Hills	200.4	187.4	-6.5
II	Road Cycling	CPIE	SP	Hills	176.4	171.1	-3.0
II	Road Cycling	CPIE	DH	Hills	165.2	156.9	-5.0
II	Road Cycling	CPIE	QH	Hills	155.5	151.9	-2.3
III	Road Cycling	CPIE	QH	Hills	165.2	158.2	-4.2
III	Road Cycling	M-M	QH	Hills	165.2	159.3	-3.6
VI	Road Cycling	M-M-S	SNW	-	170.8	161.0	-5.7
VI	Road Cycling	M-M-S	SW	Wind	177.4	168.6	-4.9
VI	Road Cycling	M-M-S	LNW	-	10351	10146	-2.0
VI	Road Cycling	M-M-S	LW	Wind	11188	11028	-1.4

Note:  $\Delta$  is the relative difference in finishing times between constant and optimal power distributions expressed as a percentage.

## 8.7 Bioenergetic model development for pacing strategy optimizations

The maximal power restriction on the M-M model (Morton, 1990) in Paper III was modified for Paper IV. However, the most comprehensive development of the bioenergetic compartment model in this thesis is presented in Paper V, in which the M-M-S model was evaluated and compared to previous empirical findings. Three different modes of exercise were simulated in Paper V to test the M-M-S model. These modes were submaximal exercise at 50 and 70% of  $rEC_0^{max}$ , supramaximal exercise at 101, 103, 110, 125, 150, and 200% of  $rEC_0^{max}$ , and all-out exercise.

### 8.7.1 Submaximal simulations

In the submaximal constant power output simulations, power was set to increase according to equation (87) and Figure 14, up to the equivalent of the pre-set rate of energy expenditure and thereafter power was kept constant. The estimated relative contributions of the various energetic systems to total energy supply for the different durations are illustrated in Figure 31.

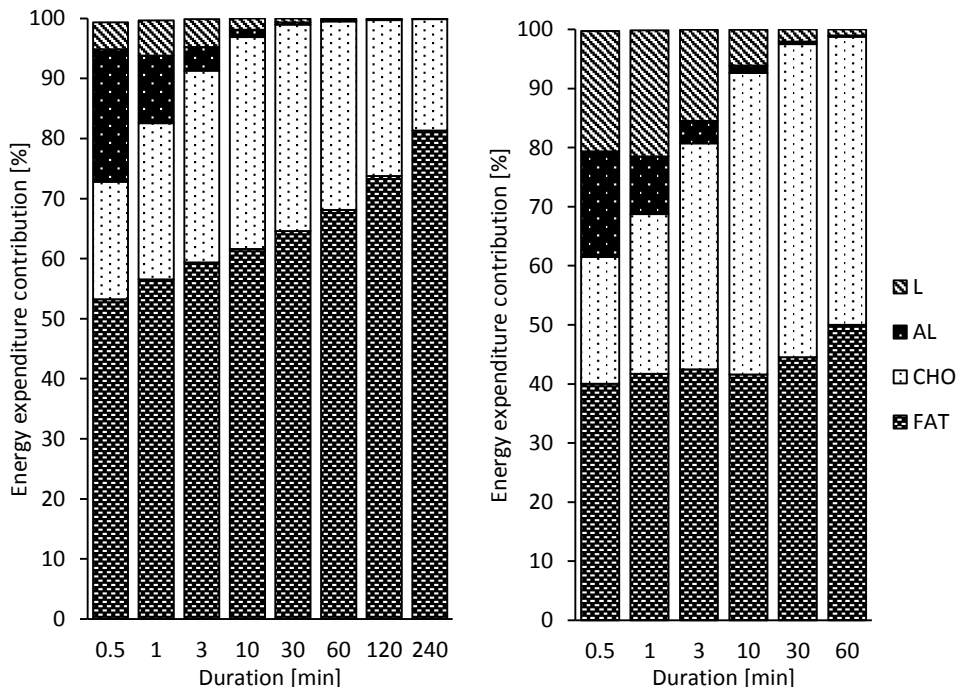


**Figure 31.** Energy substrate utilization for prolonged submaximal exercise at  $0.5 \cdot rEC_0^{max}$  (~50% of  $\dot{V}O_{2max}$ ) (left) and  $0.7 \cdot rEC_0^{max}$  (~70% of  $\dot{V}O_{2max}$ ) (right). Calculations were done using BE V (M-M-S model).

### 8.7.2 Supramaximal simulations

The supramaximal constant power output simulations were conducted in the same manner as the submaximal simulations. However, due to the higher power and the M-M-S model's constraint on maximal energy expenditure rate (equation 53), power was impelled to decrease by the interaction of equation (53). The time by which this constraint interfered was termed the time to exhaustion (TTE). Figure 32 show TTE and the estimated relative contributions of the various energetic systems to total energy supply for the different rates of energy expenditures.

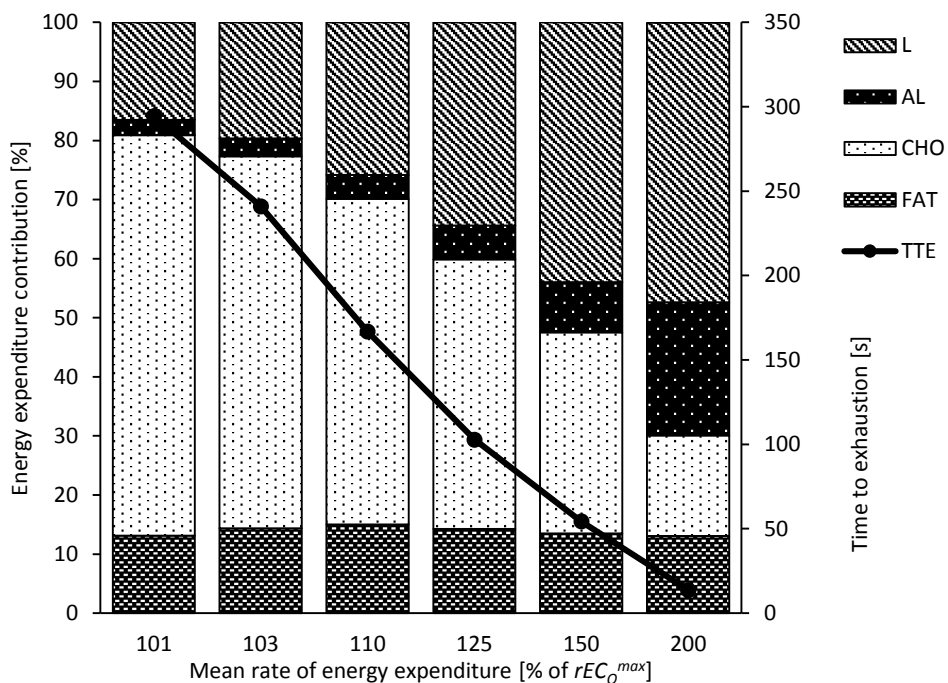


**Figure 32.** Time to exhaustion (TTE) and metabolic subsystem utilization with a duration equal to TTE for supramaximal work at constant power outputs equivalent to 101, 103, 110, 125, 150, and 200% of  $rEC_0^{max}$ . Calculations were done using BE V (M-M-S model).

To evaluate the model for empirical data, two supramaximal simulations were run for 107 and 125% of  $rEC_0^{max}$ , which were compared to study 1 of Gastin et al. (1995). The time courses of these simulations are presented in Figures 33 and 34. Compared to study 1 in Gastin et al. (1995), the relative aerobic energy contribution for the simulations were 4.2% lower and 1.5% higher for the  $1.07 \cdot rEC_0^{max}$  and  $1.25 \cdot rEC_0^{max}$  simulations respectively. Average rates of energy expenditure were slightly lower in the simulations than in Gastin's experiments (-0.3% for  $1.07 \cdot rEC_0^{max}$  and -0.7% for  $1.25 \cdot rEC_0^{max}$ ).

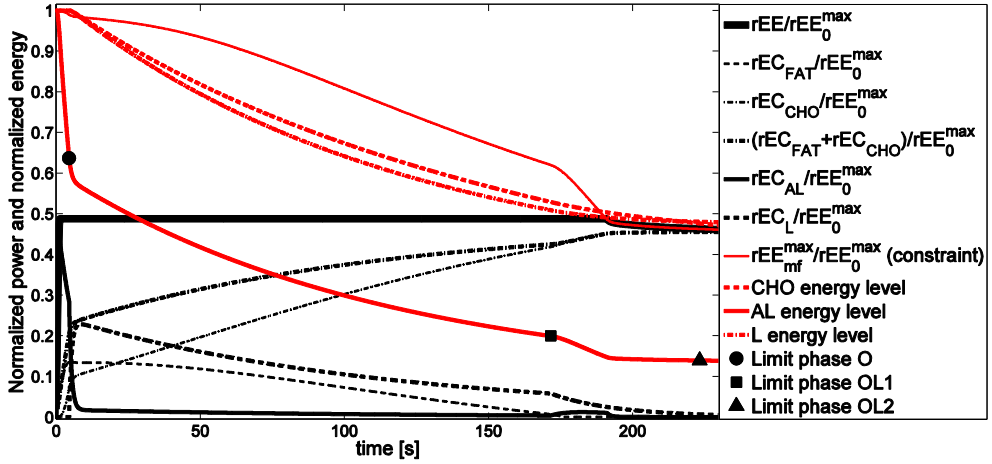


**Figure 33.** M-M-S (BE V) model time course for supramaximal exercise with constant power equivalent to a rate of energy expenditure equal to  $1.07 \cdot r_{EC}_0^{max}$  ( $\sim 107\%$  of  $\dot{V}O_{2max}$ ) for 230 s. Metabolic subsystem utilizations are expressed in normalized values.

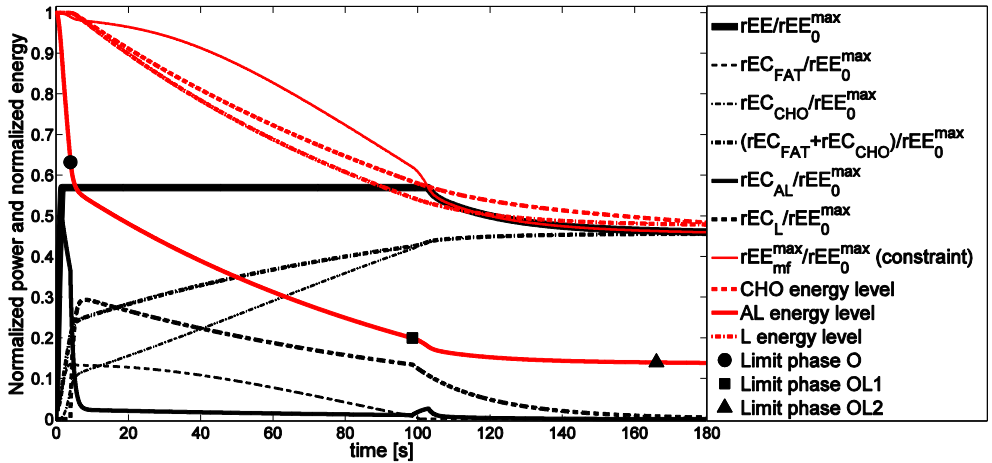


**Figure 34.** M-M-S (BE V) model time course for supramaximal exercise with constant power equivalent to a rate of energy expenditure equal to  $1.25 \cdot r_{EC}_0^{max}$  ( $\sim 125\%$  of  $\dot{V}O_{2max}$ ) for 180 s. Metabolic subsystem utilizations are expressed in normalized values.

### 8.7.3 All-out simulation

The all-out, maximal power simulation was run with an energy expenditure rate equal to the minimum of the two constraints on maximal propulsive force (equation 87) and maximal energy expenditure rate (equation 53). The all-out simulation resulted in a relative aerobic energy contribution that was 3.4% lower and the average energy expenditure rate was 8.8% higher than the reported value in study 1 of Gastin et al. (1995). The relative contributions of the various energetic systems to total energy supply for consecutive time intervals are presented for the all-out simulation in Figure 35 and the time course of that simulation is shown in Figure 36.

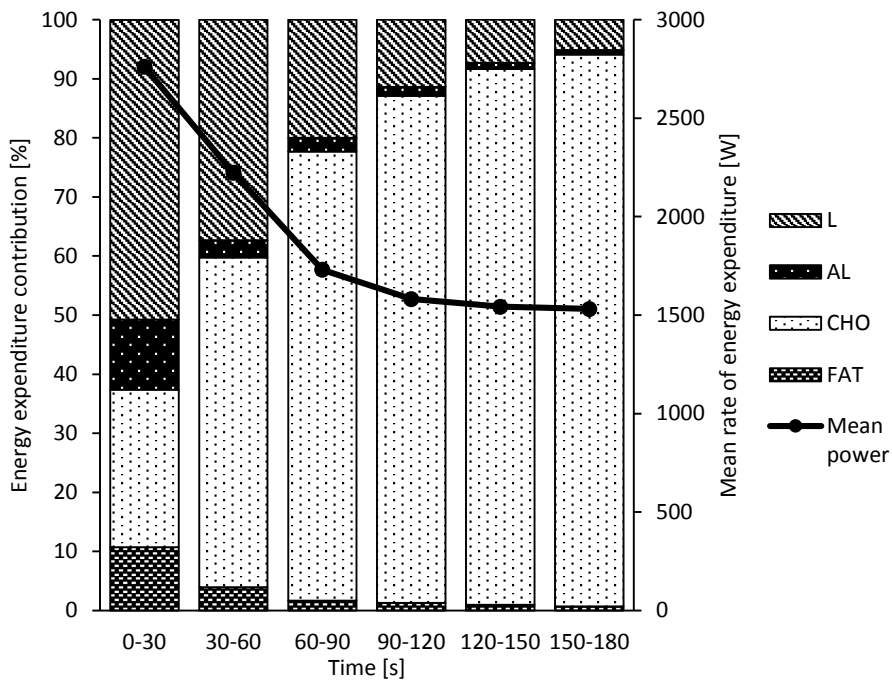


**Figure 35.** Metabolic subsystem utilization and mean power output for consecutive time periods of all-out exercise using the M-M-S model (BE V).

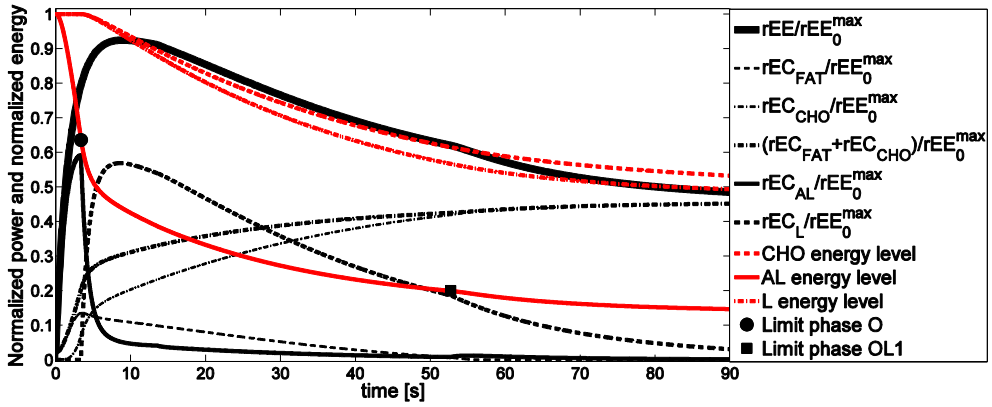


**Figure 36.** M-M-S (BE V) model time course for all-out maximal power exercise constrained by equations (53) and (87) for a duration of 90 s. Metabolic subsystem utilization is expressed in normalized values.



## **9. DISCUSSION AND CONCLUSIONS**

The results of this thesis confirm previous findings (Swain, 1997, Atkinson and Brunskill, 2000, Gordon, 2005, Atkinson et al., 2007, Cangley et al., 2011, Boswell, 2012, Dahmen, 2012b, Dahmen, 2012a, Wells et al., 2013), demonstrating that variable power output distributions are beneficial in variable ambient conditions. Furthermore, the results of Papers I, II and III specifically confirm that power output should be varied in sync with course gradient to minimize variations in speed and thereby optimize performance. Collectively, the results presented in this thesis suggest that athletes improve performance by adapting their power output with respect, not only to changing course gradients and ambient winds, but also to their own physiological and biomechanical abilities, course length, and obstacles such as sharp course bends.

### **9.1 Effect of hills on optimal pacing in cross-country skiing**

The rapid variations in power output suggested in Paper I may be questioned on the basis of human exercise bioenergetics. However, it might be argued that these variations are the result of the simplistic constraint that only restricts average, minimal and maximal power. Still, the calculated time saving of 6.5% from opting an optimal power distribution instead of constant power in Paper I, is well beyond the standard deviation of finishing times (3.6%) in elite cross-country skiers performing a similar sprint race (Andersson et al., 2010). Due to the simplistic bioenergetic model, significant time gains at the highest level of performance might be much smaller than those in Paper I, which still suggests that pacing strategy optimization may have a decisive effect on performance in cross-country sprint skiing. Overlooking the shortcomings of bioenergetics, the results of Paper I show that power should be varied heavily in parallel with course inclination to optimize performance in sprint cross-country skiing.

### **9.2 Effect of hills on optimal pacing in road cycling**

The results of Paper II show that courses with the same total elevation but with different numbers of hills need different pacing strategies. Just like the findings of Boswell (2012), the finishing times of the optimal pacing strategies in Paper II were faster when hills had lower accumulated elevations. These findings agreed with the hypothesis that hills with lower accumulated elevations (QH) would create lower speed variance and therefore lower finishing times than courses with higher hills. Key to this is the point at which anaerobic work capacity is depleted with no further replenishment. This point occurs close to the top of the last uphill on each course and therefore occurs further into the race for the courses with hills closer to the finish

line. It was suggested by Swain (1997) that constant speed is optimal but not always achievable. In such circumstances, one might argue that performance can be improved if physiological stress is kept within acceptable limits while minimizing variations in speed. In Paper I, it is concluded that this constant speed optimality is the result of the aerodynamic drag's dependence on speed squared (equations 12 and 13).

Moreover, in accordance with the findings of Swain (1997), Atkinson et al. (2007), and Boswell (2012), Paper II found that differing numbers of hills induce varying potential for improvement by applying optimal pacing strategies. However, in contrast to these studies, Paper II resulted in larger improvements for both the course with one long hill (SP) and two medium hills (DH) compared to four shorter hills (QH). It might be argued that the optimization of the pacing strategy on four hills had not reached an absolute optimum before the iterative routine was terminated. Still, it is also evident that direct comparisons cannot be made with the preceding studies (Swain, 1997, Atkinson et al., 2007, Boswell, 2012), as they did not compensate for accumulated elevations (ascent) in their simulations. In conclusion, the different hill set-ups affected the optimal pacing strategy in a similar way, resulting in power distributions varied in parallel with course gradient up to the top of the last uphill. From there, power was maintained constant at the critical power all the way to the finish line.

### **9.3 Impact of sharp course bends on optimal pacing in road cycling**

The results of Paper IV show that sharp course bends may pose considerable obstacles to road cycling performance. For example, a sharp corner with a minimal turning radius of 7.5 m on a 1000 m course slowed down the rider by 9% compared to the same course without a corner. Moreover, considering the lower turning radius as an inferior racing line of the same course bend to the 10 m turning radius, it may be argued that the inferior racing line impairs performance by more than 1% over the 1000 m course. This makes a distance gap of 13 m between the two racing lines after the bend, if average speed is assumed. It was further shown in Paper IV that greater kinetic energy lost due to braking matched a lower average power output and greater finishing time. Additionally, the differences in finishing times between the various courses could also be explained by the differences in speed variance. Therefore, based on the results in Paper VI, it was concluded that the choice of racing line or the ability to reduce the minimal turning radius in cornering influence performance substantially.

In Paper IV, it was also concluded that optimal power distribution for course bends includes four different phases in addition to the initial all-out acceleration that originates from the initial acceleration of inertia. These four consecutive phases include a steady-state power phase, a rolling phase, a braking phase, and an all-out acceleration phase. It is rational to conceive of the steady-state phase as a way of keeping the speed reached in the acceleration phase of the locomotion, and the rolling phase as an attempt to recover and save energy for the acceleration phase coming up. Braking is of course the way to reach the maximal speed attainable without slipping (Paper IV) or avoiding the maximal total acceleration corresponding to the grip limit (Paper b). The last phase of all-out acceleration is an attempt to reach high speed as soon as possible, in order to finish in minimal time. Therefore, the optimal power distribution for course bends balances these phases to minimize the variations in speed. This aim of minimizing the variations in speed conforms to previous experimental findings for pacing in variable terrain (Cangley et al., 2011). In contrast to Paper IV, Paper b showed no visible steady-state power phase. The shorter course used in Paper b may explain this difference in optimal solution phases. The shorter distance from the course bend to the finish line may require less recovery ahead of the course bend, resulting in a relatively greater initial acceleration which consumes the steady-state power phase. A closer look at the braking phase in Figure 23 reveals that optimal braking for course bends is executed directly preceding the apex (minimal turning radius) of the bend. Furthermore, optimal braking ensures that the total acceleration in the plane of the bend is below the maximal allowable acceleration corresponding to the maximal frictional force between the road and the tires (Paper b). In addition, optimal braking for a course bend on a 500 m course consisted of substantial contributions of both tangential and normal acceleration components. Therefore, it is concluded that the interaction of these components is a key to optimal braking. It is of course evident that longer courses or less sharp course bends would not require braking to avoid slippage, so in these cases the braking phase may be cancelled.

#### **9.4 Impact of ambient wind with changing direction on optimal pacing in road cycling**

The results of Paper VI show that ambient wind has a substantial effect on performance and that the lay-out of optimal power distributions may also be affected. The simulations in Paper VI show that optimal pacing in ambient wind is almost identical to optimal pacing without ambient wind on a 2000 m flat course (Figures 24 and 25). These two simulations (OSNW and OSW) were both described by an all-out pacing strategy. However, on the 100 km flat course, optimal pacing showed considerable variations in the power distribution to manage the variable ambient wind conditions in OLW (Figure 27). This supports the findings of Swain (1997) and Atkinson et al. (2007) that substantial time savings can be achieved if

power is varied in parallel with wind direction. Furthermore, the optimal pacing strategies on the 100 km course in Paper VI were generally described by a high speed and high power start followed by an overall positive pacing strategy.

The power distribution in OSNW and OSW (Paper IV) shows a distinct resemblance to the optimal power distribution on the flat 1000 m course ( $C_{\infty}$ ) without ambient wind constrained by the M-M model (BE IV) in Paper IV (PSO IV) (Figure 21). Furthermore, these power distributions support the conclusion of Morton et al. (2009) that any bioenergetic model with a maximum power feedback coupling, dependent in a monotonically decreasing fashion on the amount of some fuel substrate remaining, would require all-out effort for optimal performance. However, apparently this does not hold for the OLNW and OLW simulations (Paper VI), potentially due to longer courses and the additional constraints which restricts power to being lower than the maximum constraint in equations (53) and (131).

The all-out pacing strategies for the 2000 m courses acquired from the optimization in Paper VI (Figures 24 and 25) are all in line with the findings of de Koning et al. (1999) for a 1000 m course. The reason for this strategy being optimal is the high power needed for the initial acceleration, which is there to reduce the time spent at low speed far from the average speed. Moreover, high speed is more beneficial at the initial stages of the course, from where momentum can be transferred into locomotion at subsequent stages. On the contrary, all momentum will be wasted at the finish line and thus too high a speed at the finish line is suboptimal. All these effects can be owed to inertia. However, there is a complementary effect on performance from the  $\dot{V}O_2$  kinetics related to high power starts. Empirical studies show that the time to reach  $\dot{V}O_{2max}$  is inversely related to exercise intensity (Jones et al., 2008, Hill and Ferguson, 1999). This effect is also evident in the M-M and M-M-S models and implies that high power starts result in higher average aerobic energy expenditure rates than lower power starts, which are naturally beneficial for performance.

Judging by the results of Swain (1997) and Atkinson et al. (2007), the power distribution in OSW would have varied in parallel to the ambient wind direction. However, the results (Figure 25) showed that the power distribution was close to similar to OSNW (Figure 24), describing an all-out power distribution. The reason for this might be that the influences of inertia and  $\dot{V}O_2$  kinetics are greater than the effect of varying power relative to ambient wind direction. Consequently, the optimal pacing strategy overlooks the effects of ambient wind direction in favor of the effects of inertia and  $\dot{V}O_2$  kinetics. For the long course of 100 km, the effect of initial acceleration and  $\dot{V}O_2$  kinetics are less pronounced and the ambient wind

direction has a greater effect on the optimal power distribution in the OLW simulation than in the OSW simulation.

The OLNW simulation in Paper VI resulted in a distinct high power start influenced by initial acceleration and  $\dot{V}O_2$  kinetics (Figure 26). Subsequently, power decreased to reach a somewhat constant level at the point where the carbohydrate store was depleted. Another observation, not initially obvious, is that some carbohydrates are first expended anaerobically through glycolysis ( $rEC_L$ ), then restored through gluconeogenesis ( $rEC_R$ ) and at last expended through oxidative phosphorylation ( $rEC_{CHO}$ ). The advantage of this pathway of energy extraction is that the anaerobic depletion in the initial stages of the course will increase the rate of aerobic energy conversion. Due to the formulation of the bioenergetic model (M-M-S, BE VI), such a great aerobic energy conversion rate is impossible to sustain at the late stages of the race because of the limited stores of carbohydrates (equations 50 and 128). In the M-M-S model (BE VI), the effect of impaired efficiency in motor units sustaining fatigue is not considered. In reality this effect might shift the optimal pacing strategy from positive pacing to a more negative pacing scheme or possibly a U-shaped or reverse J-shaped pacing strategy (Abbiss and Laursen, 2008).

The OLW simulation in Paper VI resulted in a similar power distribution to the OLNW simulation, save for the substantial ambient wind adaptations (Figure 27). The power variations seen in the OLW simulation could be regarded as a compromise between the mechanical model and the bioenergetic model. Optimization of the pacing strategy, subject to the mechanical model, induces power variations but the bioenergetic model strives to reduce the variations of power to minimize the disturbance to physiological homeostasis.

## **9.5 Effect of various bioenergetic models on the results in pacing strategy optimization**

Course QH in Paper II with four hills, each with 10 m elevation, was used in Paper III to investigate the influence of various types of bioenergetic constraints on the optimization of pacing strategies. Unsurprisingly, that study showed that the optimization of pacing strategy resulted in improved performance and that the CPIE model (BE III b) induced a lower finishing time than the M-M model (BE III c). The formulation of the CPIE model without a maximal power constraint applies more relaxed restrictions on the power output than the M-M model. Therefore, it was expected that the greater performance would be observed in the CPIE optimization. However, judging by the results presented in Paper III, it is conceivable to assume that the M-M model better describes the real human body's restriction on power output. The gradual decrease in power observed in the distribution corresponding to the M-M model is more realistic than the almost unfatigued characteristics of the

power distribution observed in the optimal C PIE model optimization. It has been established that muscle fatigue is highly related to the intra-muscular concentration of inorganic phosphate that is released during supramaximal exercise (Westerblad et al., 2002). Therefore, the high power output attained by the C PIE model in the last uphill section in Paper III seems unrealistically high, as such great exertion should inhibit high power outputs.

The fast and slow components of  $\dot{V}O_2$ -kinetics are absent in the C PIE model, but are, however, implicitly included in the M-M model. There is empirical evidence showing that the time to reach  $\dot{V}O_{2_{max}}$  is inversely related to exercise intensity (Hill and Ferguson, 1999, Jones et al., 2008), which is congruent with the dynamic behavior of the M-M model. Furthermore, along with the mechanical basis of high power starts being optimal (de Koning et al., 1999) this implicit  $\dot{V}O_2$ -kinetic of the M-M model further benefits high power starts to generate high aerobic energy expenditures. Consequently, it is conceivable to assume that the M-M model is preferable in comparison to the C PIE model, for the application of optimal pacing strategies in real-world competition. In conclusion, the C PIE model resulted in the best estimated performance, but the M-M model resulted in more realistic distributions of power and speed. Furthermore, The CPS strategy resulted in poor performance compared to the C PIE and M-M models on a hilly course.

## **9.6 Effect of optimal pacing strategies on performance**

From the comparison of estimated performance improvements in Table 6, it may be concluded that short courses realize greater improvements than long courses from adopting an optimal pacing strategy. Furthermore, it may be concluded that greater improvements are also realized for less sophisticated bioenergetic constraints, such as the average power or C PIE models, than for the more sophisticated M-M model. These results also showed that greater time gains from adopting an optimal pacing strategy might be achieved in variable ambient wind conditions than in calm or no winds. The experimentally achieved time gain from adopting an optimal pacing strategy in time-trial road cycling, reported by Cangle et al. (2011), was 2.9% on a hilly 4000 m course. Numerically estimates of performance improvements presented in Papers II and III were 2.3 to 5.0% on a hilly 2000 m course. Moreover, Swain (1997) reported performance improvement estimates of up to ~10% from optimized power distributions in numerical road cycling simulations. In conclusion, the results in section 8.6 showed an optimal pacing strategy performance improvement in the range of 1.4 to 6.5%, which is in the proximity of previously reported values.

## **9.7 Methodological considerations**

### **9.7.1 Mechanics of locomotion**

The various mechanical models applied to the studies presented in this thesis are all formulated as motion equations by using Newton's second law of motion and solved using numerical differential equation solvers. These models consider both inertial resistance to motion and all the major external forces acting on the athlete and his/her equipment. This enables valid simulations of the athlete's locomotion (Martin et al., 1998) assuming all parameters of the model conform with the athlete's properties and the ambient conditions. In this respect, the validity of mechanical locomotion modeling directly reflects the validity of athlete and environment measurements. The validity of these measurements is of course functions of the accuracy and precision of measurements which, as such, relates to the measurement methods used and the administration of such methods. However, for the purpose of answering general research questions regarding locomotion or pacing strategy, reasonable parameter settings at least work to simulate the general dynamics of locomotion.

In Paper I, drag area was set to vary with speed, mostly due to the crouching occurring at high speeds in cross-country skiing. However, it is evident that cross-country skiers tend to move in a manner that cause fluctuations in the drag area within each sub-technique cycle. The effect of these variations upon the drag area have not been studied to date but might have substantial effects on the modeling of cross-country skiing locomotion. Furthermore, different sub-techniques and/or gears may also be associated with differences in efficiency (Ainegren et al., 2013) which may influence the validity of the results in Paper I.

### **9.7.2 Bioenergetics**

No study to date has investigated the validity of the M-M or the M-M-S models and, therefore, not much can be claimed about the validity of these bioenergetic models. The lack of any validation of these bioenergetic models may be regarded as a deficiency in their reliability. However, concerning the direct transmission of corroborated physiological facts to these models and their credible output results (Papers III, IV, V, and VI), support their application in pacing strategy optimization. Just like the mechanical models, the validity of bioenergetic models is also dependent on the validity of measures for the various included parameters. Some of these measures are readily available through simple sample-taking or indirect calorimetry in exercise testing. However, other measures, such as the maximal rate of energy conversion due to lactic formation, are harder to assess. Validating bioenergetic models has not been the scope of this thesis. Still, it is of great interest

that some research efforts from sports physiologists is directed into this area, especially regarding the more sophisticated M-M and M-M-S models. The vast number of parameters in the M-M-S model may be its greatest drawback. Still, every parameter in the M-M-S model has a reason to be included and serves a certain functionality, which also is its greatest advantage.

### **9.7.3 Optimization**

The optimization method used in all the studies included in this thesis has proven to work well for all the posed pacing strategy optimization problems. Several other optimization methods, including the interior point method, the sequential quadratic programming method, and the generalized pattern search method were evaluated but none worked better than MMA. The pattern search method, which is a non-gradient based method, was evaluated for its advantageous ability to find global optima but it was rejected on the basis of its long computational time requirements. In most cases, default values of the MMA algorithm were used with good results but in some cases, especially the lower and upper asymptotes had to be tightened to achieve stable converging solutions.

The resolution of the optimal pacing strategy is primarily dependent on the number of the optimization variable density. Therefore, a greater number of optimization variables will generate a better pacing strategy. However, the computation time is more or less linearly dependent on the number of optimization variables, which results in extended computation times if high accuracy is desired. Furthermore, a high number of optimization variables may result in badly formulated numerical calculations of the gradients which are necessary for the optimization. A decent compromise is to increase optimization variable density in sections where propulsive force alterations are more likely due to the approach of speed conservation. Another possible solution is to post-process such sections with more detailed variable settings.

Instead of using convergence criteria, all the optimizations in thesis were run for a preset number of iterations from which the best feasible solution was chosen. In some instances, such as Paper II, it might have been better to use a convergence criterion to be sure of convergence. However, a convergence measure was used in Paper VI to ensure all solutions had converged to a stable solution.



## 10. PERSPECTIVES AND FUTURE DEVELOPMENT

The numerical models presented in thesis may be used as means of optimizing performance for individual athletes seeking to improve performance in their locomotive endurance sports. However, at present, all models are not straightforward and user friendly to the novice user and might need engineering and physiology expertise to make full use of. These models are of course not just in the interest of elite athletes but may as well be worthwhile to the dedicated leisure athlete seeking to improve on her/his favorite segment or Grand Fondo race. The possibility to form a service of these models and make it commercially available, could eventually increase user numbers. This service could be integrated into the cyclist's power meter or the skier's GNSS-based (global navigation satellite systems) wristwatch as an on-the-fly aid for optimal pacing. From this device visual or audio-based communication systems could inform the athlete of the present status in relation to the optimal pacing strategy. Still, prior to such service is commercially available, athletes may be assisted by the general outlines of the results presented in section 8. For instance in the event of course bends in road cycling that need braking, these results (Figures 21 to 23) may be studied to consciously adapt pacing in a way that, according to these results, improves performance. A perhaps even more helpful result to any road cyclist competing in time-trials is the results of Paper VI for the 100 km course. Although such long time-trial races are rare, courses which experience ambient winds on an out-and-back or closed circuit race course are common. Therefore, direction of travel will vary over the course distance, as will the effect of ambient winds. The general outline of power distribution in Figure 27 thus suggest that power should be varied in parallel with these changes in ambient wind, still allow a high power start and an overall decreasing power distribution.

The question may arise, whether or not athletes are opting for optimal pacing strategies already, as a natural inherent ability or as a result of experience. If so, this work on optimal pacing strategy in locomotive sports would be a complete waste of time and resources. In this context it must be resembled that in-competition variabilities in pacing are frequently observed by split timing of athletes along the course distance. It may be that optimal pacing varies between individuals, resulting in these differences in split times. However, more likely, athletes frequently opt for suboptimal pacing strategies resulting in impaired performance. Furthermore, there exist several examples not mentioned in this thesis where obviously suboptimal pacing has been adopted by competitive athletes.

One might argue that science and technology undermine the excitement of sports by reducing the impact of the athletes own endeavor or the conscious and subconscious

actions that are learned by experience. In the worst case, technology may sideline the ethics of fair play in sports. However, it must be stressed that in the modern era of sports, athletes have always been influenced by other athletes, coaches, scientists, and the technological development. The challenge for the governing bodies of sports are to formulate their regulations on the use of technology, in a manner that facilitates fair play. On the other hand, the application of science and technology may also facilitate fair play. For instance, the formation of a cross-country skiing course may be designed with an optimal distribution of uphill, downhill, and flat sections so that performance is independent of the skiers' body mass (Bergh, 1987, Moxnes and Hausken, 2008).

A meaningful scientific contribution to the work presented in this thesis would be a comprehensive sensitivity analysis of, for instance, PSO VI. As already proposed in section 9.2.2, future development must also include validation of the more sophisticated bioenergetic models. It was clearly shown in Paper III that the bioenergetic model substantially affects the distribution of power and therefore the pacing strategy. Furthermore, regarding the bioenergetic model, several points for further development are possible. Discretization of compartments into muscle fiber motor units and the prioritization of fiber type activation similar to previous studies (Liu et al., 2002, Xia and Fray Law, 2008, James and Green, 2012, Sih et al., 2012, Gede and Hubbard, 2014) is one possible extension to the M-M-S model. This also enables the modelling of efficiency variations in various fiber types. The M-M-S model has a large number of parameters and therefore, it would be favorable to reduce this number and thereby attain a simpler model. However, it may be difficult to reduce this number without losing important functionality.

Considering the mechanical model of locomotion, varying glide friction for cross-country skiing and varying rolling resistance would contribute to further possibilities for studying optimal pacing strategies. In real world circumstances, snow conditions may vary between different positions on the skiing track due to local geographical differences and the natural variation in preparing the tracks (grooming). The classical technique tracks usually induce less frictional resistance than skating technique tracks which are commonly situated alongside the classical tracks. Consequently, the classical tracks may be a beneficial choice for athletes performing the skating technique in downhills where no propulsive force is generated by the athlete (above  $\sim 10 \text{ m}\cdot\text{s}^{-1}$ ). Moreover, some road cycling competitions make use of cobblestoned roads with various surface roughnesses which are often decisive for the competition's outcome.

Another variable parameter that was not allowed to vary in Paper I is the efficiency. It has been shown that efficiency varies with different gears in cross-country skiing (Ainegren et al., 2013). Modelling this variability might result in a tendency to where power is increased more in sections where gears of high efficiency is employed. At the same time, power would decrease in sections where gears associated with low efficiency is employed. These tendencies would of course be relative to power distributions computed without efficiency variability in contrast to absolute tendencies.

Widening the perspectives of this thesis, the approach of optimizing pacing strategies in cross-country skiing and road cycling presented in this thesis may also be applied to other locomotive sports, such as running, speed skating, and rowing. Similar models can also be used to minimize fuel consumption in, for instance, combustion engine vehicles. In this approach the finishing time will be a constraint and the expenditure of fuel will be the objective function.



## REFERENCES

- Abbiss, C. R. & Laursen, P. B. 2008. Describing and understanding pacing strategies during athletic competition. *Sports Medicine*, 38, 239-252.
- Ainegren, M., Carlsson, P., Tinnsten, M. & Laaksonen, M. S. 2013. Skiing economy and efficiency in recreational and elite cross-country skiers. *J Strength Cond Res*, 27, 1239-52.
- Andersson, E., Supej, M., Sandbakk, O., Sperlich, B., Stoggl, T. & Holmberg, H. C. 2010. Analysis of sprint cross-country skiing using a differential global navigation satellite system. *European Journal of Applied Physiology*, 110, 585-595.
- Atkinson, G. & Brunskill, A. 2000. Pacing strategies during a cycling time trial with simulated headwinds and tailwinds. *Ergonomics*, 43, 1449-1460.
- Atkinson, G., Davison, R., Jeukendrup, A. & Passfield, L. 2003. Science and cycling: current knowledge and future directions for research. *Journal of Sports Sciences*, 21, 767-787.
- Atkinson, G., Peacock, O. & Passfield, L. 2007. Variable versus constant power strategies during cycling time-trials: Prediction of time savings using an up-to-date mathematical model. *Journal of Sports Sciences*, 25, 1001-1009.
- Behncke, H. 1993. A mathematical model for the force and energetics in competitive running. *Journal of Mathematical Biology*, 31, 853-878.
- Bergh, U. 1987. The influence of body-mass in cross-country skiing. *Medicine and Science in Sports and Exercise*, 19, 324-331.
- Boswell, G. P. 2012. Power variation strategies for cycling time trials: a differential equation model. *Journal of Sports Sciences*, 30, 651-9.
- Cangley, P., Passfield, L., Carter, H. & Bailey, M. 2011. The effect of variable gradients on pacing in cycling time-trials. *International Journal of Sports Medicine*, 32, 132-6.
- Carlsson, P., Tinnsten, M. & Ainegren, M. 2011. Numerical simulation of cross-country skiing. *Computer Methods in Biomechanics and Biomedical Engineering*, 14, 741-6.
- Chenevière, X., Malatesta, D., Peters, E. M. & Borrani, F. 2009. A mathematical model to describe fat oxidation kinetics during graded exercise. *Medicine and Science in Sports and Exercise*, 41, 1615-1625.
- Colbeck, S. C. 1994. A review of the friction of snow skis. *Journal of Sports Sciences*, 12, 285-295.
- Dahmen, T. Computing a field of optimal pacing strategies for cycling time trials. Symposium der dvs-Sektion Sportinformatik, 2012a Konstanz, Germany.
- Dahmen, T. Optimization of pacing strategies for cycling time trials using a smooth 6-parameter endurance model. Pre-olympic congress on sports science and computer science in sport (IACSS2012), 2012b Liverpool. IACSS Press.

- Dahmen, T. & Saupe, D. 2011. Calibration of a power-velocity-model for road cycling using real power and height data. *International Journal of Computer Science in Sport*, 10, 18-36.
- Dahmen, T. & Saupe, D. 2015. Normalized and xPower to generate pacing strategies in road cycling. *IFAC-PapersOnLine*, 48, 780-781.
- Dahn, K., Mai, L., Poland, J. & Jenkins, C. 1991. Frictional resistance in bicycle wheel bearings. *Cycling Science*, 3, 28-32.
- De Koning, J. J., Bobbert, M. F. & Foster, C. 1999. Determination of optimal pacing strategy in track cycling with an energy flow model. *Journal of Science and Medicine in Sport*, 2, 266-77.
- Di Prampero, P. E., Cortili, G., Mognoni, P. & Saibene, F. 1979. Equation of motion of a cyclist. *Journal of Applied Physiology*, 47, 201-6.
- Fehlberg, E. 1969. Low-order classical runge-kutta formulas with stepsize control and their application to some heat transfer problems. *NASA technical report*. Marshall, Alabama: National aeronautics and space administration.
- Fintelman, D. M., Sterling, M., Hemida, H. & Li, F. X. 2014. The effect of crosswinds on cyclists: an experimental study. *Procedia Engineering*, 72, 720-725.
- Formenti, D., Rossi, A., Calogiuri, G., Thomassen, T. O., Scurati, R. & Weydahl, A. 2015. Exercise intensity and pacing strategy of cross-country skiers during a 10 km skating simulated race. *Res Sports Med*, 23, 126-39.
- Foster, C., Snyder, A. C., Thompson, N. N., Green, M. A., Foley, M. & Schragar, M. 1993. Effect of pacing strategy on cycle time trial performance. *Medicine and Science in Sports and Exercise*, 25, 383-388.
- Gaesser, G. A. & Brooks, G. A. 1975. Muscular efficiency during steady-rate exercise: effects of speed and work rate. *J Appl Physiol*, 38, 1132-9.
- Gastin, P. B. 2001. Energy system interaction and relative contribution during maximal exercise. *Sports Medicine*, 31, 725-741.
- Gastin, P. B., Costill, D. L., Lawson, D. L., Krzeminski, K. & Mcconell, G. K. 1995. Accumulated oxygen deficit during supramaximal all-out and constant intensity exercise. *Med Sci Sports Exerc*, 27, 255-63.
- Gede, G. & Hubbard, M. 2014. A bioenergetic model for simulating athletic performance of intermediate duration. *Journal of Biomechanics*, 47, 3448-3453.
- Gordon, S. 2005. Optimising distribution of power during a cycling time trial. *Sports Engineering*, 8, 81-90.
- Grappe, F., Candau, R., Barbier, B., Hoffman, M. D., Belli, A. & Rouillon, J. D. 1999. Influence of tyre pressure and vertical load on coefficient of rolling resistance and simulated cycling performance. *Ergonomics*, 42, 1361-1371.
- Heil, D. P. 2001. Body mass scaling of projected frontal area in competitive cyclists. *European Journal of Applied Physiology*, 85, 358-366.
- Heil, D. P. 2002. Body mass scaling of frontal area in competitive cyclists not using aero-handlebars. *European Journal of Applied Physiology*, 87, 520-528.

- Hill, A. V. 1938. The heat of shortening and the dynamic constants of muscle. *The Royal Society*, 126, 136-195.
- Hill, D. W. & Ferguson, C. S. 1999. A physiological description of critical velocity. *European Journal of Applied Physiology and Occupational Physiology*, 79, 290-293.
- James, A. & Green, S. 2012. A phenomenological model of muscle fatigue and the power-endurance relationship. *J Appl Physiol*, 113, 1643-51.
- Jones, A. M., Wilkerson, D. P., Vanhatalo, A. & Burnley, M. 2008. Influence of pacing strategy on O<sub>2</sub> uptake and exercise tolerance. *Scandinavian Journal of Medicine and Science in Sports*, 18, 615-26.
- Joyner, M. J. & Coyle, E. F. 2008. Endurance exercise performance: the physiology of champions. *The Journal of Physiology*, 586, 35-44.
- Kennelly, A. E. 1906. An approximate law of fatigue in the speeds of racing animals. *Proceedings of the American Academy of Arts and Sciences*, 42, 275-331.
- Kutta, W. 1901. *Beitrag zur näherungsweise integration totaler differentialgleichungen*. Doctoral, der K. Ludwig-Maximilians-Universität München.
- Kyle, C. R. 1996. Selecting cycling equipment. In: BURKE, E. R. (ed.) *High Tech Cycling*. Campaign: Human Kinetics.
- Liu, J. Z., Brown, R. W. & Yue, G. H. 2002. A dynamical model of muscle activation, fatigue, and recovery. *Biophys J*, 82, 2344-59.
- Margaria, R. 1976. *Biomechanics and energetics of muscular exercise*, Clarendon Press Oxford.
- Maróński, R. 1994. On optimal velocity during cycling. *Journal of Biomechanics*, 27, 205-13.
- Martin, J. C., Milliken, D. L., Cobb, J. E., Mcfadden, K. L. & Coggan, A. R. 1998. Validation of a mathematical model for road cycling power. *Journal of Applied Biomechanics*, 14, 276-291.
- Mcgilvery, R. W. & Murray, T. W. 1974. Calculated equilibria of phosphocreatine and adenosine phosphates during utilization of high energy phosphate by muscle. *Journal of Biological Chemistry*, 249, 5845-50.
- Monod, H. & Scherrer, J. 1965. The work capacity of a synergic muscular group. *Ergonomics*, 8, 329-338.
- Morton, R. H. 1985. On a model of human bioenergetics. *Eur J Appl Physiol Occup Physiol*, 54, 285-90.
- Morton, R. H. 1986a. On a model of human bioenergetics. II. Maximal power and endurance. *European Journal of Applied Physiology and Occupational Physiology*, 55, 413-8.
- Morton, R. H. 1986b. A three component model of human bioenergetics. *Journal of Mathematical Biology*, 24, 451-66.
- Morton, R. H. 1990. Modelling human power and endurance. *Journal of Mathematical Biology*, 28, 49-64.
- Morton, R. H. 1996. A 3-parameter critical power model. *Ergonomics*, 39, 611-9.

- Morton, R. H. 2009. A new modelling approach demonstrating the inability to make up for lost time in endurance running events. *Ima Journal of Management Mathematics*, 20, 109-120.
- Morton, R. H. & Billat, L. V. 2004. The critical power model for intermittent exercise. *European Journal of Applied Physiology*, 91, 303-7.
- Moxnes, J. F. & Hausken, K. 2008. Cross-country skiing motion equations, locomotive forces and mass scaling laws. *Mathematical and Computer Modelling of Dynamical Systems*, 14, 535-569.
- Moxnes, J. F., Sandbakk, O. & Hausken, K. 2013. A simulation of cross-country skiing on varying terrain by using a mathematical power balance model. *Open Access Journal of Sports Medicine*, 4, 127-39.
- Moxnes, J. F., Sandbakk, O. & Hausken, K. 2014. Using the power balance model to simulate cross-country skiing on varying terrain. *Open Access J Sports Med*, 5, 89-98.
- Olds, T. S., Norton, K. I. & Craig, N. P. 1993. Mathematical model of cycling performance. *Journal of Applied Physiology*, 75, 730-737.
- Pugh, L. G. 1974. The relation of oxygen intake and speed in competition cycling and comparative observations on the bicycle ergometer. *Journal of Physiology*, 241, 795-808.
- Robinson, S., Edwards, H. T. & Dill, D. B. 1937. New records in human power. *Science*, 85, 409-410.
- Robinson, S., Robinson, D. L., Mountjoy, R. J. & Bullard, R. W. 1958. Influence of fatigue on the efficiency of men during exhausting runs. *Journal of Applied Physiology*, 12, 197-201.
- Sahlin, K. 1986. Metabolic changes limiting muscle performance. In: SALTIN, B. (ed.) *Biochemistry of exercise VI. Human Kinetics*.
- Sandbakk, O., Holmberg, H. C., Leirdal, S. & Ettema, G. 2010. Metabolic rate and gross efficiency at high work rates in world class and national level sprint skiers. *European Journal of Applied Physiology*, 109, 473-481.
- Sidossis, L. S., Horowitz, J. F. & Coyle, E. F. 1992. Load and velocity of contraction influence gross and delta mechanical efficiency. *International Journal of Sports Medicine*, 13, 407-11.
- Sih, B., Ng, L. & Stuhmiller, J. 2012. Generalization of a model based on biophysical concepts of muscle activation, fatigue and recovery that explains exercise performance. *International Journal of Sports Medicine*, 33, 258-267.
- Sundström, D. 2013. *Optimized pacing strategies in cross-country skiing and time-trial road cycling*. Licentiate thesis, Mid Sweden University.
- Swain, D. P. 1997. A model for optimizing cycling performance by varying power on hills and in wind. *Medicine and Science in Sports and Exercise*, 29, 1104-8.
- Svanberg, K. 1987. The method of moving asymptotes: a new method for structural optimization. *International Journal for Numerical Methods in Engineering*, 24, 359-373.



- Svanberg, K. 1993. The method of moving asymptotes (MMA) with some extensions. *Optimization of Large Structural Systems*, 231, 555-566.
- Underwood, L. & Jermy, M. 2014. Determining optimal pacing strategy for the track cycling individual pursuit event with a fixed energy mathematical model. *Sports Engineering*, 17, 183-196.
- Watt, M. J., Heigenhauser, G. J., Dyck, D. J. & Spriet, L. L. 2002. Intramuscular triacylglycerol, glycogen and acetyl group metabolism during 4 h of moderate exercise in man. *Journal of Physiology*, 541, 969-78.
- Wells, M., Atkinson, G. & Marwood, S. 2013. Effects of magnitude and frequency of variations in external power output on simulated cycling time-trial performance. *J Sports Sci*, 31, 1639-46.
- Westerblad, H., Allen, D. G. & Lannergren, J. 2002. Muscle fatigue: lactic acid or inorganic phosphate the major cause? *News Physiol Sci*, 17, 17-21.
- Xia, T. & Fray Law, L. A. 2008. A theoretical approach for modeling peripheral muscle fatigue and recovery. *Journal of Biomechanics*, 41, 3046-3052.

